Thesis for the Master's degree in chemistry

Vladimiro Rago

Multiple organic and organometallic polymer-supported catalysts for sequential catalysis

60 study points

DEPARTMENT OF CHEMISTRY
Faculty of mathematics and natural sciences
UNIVERSITY OF OSLO 05/2013

Contents

Abbreviations and acronyms

Abbreviation	Full name
AMBN	Azobis methylbutyronitrile
DBAD	Di-tert-butyl azodicarboxylate
DCM	Dichloromethane
DMF	Dimethylformammide
DMSO	Dimethyl sulfoxide
DVB	Divinylbenzene
EGDMA	Ethylene glycol dimethacrylate
HMDS	Hexamethyldisilazane
MMA	Methyl methacrylate
MTBE	Methyl tert-butyl ether
MVK	Methyl vinyl ketone
n-BuLi	Butyllithium
***p*-TsOH**	*p*-Toluenesulfonic acid
PVA	Polyvinyl alcohol
TEA	Triethylamine
TFA	Trifluoroacetic acid
TFAA	Trifluoroacetic anhydride
THF	Tetrahydrofuran

Abstract

The catalytic efficiency of a combination of two catalysts on the same polymer bead is studied and compared to the catalytic efficiency of a combination of the same two catalysts in homogenous conditions for a range of cascade or tandem reactions. The study mostly focuses on the iminium-ion and enamine activation mechanisms, making use of easily available proline-like or imidazolidinone-based organocatalysts discovered in the last decade. Additional insight is provided on the combination between organocatalysis and organometallic catalysts in a non-synergistic fashion, and on the application of the concept to the ongoing research on polymer-supported catalysts for sequential catalysis. A bottom-up procedure for the immobilization of organometallic gold(I) species is also developed and compared to the more classical post-modification procedure.

1 Introduction

In this section the basics and early history of organocatalysis are discussed, with a focus on sequential enamine and iminium-ion catalysis (Sections 1.1 and 1.2). The topic is discussed in relation to sequential catalysis and is further extended to cover the combined applications of cascade/tandem reactions on polymer support (Section 1.3 and 1.4). A description of the performed reactions is provided, along with the explanation of the criteria leading to the choice of the benchmark reactions and the polymeric materials (Section 1.5).

1.1 Sequential catalysis: the concept

Organic syntheses are commonly carried out both at laboratory and industry scale as chains of well-distinct steps, each comprising only one reaction. In step-wise synthesis the separation of reactions in different vessels is a direct method to achieve accurate and control of all non-interdependent factors (temperature, pressure, concentration, etc.). The step-wise approach however imposes purification operations after every chemical process, increasing the amount of energy, chemicals and efforts required for the whole synthesis (Figure 1.1a).

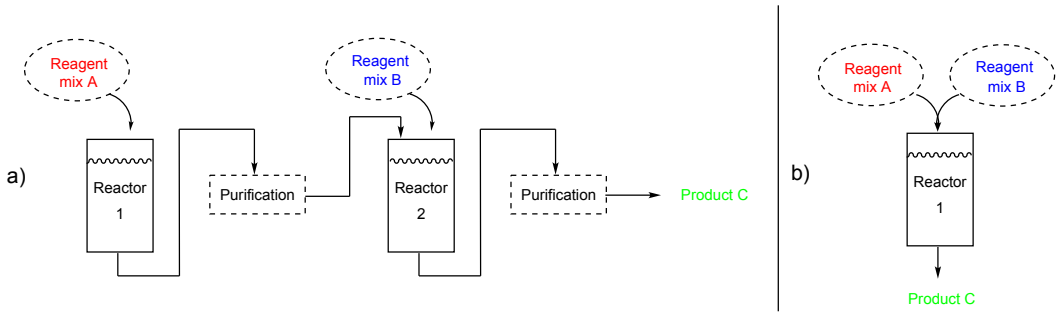

Figure 1.1: a) Step-wise synthesis; b) one-pot sequential synthesis.

An alternative to the step-wise approach is the "sequential" strategy. In sequential synthesis several steps are carried out in the same reaction, in one-pot conditions. Compared to the step-wise approach, sequential processes can easily require less time, chemicals and work to achieve the same results (Figure1.1b).

Early and successful attempts to achieve one-pot sequential reactivity based their strategy on the emulation of known natural sequences. A very good example is the one-pot synthesis of precorrin-6x, an advanced precursors in the total synthesis of vitamin B_{12}.[1] In this case

the total synthesis was possible by the complete in-vitro replication of the minimal cell conditions observed in *E. coli* and *P. denitrificans* required for each step. The astonishing number of 17 consecutive reactions yields precorrin-6x with overall 20% yield. The efficiency of the system is clearly a consequence of the intrinsic activity and selectivity of the enzymes used, whose potential for improvement however is severely limited by the small degree of tunability of enzymes. Enzymatic complexes can catalyze only a small pool of reactions, and are notoriously more fussy with diverse substrates than most other standard organic reactions.

Another far more successful strategy towards sequential catalysis takes its first steps from enzymatic catalysis, but assumes that the only enzymatic properties of interest are those of its catalytic site, which can be interpreted as the presence of a limited number of groups, in a fixed conformation. Many attempts have been made in order to recreate the unique catalytic properties of enzymes through small peptide synthesis.[2]

One of most intriguing discoveries in this field was achieved by List and Barbas in 2001.[3,4] Their study showed how the smallest part in the catalytic site of Class I Aldolases, the proline amino acid, could effectively and with good stereoselectivity catalyze aldol reactions. The study would later be regarded as a breakthrough in organic chemistry, because, starting from the simple and widely available proline molecule, many other slightly different catalysts could be synthesized, all based on the same reaction mechanisms, but operating on a much broader range of reactions compared to enzymatic catalysis and small peptide catalysis. One decade after this branch of chemistry now goes under the name of organocatalysis, and is by far the most effective strategy towards highly stereoselective, high yielding sequential reactions, due to the large number of reactions it features, most notably α-functionalization of aldehydes and ketones, aldol reactions, Michael reactions, Mannich reactions, Diels-Alder and several derivations thereof (Figure 1.2).[5,6]

In addition to the broad scope of this strategy, organocatalysis comes with the combined advantage of using small highly customizable molecules, opening the way to perfect tuning of the catalyst and to facile reversion of stereoconfiguration, both lacking features in the enzymatic approach.

The reactions based on activation by a secondary amine, such as proline, typically rely on two activation mechanisms: the enamine activation, and the iminium-ion activation. (Figure 1.3).[7]

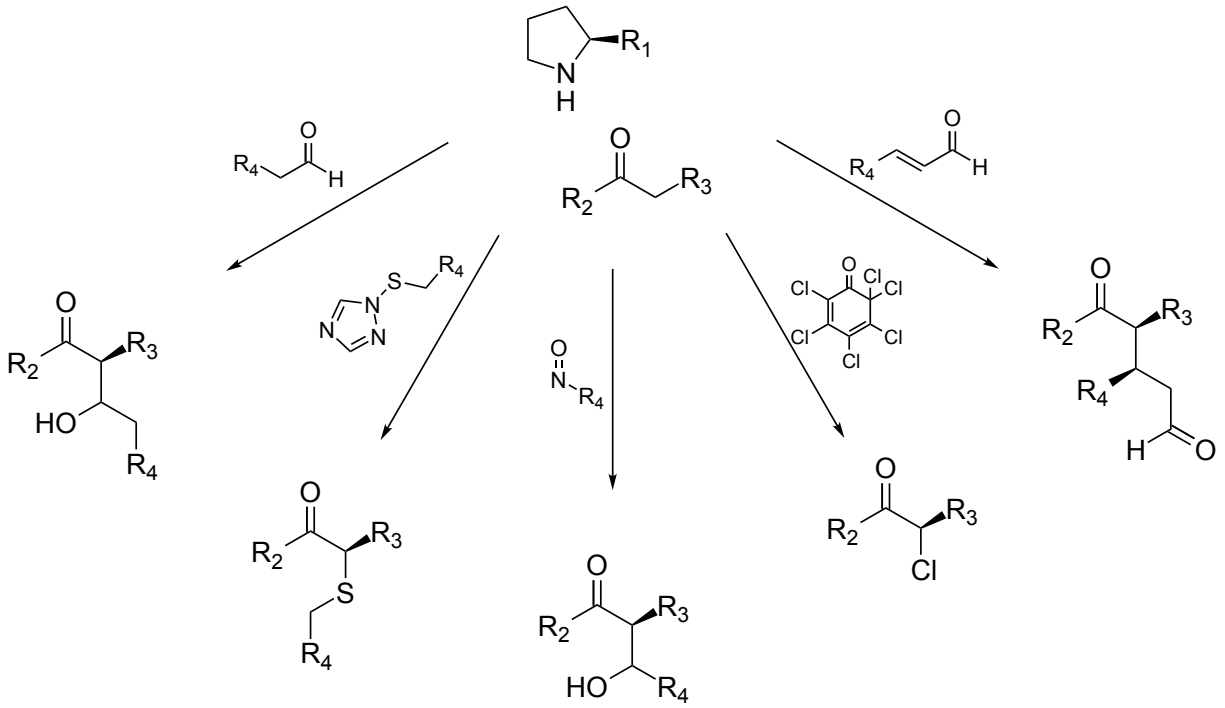

Figure 1.2: Examples of stereoselective amine-catalyzed reactions.

Enamine activation requires that proline, the secondary amine, reacts with the aldehyde, in order to form an enamine and water. The enamine thus formed is much more active towards electrophilic attack than the free aldehyde, and thus reacts very easily with another aldehyde molecule in an aldol reaction, or, depending on the reagents used, can undergo to α-functionalizations, such as chlorinations, sulfenylations, fluorinations, aminations, etc. Once this occurs, an iminium ion is formed. Subsequent hydrolyzation and deprotonation of the iminium ion yields the reaction product and regenerates the catalyst. The secondary amine can achieve the same type of reactivity on ketones as well.

Iminium ion activation requires that an iminium ion, such as proline in acidic conditions, joins to an aldehyde to form the active catalyst-substrate complex. Once this occurs, the complex is far more reactive towards 1,4-nucleophilic attack for electronic reasons, and Diels-Alder reactions due to LUMO-lowering analogous to Lewis acid activation. After the reaction, the aldehyde can reversibly detach from proline with the addition of water, which regenerates the catalyst. Once again, the mechanism works equally well with aldehydes and ketones.

Stereoselectivity is achieved in the same way for both mechanisms. The carboxylic moiety on proline can coordinate the incoming reagent and selectively direct the attack. This mech-

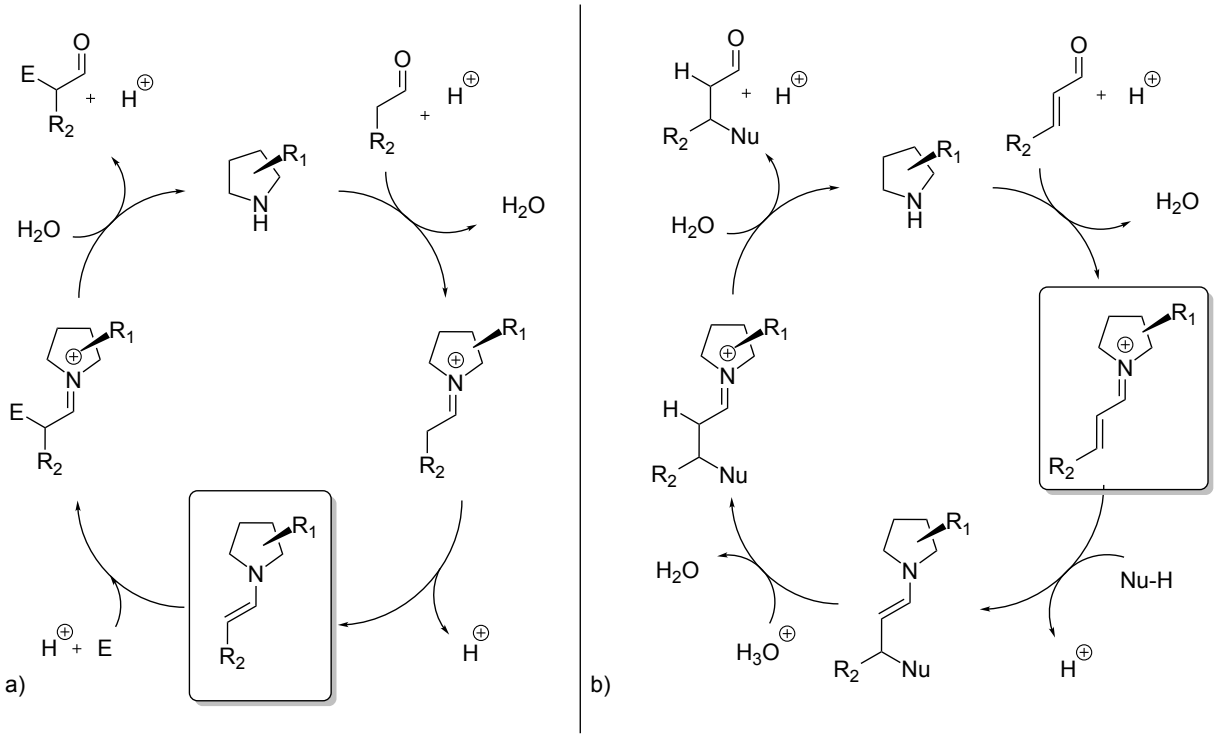

Figure 1.3: a) Enamine activation mechanism; b) Iminium ion activation mechanism. Nielsen, M.; Worgull, D.; Zweifel, T.; Gschwend, B.; Bertelsen, S.; Jørgensen, K. A. *Chem. Commun.* **2011**, 47, 632–649.

anism is most easily depicted in the case of the aldol reaction with the Zimmerman-Traxler model, in which the incoming aldehyde is coordinated to the acid moiety of the catalyst through its carbonyl group (Figure 1.4).[4] In different scenarios where such coordination is not possible or not effective, the carboxylic acid on proline can be substituted with a bulky group, most commonly phenyl, *t*-butyl and 3,5-Bis(trifluoromethyl)phenyl. Steric hindrance blocks attack from one side, enhancing selectivity. In all cases, depending on the initial configuration of proline, either side of the catalyst-substrate complex can be favored/blocked

.

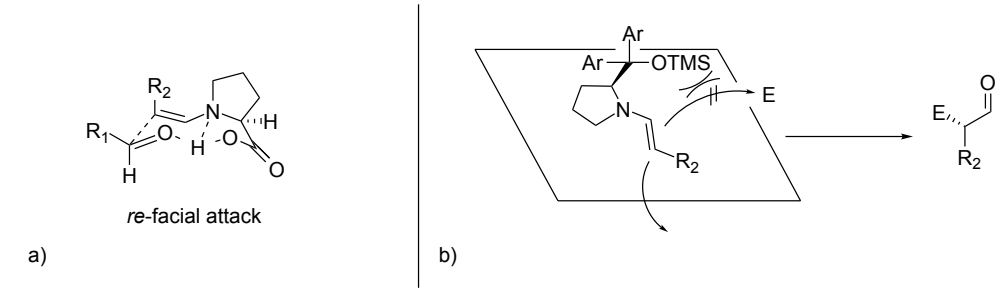

Figure 1.4: a) Zimmerman-Traxler transition state for the coordination-controlled proline-catalyzed aldol reaction; b) rationalization of sterically controlled α-functionalization reactions.

Organocatalysis can be the key to sequential catalysis for several factors. At any moment during the course of the sequential reactions several chemicals are present in the mixture, be it starting materials, intermediates, products and by-products. Enzymes can discern easily the right substrates mostly due to the perfectly fitting configuration of the catalytic site. In the case of synthetic organocatalysts this ability can be obtained by careful choice of the coordinating/sterically hindering substituents on the 1 and 5 positions of the proline ring (Figure 1.5).

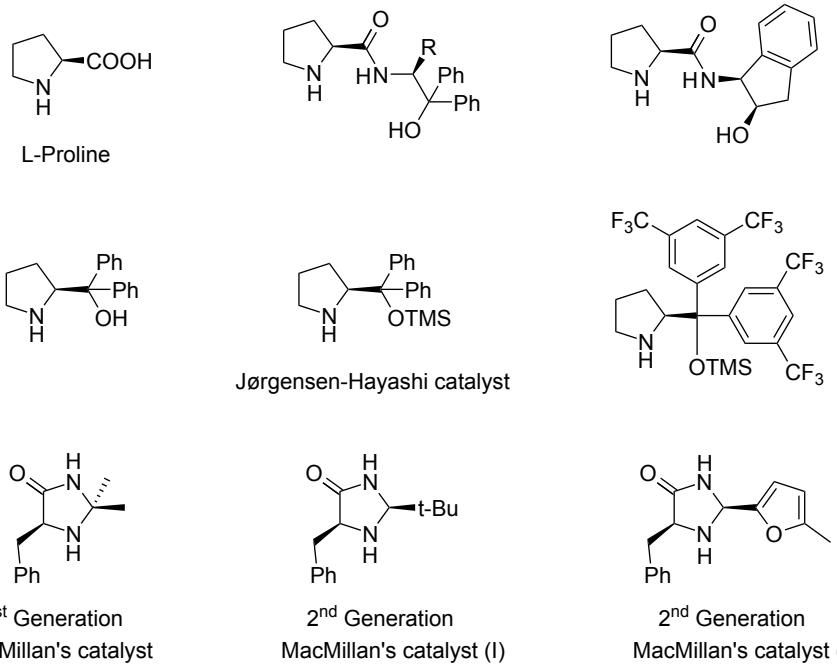

Figure 1.5: Most common organocatalysts based on proline-like structures and oxazolidinones.

In addition to the selectivity and the customization properties, secondary amine organocatalysts are particularly fit for "sequential catalysis", for they can operate via two different mechanisms, as previously explained, carrying out two or even three stereoselective reactions in rapid sequence. A very elegant case where this strategy was used is in the development of the synthesis of α-Tocopherol (Figure 1.6).[8]

The enamine-iminium ion sequence here was successfully employed in order to produce the right configuration of the quaternary stereocenter via formation of a rigid tricyclic structure partially disassembled in the later steps of the the total synthesis. Several more examples of sequential enamine-iminium ion, iminium ion/enamine, and other sequences have been reported. An extensive review on the subject is available.[9]

Within the broad concept of "sequential catalysis" there are a range of different processes.

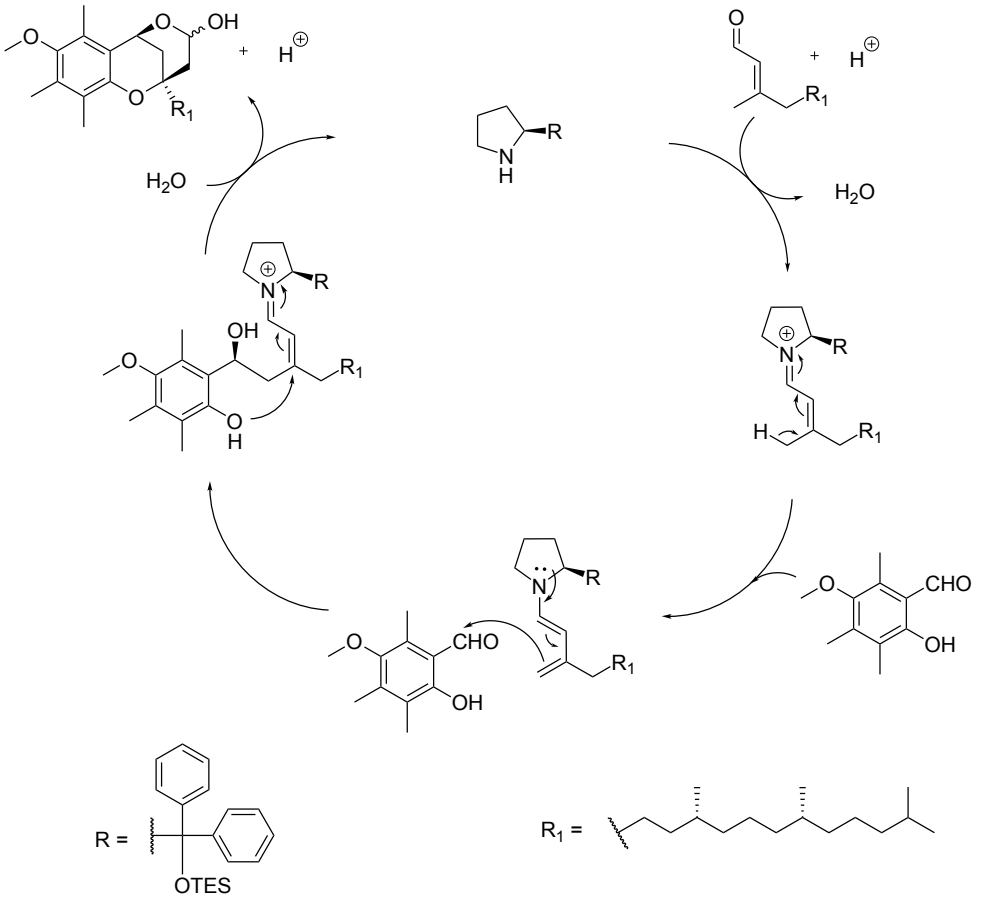

Figure 1.6: Organocatalyzed cascade employed in the synthesis of α-Tocopherol.[8]

The most common definitions are the following:

Cascade (Domino) The definition provided by Tietze in 1996 is that of "*two or more bond-forming transformations which take place under the same reaction conditions, without adding additional reagents and catalysts, and in which the subsequent reactions result as a consequence of the functionality formed in the previous step*".[10] An early example of domino reaction was reported in 1998 by Terashima with a Michael addition/aldol reaction sequence. After the amine-catalyzed Michael reaction occurred selectively, the aldol reactions follows up immediately (Figure 1.7).[11]

Tandem In this category fall the sequences composed by well distinct chemical processes, which may or may not be orthogonal or externally assisted during the course of the sequence, but are fundamentally discrete. It is most common that intermediates in tandem reactions are isolable, and in some cases it is even possible to operate the single reactions in a step-wise fashion.[12] Three examples of tandem reactions will be later described in section 1.5.2.

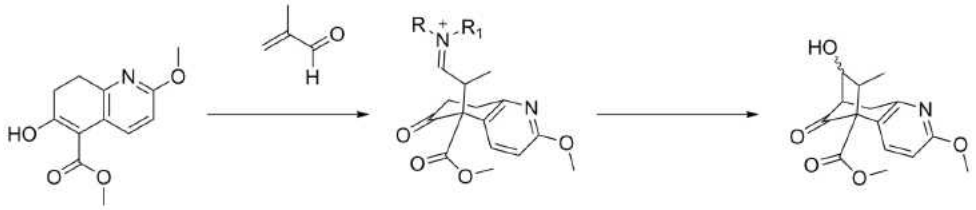

Figure 1.7: Amine-catalyzed cascade Michael addition, followed by aldol reaction.

1.2 The need for multiple catalysts

The categories of organocatalysts discussed so far (Figure 1.5) are characterized by high levels of stereocontrol. Average values reported in literature range from 60% to 90% enantiomeric excess. Optimization of reaction conditions improves these values up to virtually pure products in most cases (99% e.e.).[13] This is also the case in sequential organocatalytic reactions, which usually proceed with high selectivity toward one major isomer out of many possible combinations: depending on the number of steps (n) included in the cascade, a maximum of 2^n isomers are possible, but usually only one or two main isomers are formed.[14] This implies that, regardless of the number of steps involved in the cascade reaction, no more than the two main enantiomers are viable products, that is the enantiomers obtained with either configuration of the chiral catalyst (Figure 1.8).

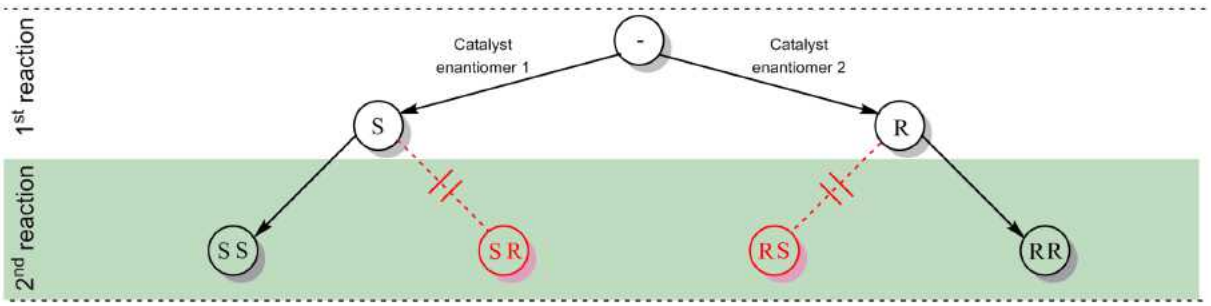

Figure 1.8: Stereochemical limitations of sequential catalysis by the use of a single chiral catalyst for multiple reactions.

The cascade reaction developed by Enders in 2006 is an excellent example of sequential reaction heavily limited by the use of a single catalyst (Figure 1.9).[15] In this case the cascade features three organocatalyzed reactions, all based on enamine or iminium ion activation by catalyst **1**: the preliminary formation of a chiral enamine activates a linear aldehyde towards Michael addition to an α,β-unsaturated alkene; formation of an iminium ion with an α,β-unsaturated aldehyde enables the second conjugate addition and generates a reactive enamine. Aldol condensation and subsequent hydrolysis close the catalytic cycle. The final product of the cascade is a highly substituted six-membered ring with

four new stereocenters. In case of achiral synthesis, the final mixture could contain 16 different isomers. The presence of the organocatalyst heavily reduces the number of isomers formed in the reaction to two diastereoisomers (minimum d.e. experimentally observed is approximately 4:1); inversion of the catalyst's stereoconfiguration can yield their two enantiomers. Without a second catalyst or an otherwise different source of stereogenicity, none of the remaining 12 isomers can be achieved.

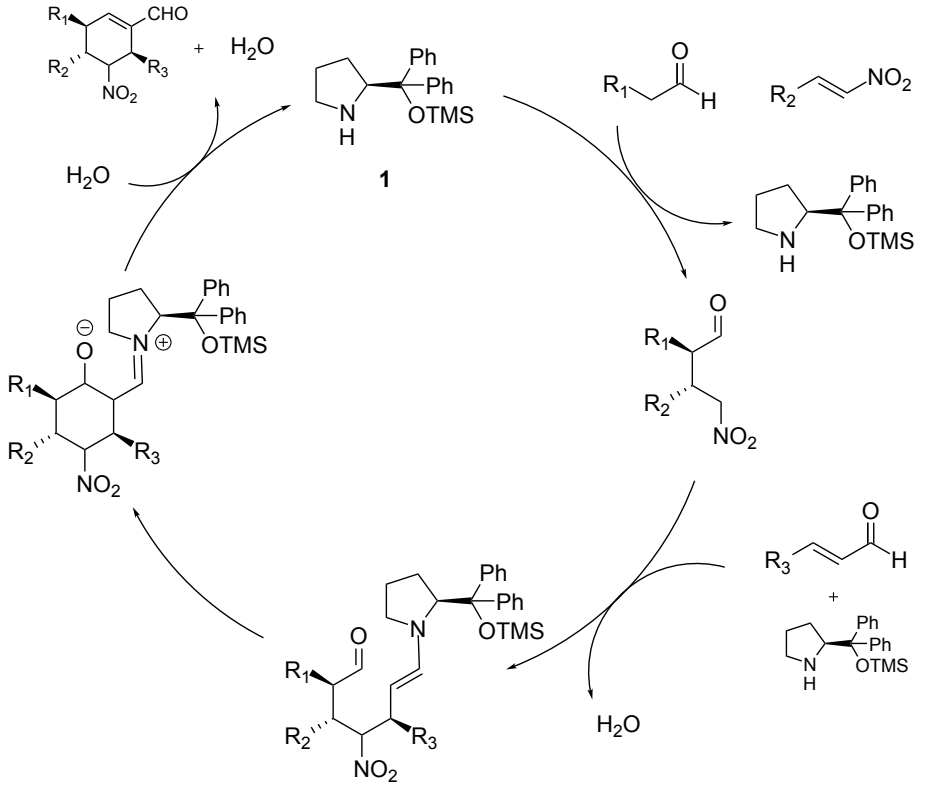

Figure 1.9: Ender's cascade. Enders, D.; Hüttl, M. R. M.; Grondal, C.; Raabe, G. *Nature* **2006**, 441, 861–863.

To expand the scope of cascade or tandem reactions, and retain sequentiality in the process, the most obvious approach is the combination of multiple chiral catalysts, operative in the same reaction conditions, but active only in a single step of the entire cascade. This strategy has already been employed with remarkable success in a variety of original syntheses, as well as in the production of complex bioactive molecules.[9]

Combination of multiple catalysts can achieve far more elaborate results than the simple "unification" of different chemical processes. The one-pot combination of multiple catalysts can lead to a variety of activation pathways which are normally unattainable by the means of single-catalyst chemistry. Pretty much like multiple enzymes can form enzymatic complexes active toward a single reaction, organocatalysts can be combined with a variety

of other known catalysts, such as other organocatalysts, metallic catalysts and Lewis acids. Combination of several catalysts in a single catalytic process can lead to the four different types of catalysis: cascade, double-activation, synergistic and bifunctional (Figure 1.10):[16]

- cascade catalysis was discussed in section 1.1; when multiple catalysts are used, separate steps of the cascade are carried out by different catalysts.

- double-activation catalysis involves the activation of the substrate by two different catalysts in a single step; once activated, the substrate proceeds towards its chemical transformation;

- synergistic catalysis bears some resemblance to double-activation in that both catalysts operate during the same step; the difference lies in the fact that each catalyst activates a different substrate, which in turn can react with each other.

- bifunctional catalysis occurs when the same catalyst activates the substrates at the same time using two different catalytic sites.

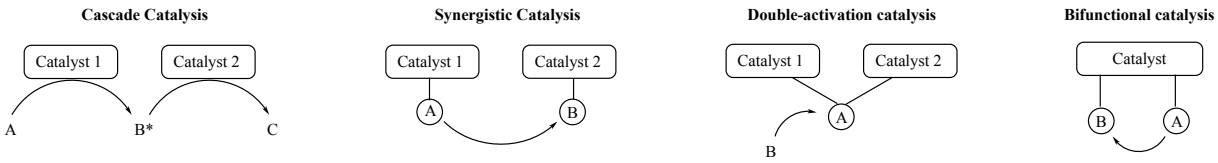

Figure 1.10: Multiple catalysis classification.

A good example of synergistic catalysis is the combination of proline-mediated activation of carbonyls and Palladium-mediated activation of allylic alcohols, reported by Breit's group in 2009 (Figure 1.11).[17] Proline activation of a carbonyl generates a nucleophilic enamine, as discussed previously (Section 1.1), while palladium activation of an allylic alcohol generates a reactive electrophile. The double activation proceeds smoothly to afford the final 1,2-addition product in high yield. Many similar activation mechanism are known for combinations of organocatalysts and organometallic catalysts, and several reviews have been written on the subject.[16,18–20]

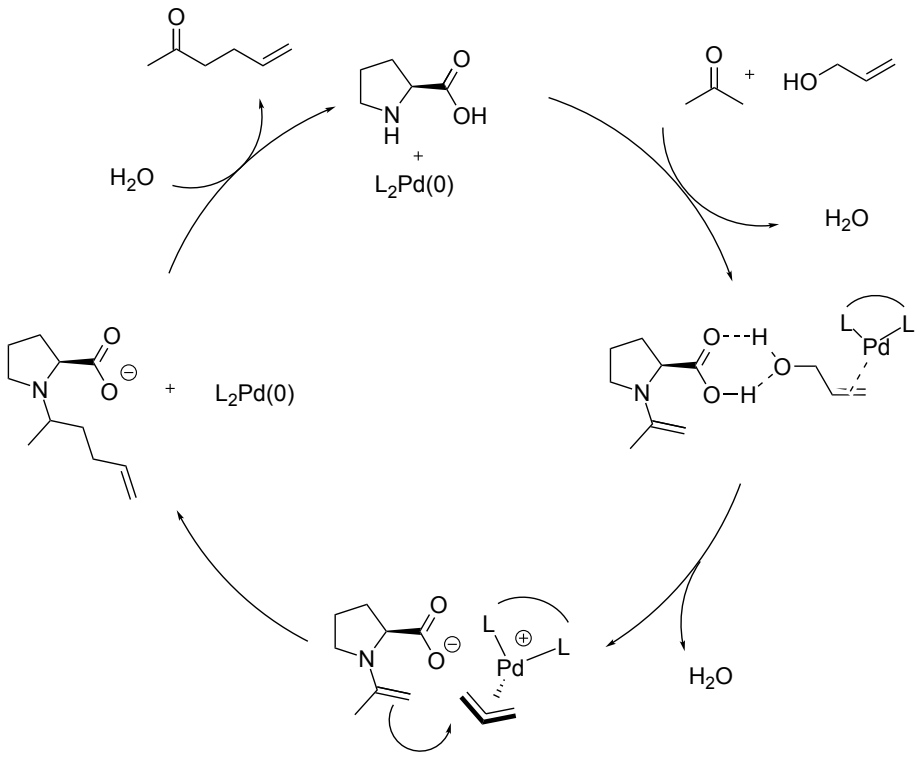

Figure 1.11: Synergistic catalysis. Usui, I.; Schmidt, S.; Breit, B. *Organic letters* **2009**, 11, 1453–1456.

1.3 Getting things together: adding polymers to the mix

Sequential catalysis, while good on paper, is far more troublesome and subject to constraints when attempted in reality. The largest limitation is clearly the compatibilty of all the reagents required. In homogeneous conditions the entire sequence is always a non-compartmentalized one-pot procedure, and will therefore have a unique solvent, pH, concentration, temperature, etc. Ideally, in the complex mixture of reagents, any component should be chemically inert until activated by the catalyst, and even then, the activated substrate should only react with another single chemical specie present. Every catalyst-substrate complex formed must be highly chemioselective. Ender's cascade achieves this type of selectivity by careful planning of the reagents.[15] Correct chemioselectivity during the initial Michael addition of the aliphatic aldehyde is ensued by the use of a very reactive α,β-unsaturated nitroalkene. If a less reactive electrophile is used, competition arises between the new reagent and the α,β-unsaturated aldehyde. While very efficient in the outcome, this strategy is clearly of limited scope, imposing a strong constrain on the range of the viable chemicals, and therefore narrowing down the range of possible products.

Fréchet and co-workers have addressed the problem in a study on the multi-catalytic cascade

reaction shown in figure 1.12.[21] The cascade involves an iminium-ion catalyzed Michael addition and the consequent enamine catalyzed conjugate addition of MVK. The enamine catalyst **2** is known to be inactive in its iminium-ion form for this type of reaction; reversely the iminium catalyst **3** is only active in its iminium-ion form, and thus requires acidic conditions. No intermediate pH conditions exist in this particular case to allow both catalytic cycles to operate. Using polymer-supported versions of each catalyst on non-interpenetrating star-polymers it is possible to create separate reaction environments capable of operating both activation mechanisms one-pot, but effectively separating the incompatible species. The large styrenic star-polymers are also easily recovered with filtration and can be recycled. Interestingly, exchange of either polymer-supported catalyst with its homogeneous analog yields little or no product at all, proving that physical separation of the "microreactors" is necessary for a successful outcome of the cascade. Proof that a closed polymeric-matrix is necessary, such as that of a star-polymer, was provided by testing the same cascade using linear polymers instead of star-polymers. Linear catalytic polymers in solution did not afford the product, proving that catalyst reactivity is lost unless direct interaction of the iminium-ion and enamine are completely inhibited.

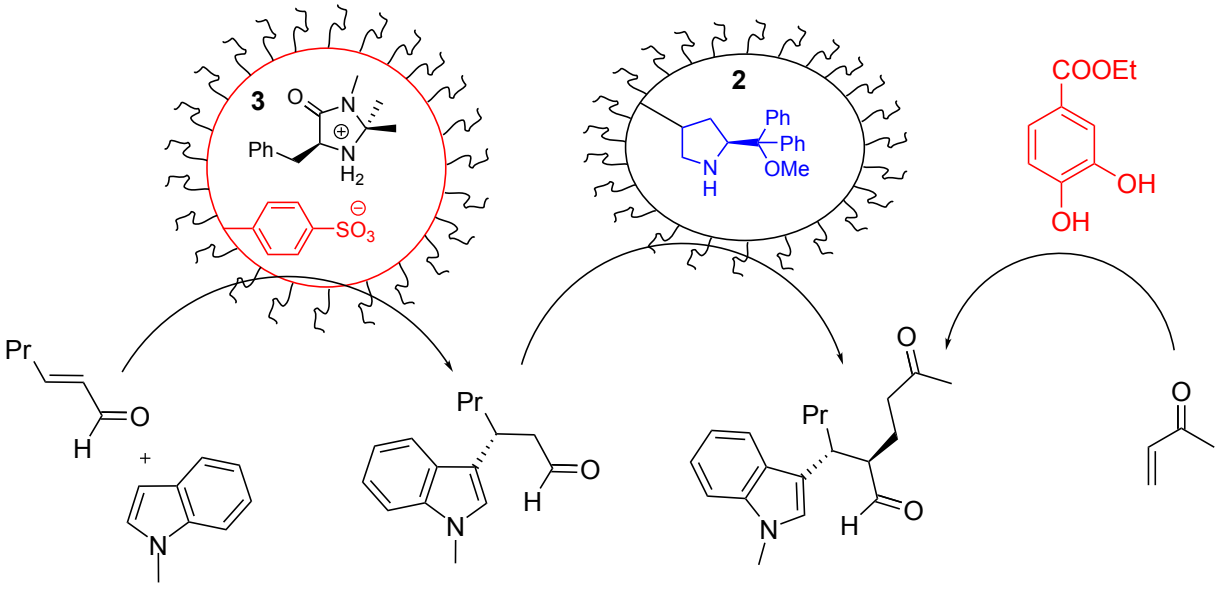

Figure 1.12: Two-catalyst cascade on polymer support. Red highlights acidic species, blue basic ones. Chi, Y.; Scroggins, S. T.; Fréchet, J. M. J. *J. Am. Chem. Soc.* **2008**, 130, 6322–6323.

Polymer supported catalysts are also known for their ease of use and applicability in flow processes. Flow processes constitute a major interest for industrial application due to several features. Most obviously, work up is reduced sensibly for flow processes, as most of the catalysts are immobilized in the reactor matrix. The conditions for the reaction are

also much easier to control in comparison with batch processing, which in turn leads to a better implementation of automated procedures for large scale synthesis of chemicals. It was also observed that reagents immobilized within flow reactors are much less subjected to deterioration, making flow processes an ideal candidate for reactions using expensive and/or sensitive catalysts. Depending on the reaction speed, the chemicals may be left to reside inside the reactor for prolonged amounts of time, or simply recycled through the same reactor. In case of straightforward purification of the product from the starting materials, recycling of starting materials through the same reactor is possible, as a crude mean to improve yields.[22]

Combining sequential reactivity to flow processing opens the way to large scale combinatorial synthesis, and therefore to the expeditious synthesis of a large number of analogues for high throughput screening. A single flow reactor containing multiple catalysts is able to achieve a two, three or more step sequence in short times, and the reactor can be quickly reused with a different combination of reagents. The flow reactor can therefore provide in short times, with little effort, and potentially with the aid of automation, an incredibly large library of small molecules.[23] The potential of cascade reactions in drug discovery can be compared to the exploratory power of multi-component transformations.[24]

1.4 Limitations on polymer support

The restricted mobility of catalysts achieved by polymer immobilization brings, in addition to the positive effect of limiting the interactions with inactivating chemicals, a negative consequence altogether. The physical constrain imposed by the polymeric matrix limits positive and negative interactions equally, and can alter quite sensibly the mechanisms and kinetics of reactions. The limiting power of polymer supports may vary sensibly on a case to case basis, and may affect dramatically yields, enantioselectivities and product ratios. Several examples of reactivity alterations on polymer supports are available for the most common organocatalyzed reactions. In 2008 Varela et al. reported the loss of catalytic activity for the polymer-supported versions of prolinol-based organocatalysts, depending on the number of anchoring sites present on the catalytic molecule (Figure 1.13). It was rationalized that in the case of a single anchoring site reactivity is retained due to the mostly unchanged mobility of the catalyst. Double anchoring site severely limits the catalyst's flexibility, therefore hindering the catalytic mechanism, and rendering the amine inactive.

The chemical nature of the polymers used in this case is styrenic.[25,26]

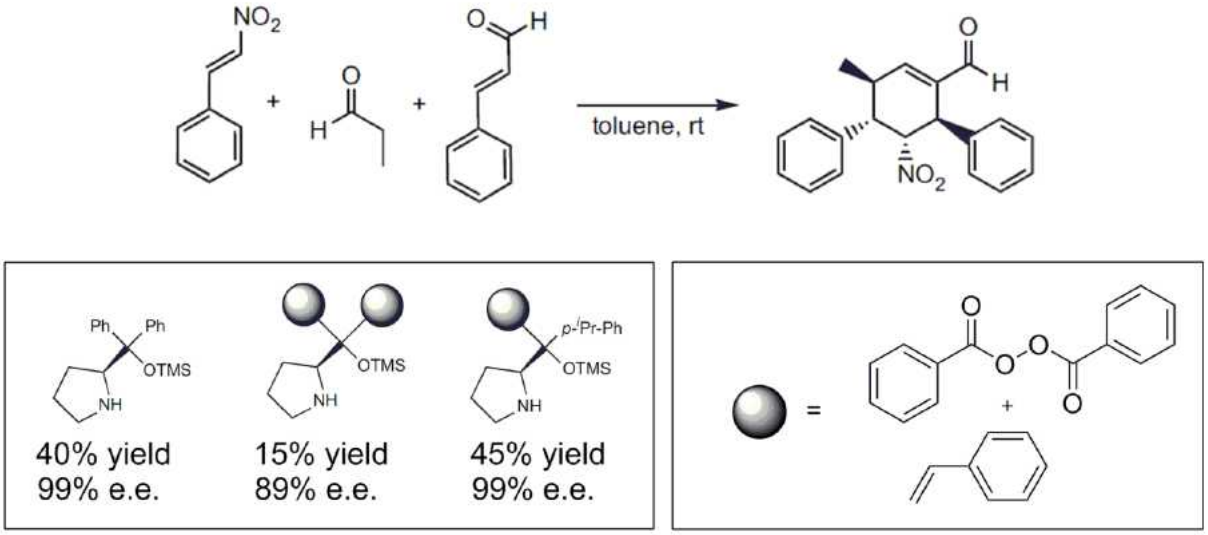

Figure 1.13: Catalytic styrenic polymers activity for pendant and cross-linking catalytic monomers. Varela, M. C.; Dixon, S. M.; Lam, K. S.; Schore, N. E. *Tetrahedron* **2008**, 64, 10087–10090.

Koskinen et al. observed divergent yields in the iminium ion catalyzed Diels-Alder reactions shown in Figure 1.14, as a function of the chemical nature of the polymer support. JandaJel^{TM}-based polymer beads produce the final Diels-Alder adduct in a mere 30% yield, while silica supported analogues achieved yield in the range of 80%. The scenario reverts when a different combination of reagents is used, showing a less active silica-supported iminium-ion catalyst, and a far more efficient styrene-supported one.[27] Additional reports by Benaglia et al. investigated the impact of a PEG-based polymer matrix on catalyst activity. The polymer supported versions in this case behave equally well to the unsupported catalyst in terms of stereoselectivity, but sensibly poorer in terms of yield.[28] It should be noted that the two studies took advantage of two different anchoring sites on the same catalyst.

1.5 Scope of the thesis

In this work the variations in the reactivity profile of multiple organic/organometallic catalysts immobilized on cross-linked polymer beads is studied. Multiple catalysts are studied in relation to sequential synthesis of small organic molecules, either via cascade or tandem catalysis. Based on previous literature knowledge, the research focused on the divergences between the catalytic activity of polymer beads bearing a single catalyst (from now on Single catalyst polymers), or two different catalysts (from now on Double

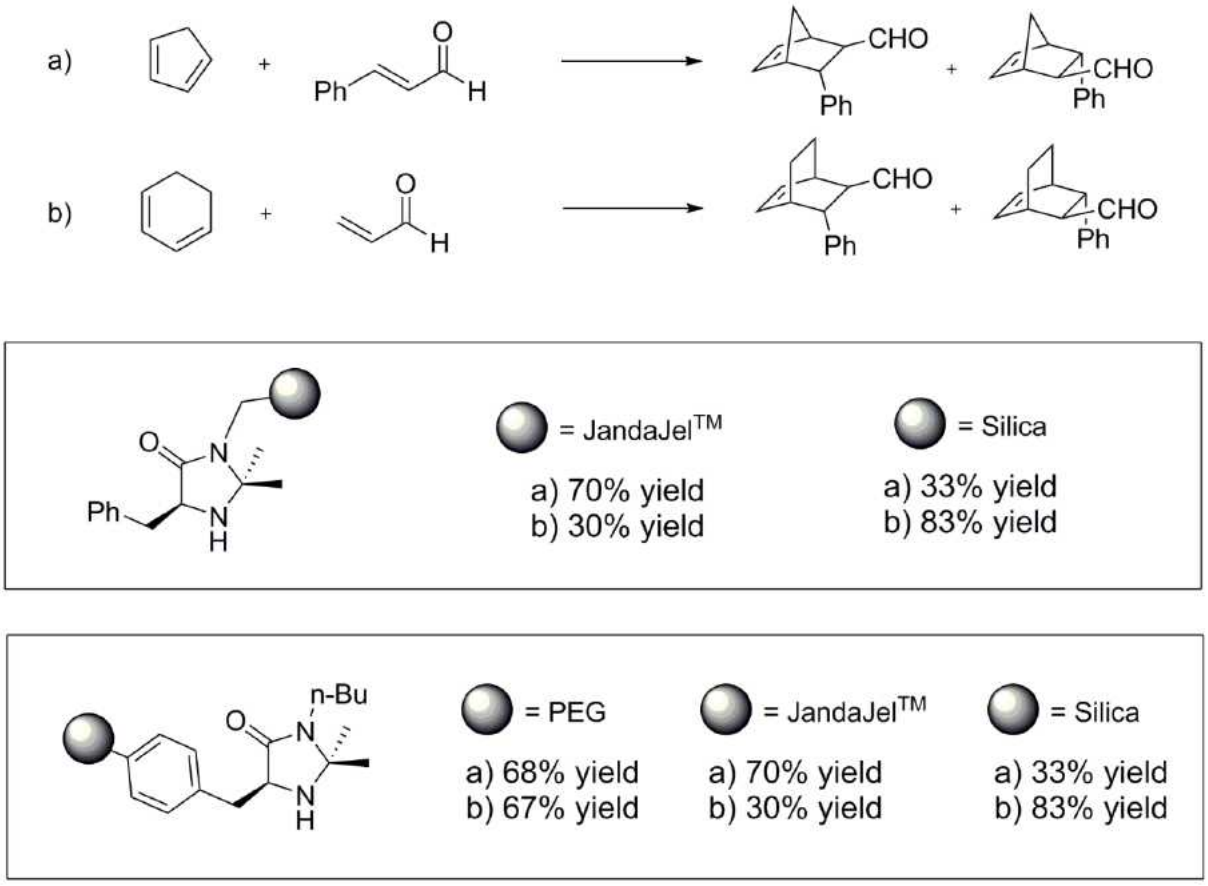

Figure 1.14: Catalytic efficiency study on JandaJel, PEG, and silica supported organocatalysts.

catalyst polymer). To provide an estimate of the reactivity profiles, mix of single catalyst polymers, non polymer-supported catalysts and double catalyst polymers were tested in one-pot procedures, and the outcome of the reactions was compared. The study mostly focused on the secondary amine catalysts **1**, **3** and **4** shown in figure 1.15, and the organometallic catalyst **5**. The choice was dictated by previous studies started on the subject,[29–32] the large interest existing on combination of these largely used catalysts in a single sequence,[33] as well as combination of different categories of catalysis which take advantage from the high stereocontrol arising from asymmetric organocatalysis.[16,18,19]

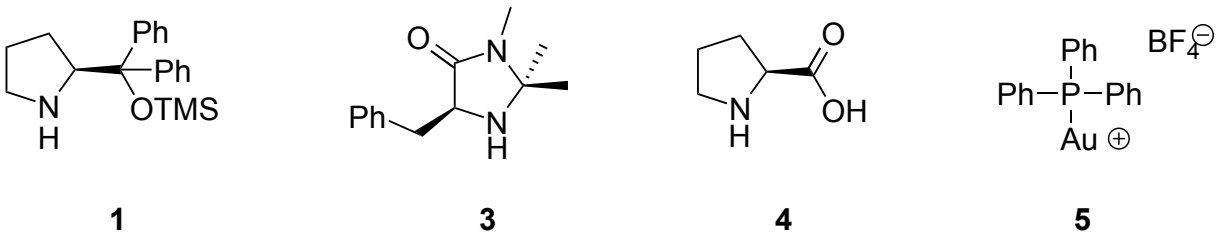

1 **3** **4** **5**

Figure 1.15: Jørgensen-Hayashi catalyst **1**, first generation MacMillan catalyst **3**, L-proline **4** and triphenylphosphino gold(I) tetrafluoroborate **5**.

More detailed discussions are available in the following sections regarding the choice of polymeric matrix (Section 1.5.1) and the choice of the benchmark reaction (Section 1.5.2), including an overview of the four reactions examined.

Double catalyst polymers can be determining factors in the attempt to achieve longer, more efficient, sequential reactions. Extending the concept described by Fréchet of non-interpenetrating reaction environments, it should be possible to include several compatible steps in a single polymer bead, and therefore achieve a mix of many different polymer beads, which in complex, are able to carry out a "sequence of sequences" (see Figure 1.16).

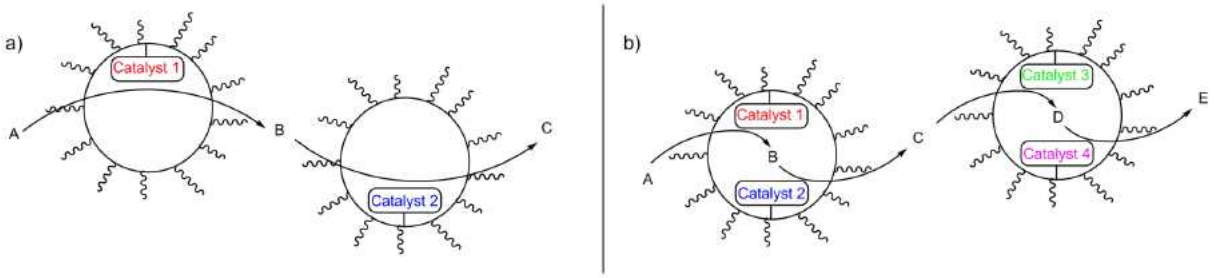

Figure 1.16: a) Schematic representation of mixed single catalyst polymers. b) schematic representation of mixed double catalytic polymers.

1.5.1 The polymeric network

The choice of the the polymer matrix is dictated by chemical compatibilty. The most common supports for chemically active polymers are styrenic due to their chemical inertness and mechanical resistance. Previous works in our group however pointed out how methacrylic polymers can be equally promising in organocatalysis, the main difference being the different range of solvent compatibility and largely different swelling properties, in exchange for a decreased chemical inertness in strong acidic and basic conditions. This is not an issue, as organocatalyzed reactions studied in this work are carried out only in mildly acidic or basic pH. Good solvent compatibilty and swelling however are fundamental conditions to achieve a large surface-to-volume ratio and further improve the catalytic activity. To continue the previous research trend this work focused on methacrylic polymers, or hybrid methacrylic-styrenic polymers.[32]

The degree of cross-linking plays a large role on the polymer reactivity. A large degree of cross-linking yields a very tight and stiff polymeric network within the beads, lowering the surface-to-volume ratio, swelling volume, and reducing the number of active catalytic sites

on the surface. On the other hand a small degree of cross-linking will produce weakly bond polymer chains, with very high swelling properties but low mechanical resistance. In this work it is highly desirable to produce a polymer bead largely capable of swelling and with a high surface-to-volume ratio. The typical amount of cross-linker used for this purpose is 2 wt.% of all other monomers.[34,35] Very tight networks (higher amount of cross-linker) are not of our interest, since steric hindrance from the polymer may affect the catalytic mechanisms.

The polymerization was carried out by free-radical polymerization in emulsion. This procedure has already been used in our group to produce polymeric beads carrying a single type of organocatalyst, affording beads of very similar dimensions (in the order of the tenth of millimeter). Narrow bead size distribution is desirable in this work, because it affects the speed at which the reagents diffuse inside and outside of the beads.[34,35] When multiple catalysts are immobilized with this synthetic protocol, a random distribution of the catalytic groups along the polymer's chains is produced, resembling the random distribution of the catalysts in homogenous conditions.

In the case of functional polymers, such as catalyst-bearing polymers, there is the possibility of choosing between a post-modification approach and a bottom-up approach. In the case of post-modification a pre-made polymer bearing functional groups on some of its monomers is reacted with the molecule which is to be immobilized; alternatively the entire synthesis of such functionality is carried out on the polymer. A very famous example of post-modified polymer is the Merrifield resin (Figure 1.17). The resin is initially polymerized using a mix of monomers very susceptible to later modification, such as containing chlorinated benzylic positions (highly electrophilic). After polymerization of the resin, the bulk material is exposed to the post-modification reagent. In the case of the Merrifield resin an N-capped amino acid will substitute the chlorine atom on the benzylic position. Post-modification occurs quantitatively on all reactive sites present on the polymer only for highly reactive groups used in large excess, and in most cases requires several identical post-modification reactions to cover all the available surface. This approach is useful for its immediacy and economy, but is unsuitable when costly reagents must be used.[34,35]

The bottom-up approach follows a completely different pathway to obtain the same result of a post-modification synthesis (Figure 1.17). The beginning of the synthesis involves the complete construction of the functional monomers. After this is complete, the mix of catalytic monomers is polymerized. In this way the composition of the reactive groups on the polymer

is exactly known, especially when several reactions are required in order to build the right functionalities on the catalyst. It is also convenient when the immobilized functionalities must have a known and exact loading, which can be controlled by the stoichiometric amount of reagents used during polymerization. It is also typical that nearly all catalytic monomers used in the bottom-up polymerization will be included in the final polymeric product.[34,35] For the case discussed in this thesis the bottom-up approach is clearly better fitted to make double catalyst polymers. Unlike the post-modification strategy, it is possible to create polymer beads with exact loadings and relative ratios between the different catalysts immobilized. The bottom-up approach will therefore be the main strategy discussed in this thesis.

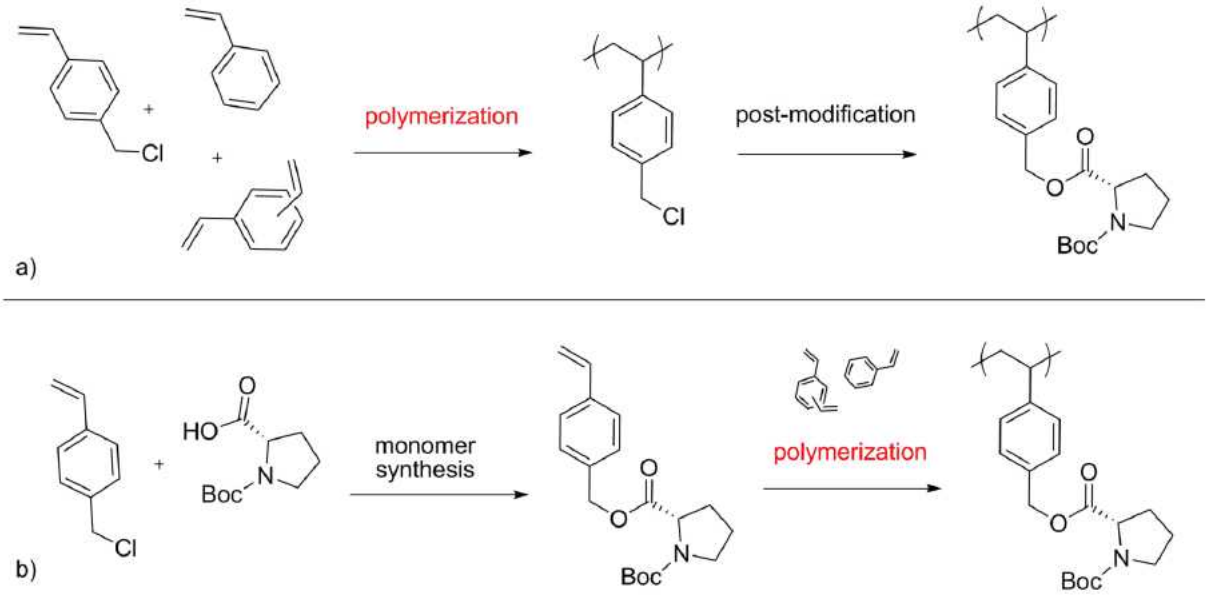

Figure 1.17: a) example of post-modification synthesis. b) example of bottom-up synthesis.

1.5.2 The benchmark reaction

To test the potential of double catalyst polymers, the benchmark reaction adopted must fulfill certain requirements. First of all the catalysis mechanism must not be synergistic. It was discussed in section 1.4 how the use of polymer supports drastically reduces catalyst mobility. To expect a synergistic mechanism to proceed unhindered, in absence of a dedicated strategy, would be an exceedingly optimistic assumption. Sufficient knowledge of the reaction's mechanism should be available or easily inferred, in order to avoid selection of an impossible catalytic mechanism. The second criterion for the choice of a benchmark reaction is the contextualization within the ongoing research on polymer-supported organocatalysis. A

large number of studies from the last decade focused on the highly stereoselective chiral secondary amines derived from proline. Most discoveries on the subject have already found many application in organic chemistry, and more recently in sequential catalysis, the major interest being catalysts **1** and **3**. This work will therefore focus mostly on these classes of catalysts, namely prolinol ethers and imidazolidinones.

A secondary criterion in the benchmark reaction choice is the compatibilty between reaction conditions and polymeric matrix.

The following four reactions were selected as benchmark reactions in the present study.

Benchmark reaction 1

Three step modified cascade: 1,2-addition, 1,4-addition, aldol condensation

The first organocatalytic cascade attempted is the cascade reaction developed by Enders et al. in 2006.[15] The cascade relies exclusively on catalyst **1** to achieve a sequence of two intermolecular conjugate additions and a final aldol condensation (Figure 1.9). As discussed in section 1.2 the cascade is limited in its outcome to two main products and two side products, out of a total of 16 potential isomers. Multiple catalysis can improve the flexibility of the cascade tuning the stereochemistry at intermediate steps.

Between the first and second step we know that the enamine catalyst must detach from its first product to activate the α,β-unsaturated aldehyde in the iminium-ion catalyzed step. Catalyst **3**, however is known to have a much higher activity in its iminium-ion form than catalyst **1**. Mixing the two catalyst should then lead to a combination of two catalytic cycles, increasing the tunability of the cascade and extending its scope (Figure 1.18).

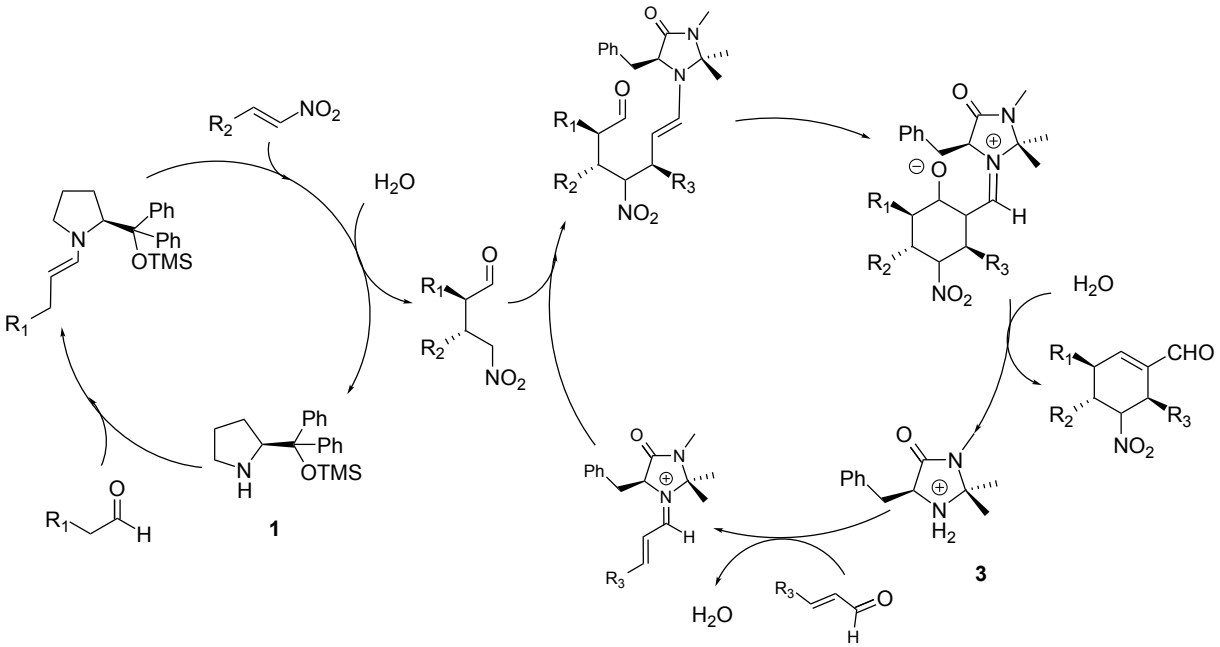

Figure 1.18: Double-catalyst Ender's cascade.

Benchmark reaction 2

Two step tandem: 1,4-addition, 1,2-addition

The second organocatalytic tandem reaction attempted was developed by MacMillan's group and further improved by Fréchet et al.[21,36] The reaction requires a combination of MacMillan's catalyst **3** and L-proline **4**; the former to achieve the 1,4-addition of N-methylpyrrole **6** on the unsaturated aldehyde **7**, the latter to operate the following 1,2-addition of DBAD **8** (Figure 1.19). The same reaction mechanism, albeit with slightly different reagents, was successfully exploited with a variety of unsaturated aldehydes, electrophiles and nucleophiles.[33]

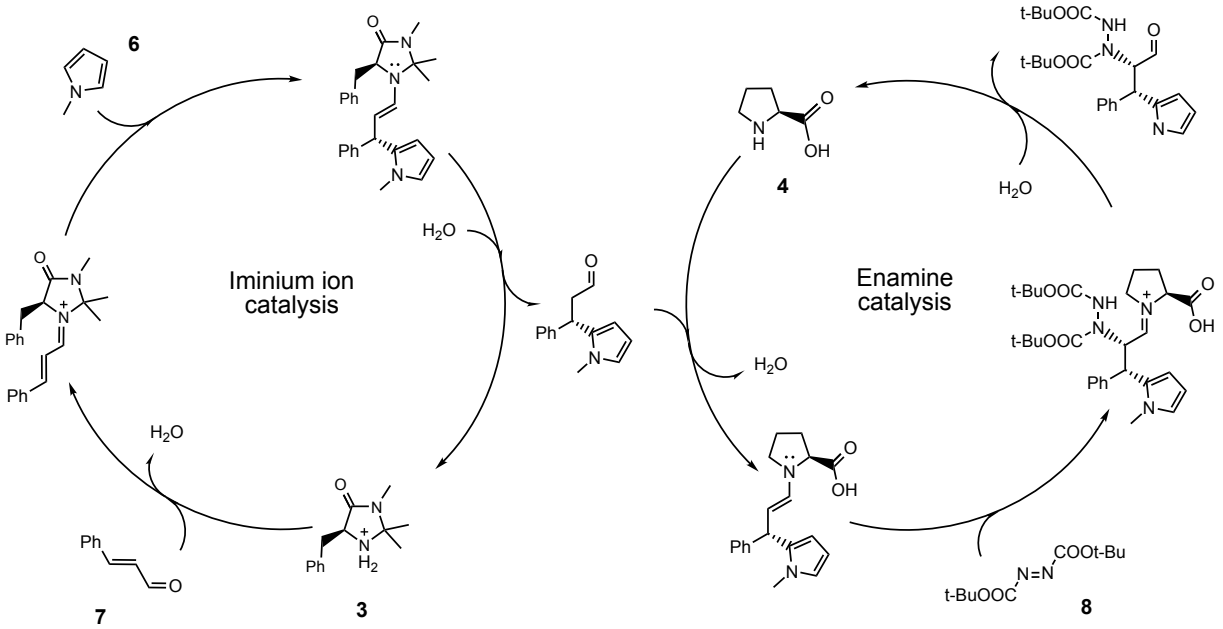

Figure 1.19: Proposed catalytic cycle for the cascade catalysis of a 1,4-addition and a 1,2 addition. In blue the starting material and in red the final product.

In this work a variant of the reported tandem reaction was tested as benchmark reaction with methacrylic-PEG supported versions of **3**.

Benchmark reactions 3 and 4

Two step novel tandem: Diels-Alder, 1,2-addition or aldol reaction

Imidazolidinone **3** received much attention for its high enantioselectivity in Michael additions, but to our knowledge no sequential reactions employing **3** for asymmetric Diels-Alder has been developed yet. As part of the studies on the benchmark reaction for polymer immobilization, a combination of the first generation MacMillan catalyst and a second enamine catalyst is investigated, to develop a simple synthetic protocol for a two-step sequence.

From previous research it is known that the Diels-Alder reactions between cinnamaldehyde and cyclopentadiene to give product **9** are compatible with the methacrylic-PEG polymer matrices.[32] Starting the sequence with a Diels-Alder reaction, the second step employs a different organocatalyst, which can either be the 1,2-addition on the position or an aldol reaction. α-Functionalization and aldol reactions can both be achieved through enamine catalysis, so preferentially employing catalysts **1** or **4**. The same combination of catalysts can therefore be used to carry out different sequences, depending on the reagents present in the mixture (Figure 1.20).

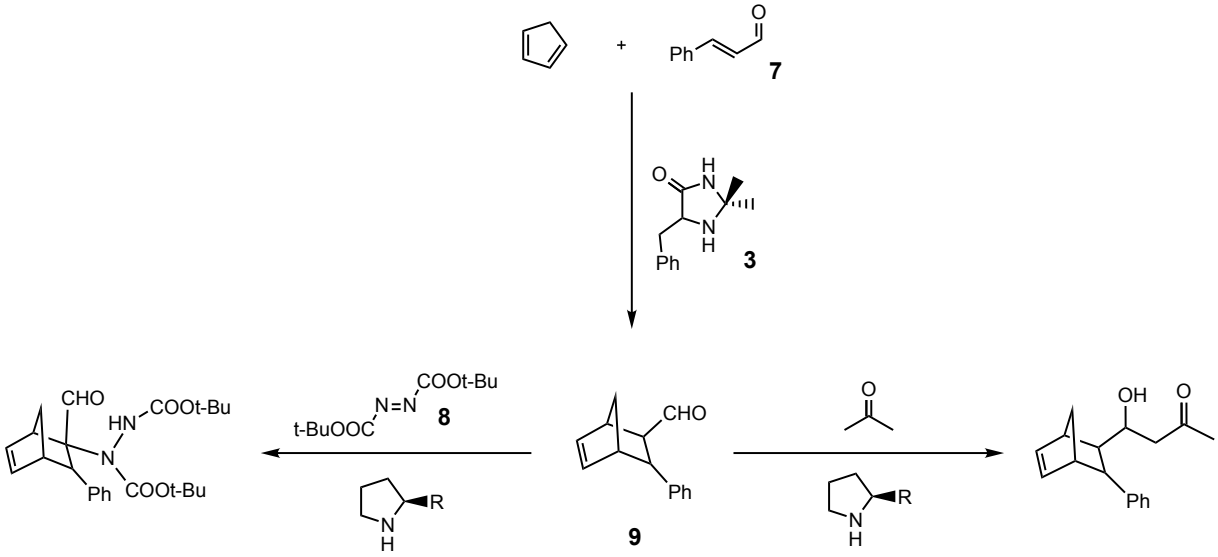

Figure 1.20: Enamine-catalyzed pathways consecutive to Diels-Alder reaction between cyclopentadiene and cinnamaldehyde.

Benchmark reaction 5

Two step organic and organometallic tandem reaction: 1,2-addition, cyclization

The combination of organocatalysis and organometallic catalysis is a recent development in chemistry, and has been extensively reviewed.[16,18,19] Most studies have explored the use of palladium and platinum in combination with typical enamine catalysts, and the mechanisms explored in most cases belong the the category of synergistic catalysis. A combination of metal- and organo- catalysis not relying on synergy was developed by Krause et al.[37] making use of gold(I) catalysts. The reaction sequence in this case includes a first asymmetric conjugate addition between isovaleraldehyde **10** and compound **11**, catalyzed by prolinol ether **1**. The second reaction, tandem-executed, is an intramolecular cyclization catalyzed by gold(I) catalyst **5**. Stereoselectivity in this case is the direct consequence of the configuration achieved during the first step (Figure 1.21).

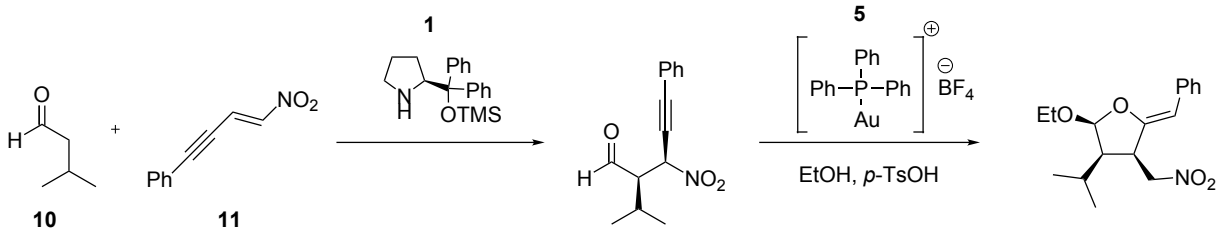

Figure 1.21: Reaction scheme for the enamine and gold (I) catalyzed tandem reaction.

2 Results and discussion

This section covers the detailed discussion of the results observed during the course of this project. Every benchmark reaction is discussed in chronological order. The most significant results for the discussion are reported in this section. For further details on the experimental proceedings see section 4. Polymerization procedures are discussed within the relevant sections.

2.1 Benchmark reaction 1
Three step cascade: 1,2-addition, 1,4-addition, aldol condensation

Ender's cascade reaction is a three step organocatalytic sequence involving two enamine-catalyzed C-C bond forming reactions followed by an iminium-ion-catalyzed aldol condensation (see 1.5.2). In its original publication this cascade employs the same catalyst **1** to activate the substrates in all steps (Figure 2.1).[15]

Catalyst **3** however is known to be a much more effective iminium-ion catalyst in terms of yield towards Michael additions on α,β-unsaturated aldehydes, as compared to catalyst **1**.[38] The incorporation of both amine **1** and oxazolidinone **3** in this cascade may therefore lead to an improvement in the yields observed for the cascade, in addition to the improved customization potential for the entire transformation. It is reckoned that the presence of two different catalyst leads to the selective formation of the most reactive catalyst-substrate complexes, as a direct consequence of the equilibrium between the free catalyst and the catalyst-substrate complex (Figure 2.2).

In this particular case it is expected that catalyst **1**, being the most active enamine catalyst of the pair, will predominantly drive the first reaction to completion. Binding of catalyst **3** to the α,β-unsaturated aldehyde on the other hand should result in a faster enamine-iminium sequence, ultimately causing the predominant completion of the second and third step by action of catalyst **3**.

Recent studies by Blackmond et al. have also pointed out the beneficial role of catalytic

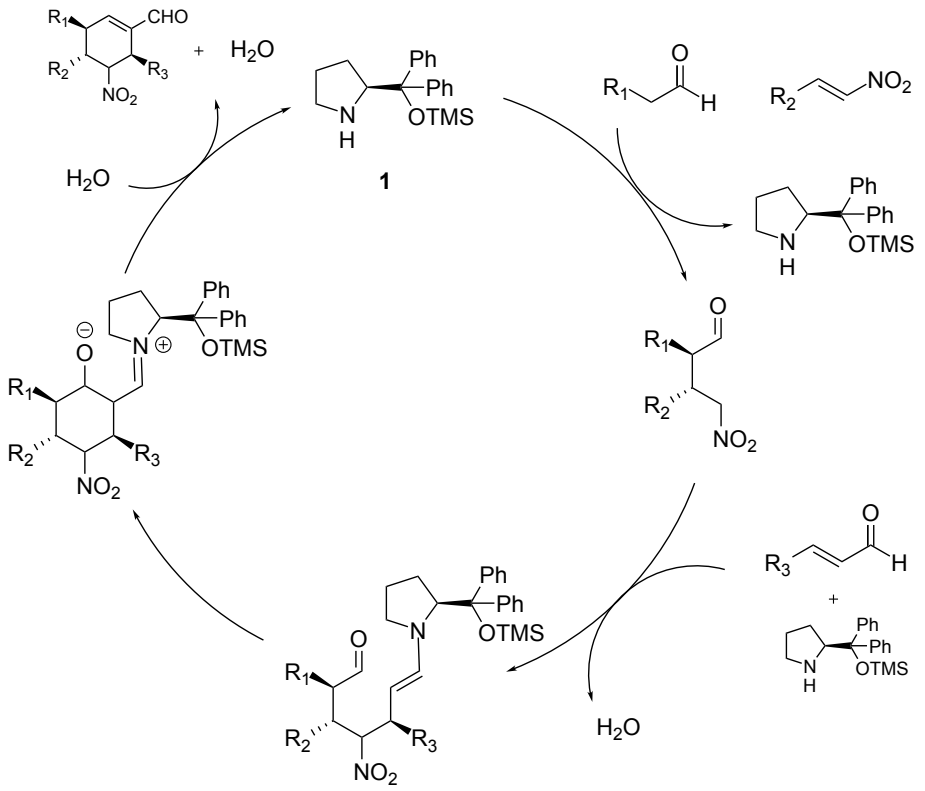

Figure 2.1: Ender's cascade. Enders, D.; Hüttl, M. R. M.; Grondal, C.; Raabe, G. *Nature* **2006**, 441, 861–863.

amounts of acetic acid towards the rate of the first step conjugate addition. Neat reaction conditions and consequent high concentration of reagents further increases the reaction rate.[39] Both these improvements over the standard procedure are much desirable in our context, improving the efficiency of catalyst **1** over **3** in the first step. The same study also reveals the lack of influence from the presence of water on the kinetics for the first step, making the two catalysts even more compatible as **3** requires small amounts of water to ensure complete solvation. In the same study it was pointed out the much larger affinity of **1** to linear aldehydes compared to α,β-unsaturated aldehydes as an additional reason to explain the success of Ender's cascade. All these considerations seem to favor the orthogonal combination of **1** with a much more effective catalyst in the second step of the cascade, such as **3**.

In our first attempt to extend the scope of Ender's cascade the sequence was carried out using a single catalyst (**1**) in neat conditions with catalytic amounts of acetic acid. For this preliminary experiment catalyst **3** was not employed to observe the direct impact of the modified reaction conditions on catalyst **1**. The reagents used were *trans*-cinnamaldehyde **7**, propionaldehyde **12** and *trans*-β-nitrostyrene **13**.

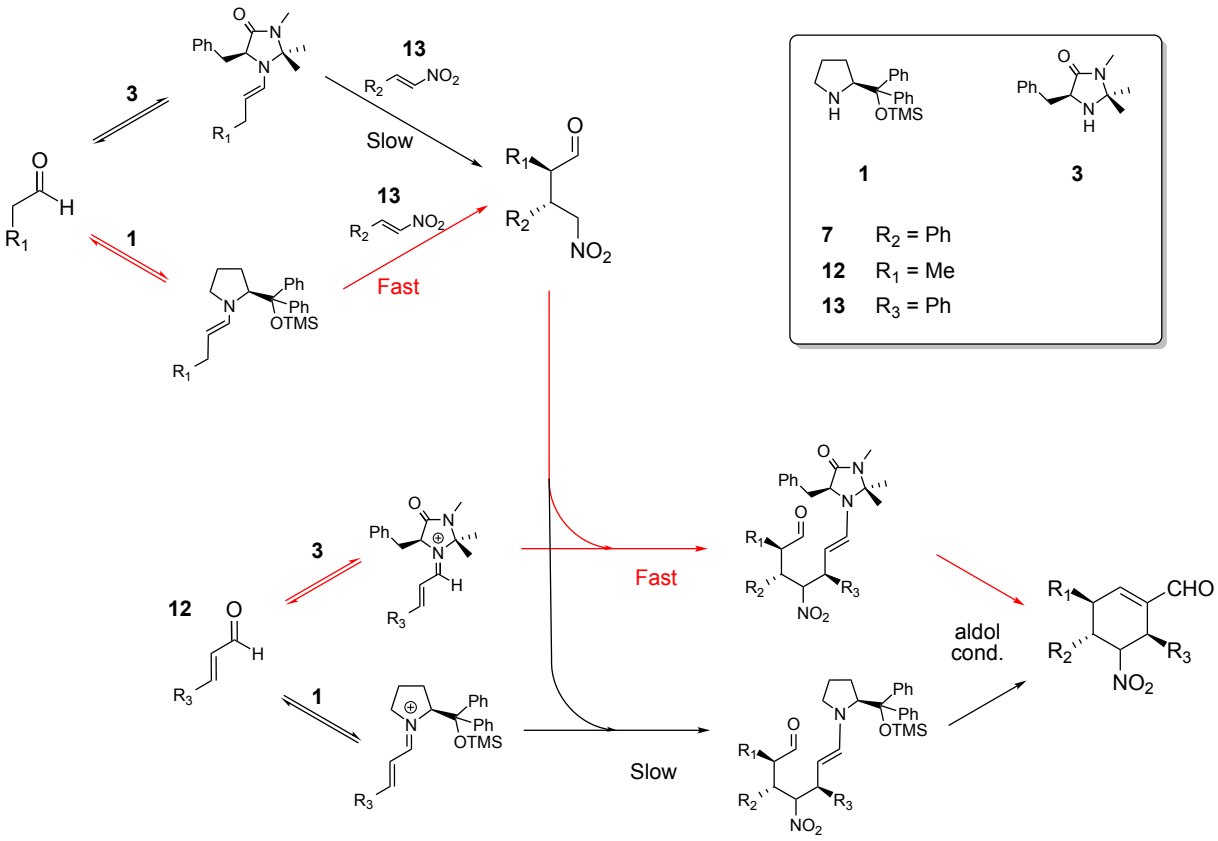

Figure 2.2: Expected kinetics for the double-catalyst Ender's cascade. The favored reaction mechanism is highlighted in red.

Neat and acidic conditions had the most immediate effect of drastically lowering the cascade yield to a disappointing 3%, as opposed to 30% observed in the original reaction conditions (Entry 1 and 2, table 2.1). Intermediate products formed after the first and second step of the cascade could not be observed. From this observation it can be deducted that the new reaction conditions have a detrimental impact on the overall efficiency of catalyst **1**. The lack of any intermediate product is an especially glaring indication of the loss of catalytic activity even in the first step conjugate addition. The following experiments were therefore carried out in the conditions reported in the original paper, using toluene as solvent and without addition of acetic acid.

Even without a protocol to selectively activate catalyst **1** towards the first step, the cascade reaction in presence of **3** was attempted (Entry 3 table 2.1). The yield observed in this case did not sensibly improve from the single-catalyst procedure, suggesting that catalyst **1** operates unaffected in presence of **3** under reported conditions. The combination of the two catalysts in the optimal reaction conditions seems to favor activation by catalyst **1** throughout the entire reaction sequence, spoiling the very point of double catalysis in this

Entry	7 [mmol]	12 [mmol]	13 [mmol]	1 [mol%]	3 [mol%]	Solvent	Yield
1	0.5	0.75	0.6	2	-	neat	3%
2	1	1.5	1.2	20	-	Toluene 1 mL	30%
3	1	1.5	1.2	20	20	Toluene 1 mL	28%[a]

Table 2.1: Reaction conditions and yields for the extended Ender's cascade.

context.

These experiments have shown how the most favorable conditions for the first step of the cascade reaction clearly erode yield values when used for the entire three step cascade (Entry 1 in table 2.1). On the other hand, the optimal conditions for this cascade do not seem to favor the useful inclusion of catalyst **3** in the catalytic cycle in place of **1** (Entry 3 in table 2.1). It was ultimately concluded that this benchmark reaction is unsuitable for the present work.

2.2 Benchmark reaction 2
Two step tandem: 1,4-addition, 1,2-addition

The second tested benchmark reaction is an adaptation of MacMillan's cycle-specific organocascade featuring a second generation MacMillan's catalyst in combination with proline. For an overview of the cascade mechanism refer to section 1.5.2. The sequence has been defined "cycle-specific" due to the selectivity observed for each catalyst toward promotion of only one catalytic cycle.[33] For our preliminary tests it was decided to adapt the first step in the sequence with an alternative combination of electrophile **6** and catalyst **3** (Figure 2.3).

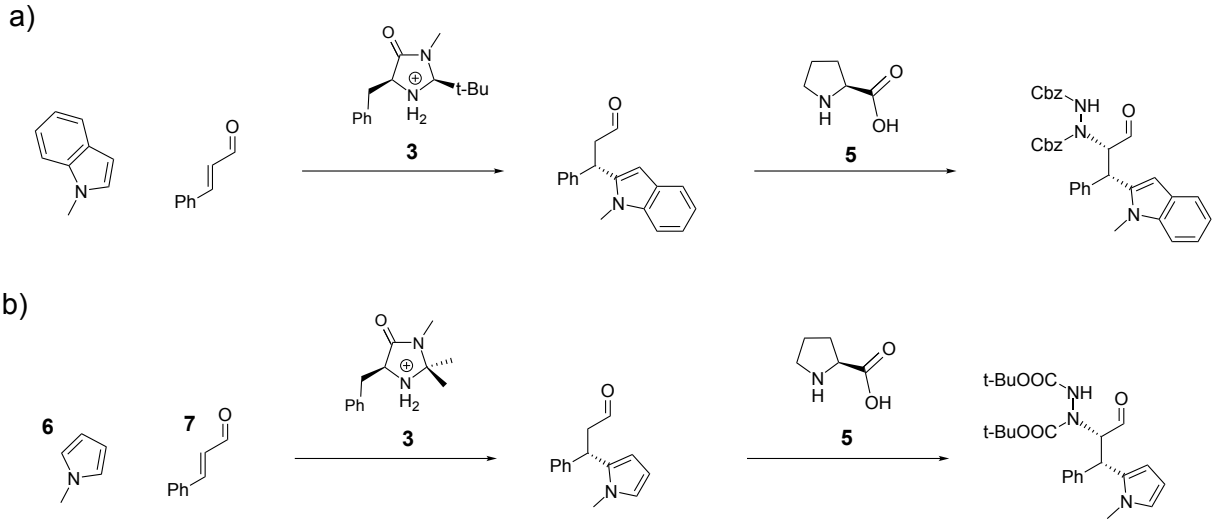

Figure 2.3: a) Reported cycle-specific tandem reaction. Simmons, B.; Walji, A. M.; MacMillan, D. W. C. *Angew. Chem., Int. Ed.* **2009**, 48, 4349–4353. b) Modified cycle-scpific tandem reaction studied in this work.

The 1,4-conjugate addition of N-methylpyrrole with cinnamaldehyde was previously reported by the same group, but it has never been included in any sequential process.[40] The choice for a different combination of catalyst and electrophile for the iminium-assisted step is dictated by the readily availability of polymer-supported analogues of the first generation MacMillan's catalyst, previously prepared in our group.[32]

Initial attempts to reproduce the entire sequence in a lower polarity solvent such as DCM were unsuccessful (Entry 1, table 2.2). However use of a higher polarity solvent mixture as THF/water re-established proper catalyst activity for both 1,2 and 1,4 conjugate additions when executed in step-wise fashion (Entry 2 and 3, table 2.2). Absence of a strongly acidic co-catalyst such as TFA, reported to improve MacMillan's catalyst efficiency, negatively affects the 1,4-conjugate addition reaction, reducing drastically the yield from a reported

Entry	7 [mmol]	6 [mmol]	8 [mmol]	3 [mol%]	4 [mol%]	Solvent	Additive	Yield
1	1	1.2	1.2	10	30	DCM	-	-
2	1	1.2	-	10	-	THF/H_2O 7:1	-	24%
3	-[a]	-	1.5	-	30	THF/H_2O 7:1	-	40%
4	1	1.5	1.4	10	30	THF/H_2O 6:1	-	-[d,e]
5	1	5	-	10[b]	-	THF/H_2O 12:1	TFA	-[e]
6	1	5	-	10[b]	-	THF/H_2O 10:1[c]	TFA	-[e]
7	1	5	-	10[b]	-	THF/H_2O 10:1	-	-[e]
8	1	5	-	10[b]	-	THF/H_2O 10:1	Ac. acid	-[e]

Table 2.2: Yields and mol % are calculated with respect to **7**. **a**) the product from entry 2 was used as starting material; **b**) **14** was used as a catalyst instead of **3**; **c**) 0.5 mL of solvent overall, monitored by ^{1}H-NMR; **d**) 48 h reaction time; **e**) no chromatography was possible due to by-products.

93% to 24%.[40] Proline-catalyzed addition of DBAD to the 1,4-addition product proceeds smoothly yielding the final product in 40% yield (10% overall).

After reactivity in homogeneous conditions was verified in both acidic and neutral media, the one-pot procedure on polymer-support was attempted using already available polymer-supported first-generation MacMillan's catalyst **14**. The polymer support consists of methacrylic beads bearing short PEG chains (8-12 units) compatible with ethers and other highly polar solvents.[32]

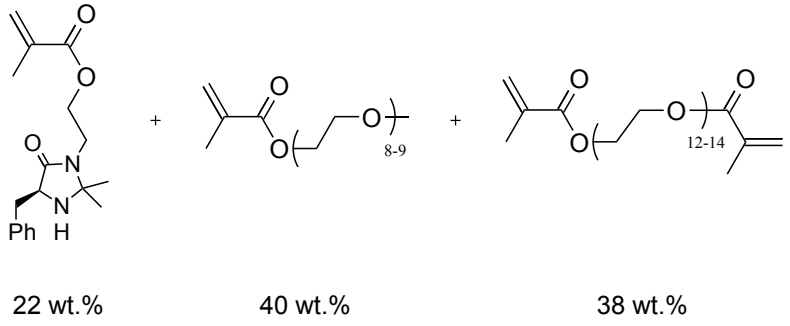

Figure 2.4: Monomer composition of PEG-methacrylic co-polymer supporting MacMillan's catalyst **14**. Kristensen, T. E.; Vestli, K.; Jakobsen, M. G.; Hansen, F. K.; Hansen, T. *J. Org. Chem.* **2010**, 75, 1620–1629.

To our surprise the polymer-supported version of MacMillan's catalyst did not afford any 1,2-addition product even after 48h reaction. Instead a very viscous brown oil was isolated as crude which could not be further purified by flash chromatography due to massive tailing. ^{1}H-NMR of the crude product revealed formation of expected 1,4-addition product, easily verified by the presence of the triplet at 4.49 ppm (Figure 2.5). Its presence however is

also an indication of a failed or minor degree of 1,2-addition. Solvent evaporation was also inefficient due to the high viscosity of the oil.

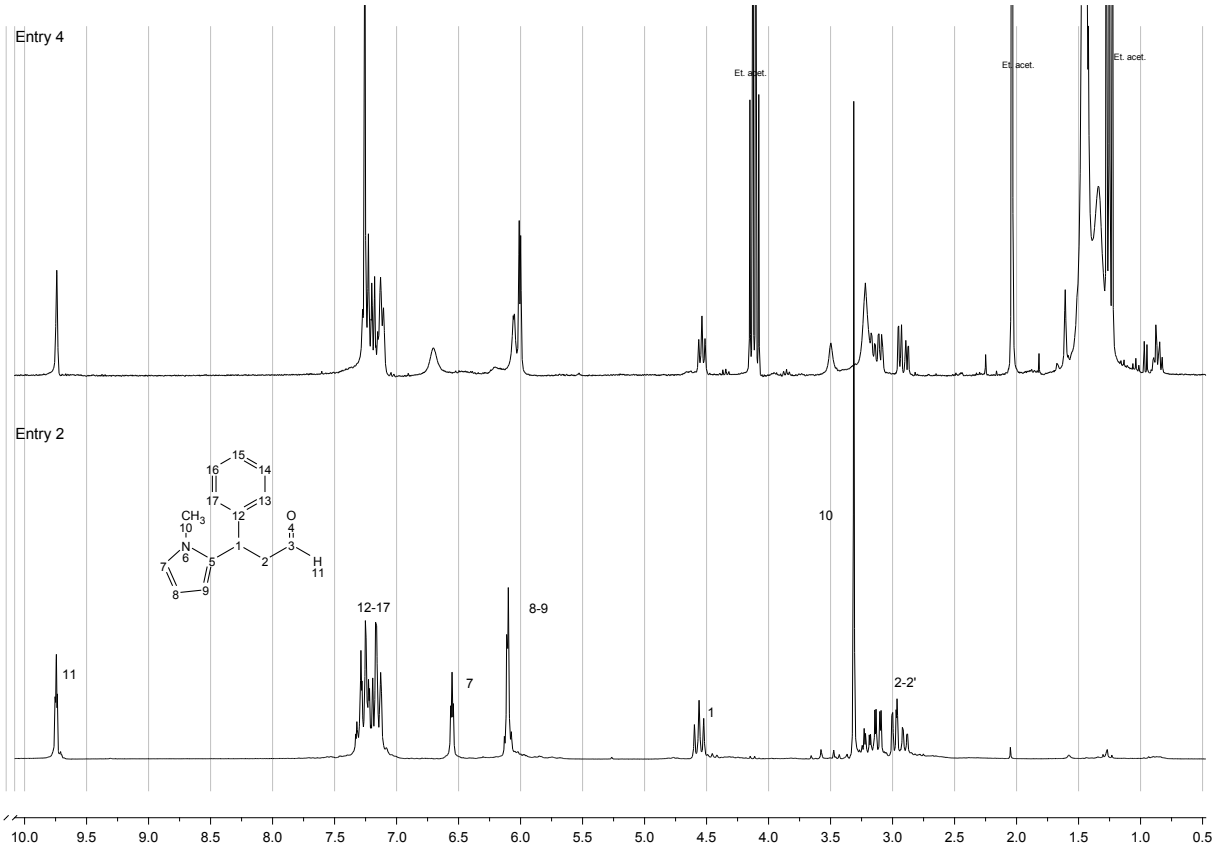

Figure 2.5: Proton NMR spectra for entries 2 and 4 in table 4.2. Solvent could not be removed effectively due to high viscosity of the product.

From the comparison of NMR spectra in figure 2.5 can be noted the unusual broadness of proton signals 7 and 10. Chemical shift is also higher for the aromatic proton in position 7, with an increase of of 0.1 ppm from the pure product. The methyl protons on position 10, in strong contrast with the pure product, produce two very broad singlets at higher and lower chemical shift from the pure product signal: 3.5 and 3.25 ppm against 3.3 ppm for the pure product signal. The aromatic protons in position 8 and 9 give rise to an apparent double doublet, albeit much broader than expected. All these alterations in the NMR spectrum were rationalized by the occurrence of multiple substitution on both position 5 and 7 of the pyrrole ring, in combination with a minor degree of condensation reaction between the 5 and 7 carbons on the pyrrole ring and the carbonyl groups (Figure 2.6).

The combination of the side reactions **a** and **b** triggers the formation of branched oligomers and, potentially, polymers with deleterious effects on purification. The occurrence of multiple substitutions of type **a** is especially notable by the apparition of the two broad doublets

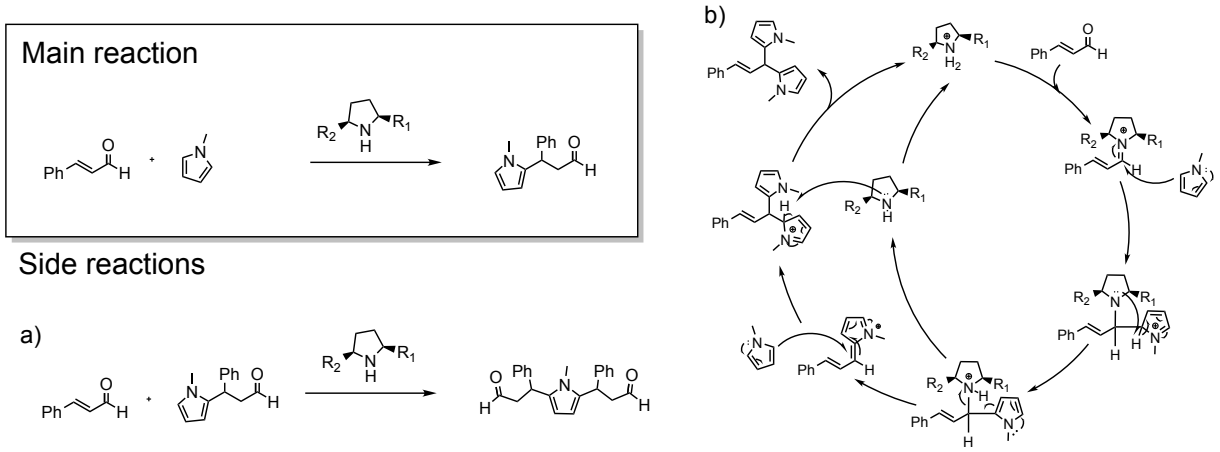

Figure 2.6: Proposed reaction schemes and catalytic cycles for the side reactions.

at 6.1 ppm, due to the protons in positions 8 and 9 being increasingly equivalent. The presence of such species can be directly observed from the pronounced tailing on TLC plate. Previous reports have pointed out the formation of analogous oligomers and polymers when pyrrolidine is used as catalyst for the same reaction.[41]

In the case at hand it was reckoned that formation of side-products is a consequence of altered reaction kinetics on polymer-support. To reduce the impact of undesired side-reactions a more detailed study of the first step reaction was conducted by variation of the most relevant factors and by analysis of the reaction mixture at regular intervals by proton NMR.

The optimized conditions for the first step conjugate addition reported by MacMillan et al. point out the importance of a strong acidic co-catalyst, such as TFA, to improve the reaction yield. When employed in combination with polymer support however TFA did not improve the final outcome of the reaction, but, in addition to the usual formation of high amounts of condensation products, complete loss of the aldehyde signal observed in the proton NMR of the crude mixture (Entry 5, table 2.2). The loss of aldehyde functionalities seems to be an indication of the enhanced reaction rate for the pyrrole-aldehyde branching condensation.

An identical reaction in the presence of TFA was monitored by ^{1}H-NMR every hour for the first 4 h, and after 24 h (Entry 6, table 2.2). The small but sensible formation of 1,4-addition products could be observed throughout the initial stages of the reaction. At longer times however both the β-proton signal and the carbonyl signals are lost (Figure 2.7).

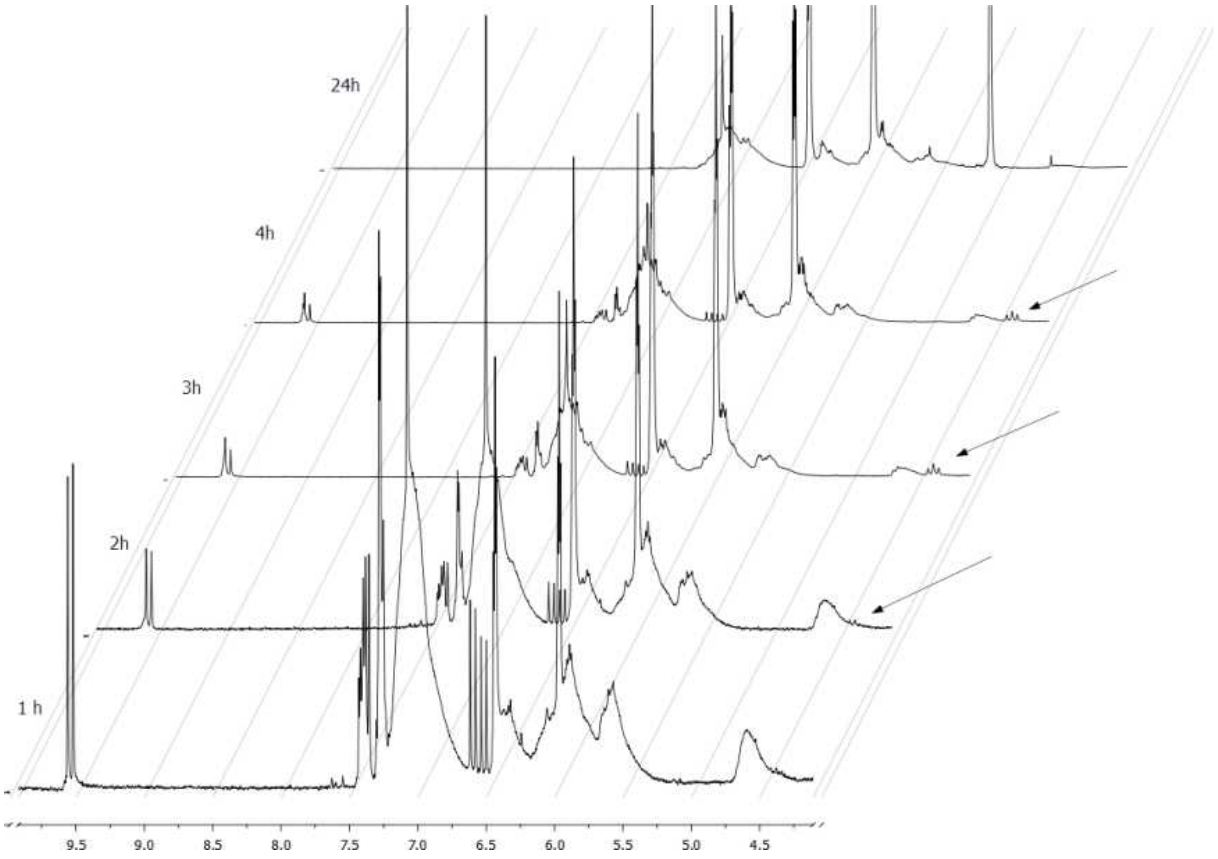

Figure 2.7: Conjugate addition between N-Methylpyrrole and cinnamaldehyde, monitored at 1 h, 2 h, 3 h, 4 h and 24 h. Intensity of signals is calibrated on the pyrrole signals between 6.0 and 6.5 ppm.

The experiment also reveals that the concentration of cinnamaldehyde drastically decreases in the initial stages of the reaction as pointed out by the steady and drastic decrease in the intensity of the doublet at 9.6 ppm and the quartet at 6.6 ppm, while the concentration of 1,4-addition product remains constant. This stems for the likely consumption of either cinnamaldehyde or 1,4-addition product in parasite side reactions.

Degradation of aldehydes in this case is most likely dependent on the strongly acidic conditions, which increase the rate of condensation reactions much more effectively than the rate of conjugate additions. Formation of condensation products was observed by TLC after less than 2 h from the start of the reaction, contemporaneously to the first traces of 1,4-addition product.

Use of acetic acid as a milder substitute of TFA, or complete lack of acidic co-catalyst did not result in any 1,4-conjugate addition and the unreacted reagents could be recovered after 24 h (Entries 7 and 8, table 2.2).

2.2.1 Experimental design considerations and results

To evaluate the interactions between the relevant parameters in the polymer-supported version of this reaction an experimental design was prepared. In this design the effect of variations of acidic co-catalyst amounts, N-methylpyrrole equivalents and temperatures were studied in relation to the degree of 1,4-addition (yield). The experimental design also provides a valid tool to estimate the non-linear interactions between all the above-mentioned factors.

A rapid system to measure the degree of conjugate addition, even if no purification is possible, is to estimate the yield of the reaction at identical times by integration of known and reliable signals in the ^{1}H-NMR spectra of the crude mixture. It was previously shown how in this case is possible to monitor the course of the main catalytic cycle by the characteristic triplet arising at 4.49 ppm from the β-proton of the conjugate addition product. The same region is clear from any other signal, and integration of this triplet is straightforward and reliable. To calculate the yield it is also required a reference peak for the starting materials. In our case it is possible to use the quartet at 6.4 - 6.6 ppm arising from the α-proton of *trans*-cinnamaldehyde; again, the signal is located in a clear region of the spectrum and the integrals can be easily measured (Figure 2.8).

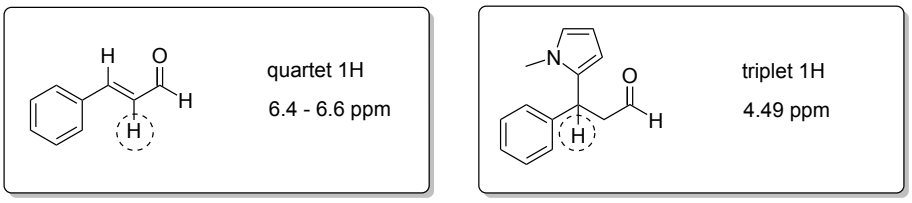

Figure 2.8: Reference signals for the experimental design and respective assignment.

Any signal from N-methylpyrrole is unsuitable for this purpose, since the concentration of it will vary from experiment to experiment. Aldehyde signals are also unreliable because of non negligible condensation reactions occurring at lower pH.

If the integral from the cinnamaldehyde quartet is calibrated at the arbitrary value of 1.00, the integral of the triplet at 4.49 ppm provides an estimate the yield by the following equation:

$$Yield = \left(\frac{x}{1.00 + x} \right) \cdot 100$$

Where x is the integral on the conjugate addition product triplet.

Each factor of interest was divided in two levels representative of well distinct reaction conditions. The effect of temperature was studied at 4 °C and r.t.; the effect of acidic co-catalyst was studied at a minimum of 0 eq. and a maximum of 0.1 eq., the latter corresponding to a 1:1 molar ratio with the catalyst; the effect of N-methylpyrrole concentration was studied at values of 1 eq. and 5 eq. The complete list of performed reactions for this experimental design and the calculated yield after 24 h are reported in table 2.3a.

Entry	Temp. [°C]	TFA [eq.]	6 [eq.]	Yield
1	r.t.	0	1	0
2	r.t.	0	5	0
3	r.t.	0.1	1	0
4	r.t.	0.1	5	traces
5-6-7	10 °C	0.05	3	19% - 22% - 15%
8	4 °C	0	1	0
9	4 °C	0	5	0
10	4 °C	0.1	1	38%
11	4 °C	0.1	5	33%

(a) Experimental design results.

Effect	Value	S_{Eff}
Main effects		
TFA	**19**	±3.3
T	**-16.5**	±3.3
N-MP eq	**2.5**	±3.3
2nd order interactions		
T*TFA	**-16.5**	±3.3
N-MP eq*TFA	**2.5**	±3.3
NMP eq*T	**0**	±3.3
3rd order interactions		
T*TFA*NMP eq	**0**	±3.3

(b) Effect table.

Table 2.3: Experimental design results and effects.

For entries 5, 6 and 7 the experiment was repeated three times at average values with respect to each parameter to calculate the reliability of this design (standard deviation). The data were processed using MODDE v. 9.1. Results are reported in effect table 2.3b.

The outcome of the experimental design clearly indicates that the amount of N-methylpyrrole has no significant impact on the degree of conjugate addition. Temperature and co-catalyst however seem to have a large effect on the rate of 1,4-addition. As expected from previous literature, high amounts of acid lead to faster reaction rates, while lower temperatures sensibly improve yields with approximate increments of 20% for every 10 °C. The most interesting event however is the correlation (2^{nd} order interaction) between temperature and acidic co-catalyst, best represented by a three-dimensional plot of temperature vs. TFA equivalents vs. yield (Figure 2.9).

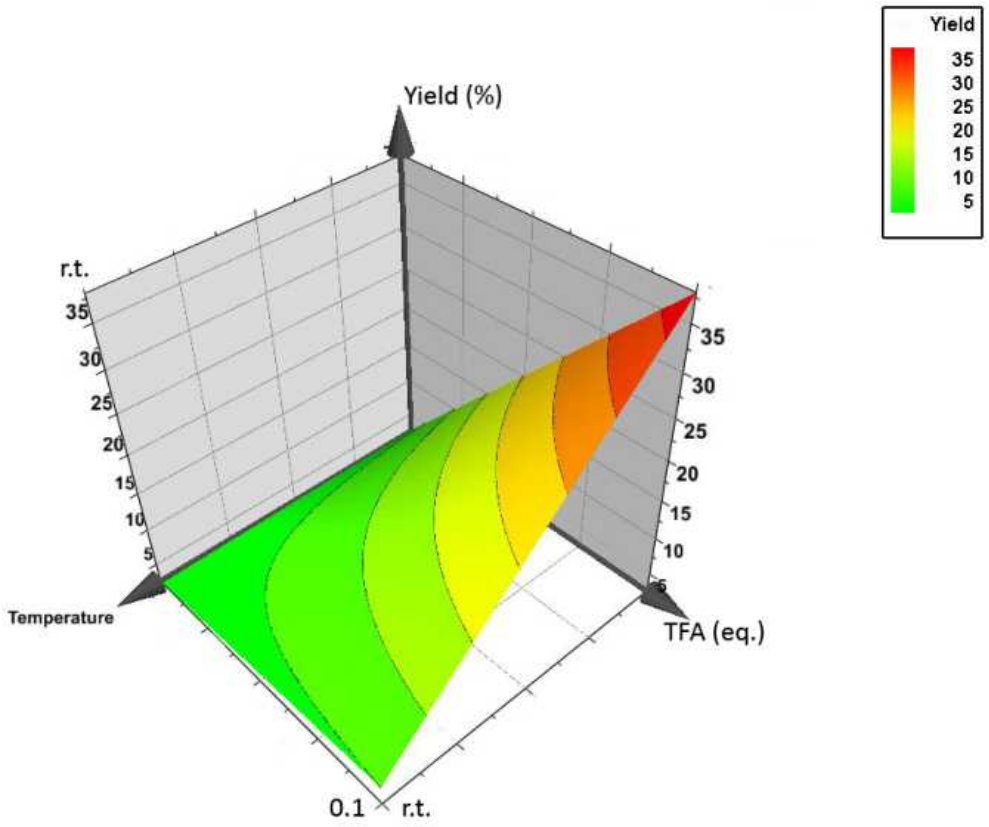

Figure 2.9: Predicted surface for the variation of temperature and TFA equivalents.

At higher temperatures little product is formed, with only a minor dependence from TFA equivalents: higher TFA loadings produce trace amounts of product (<5%). At lower temperatures however the impact of TFA equivalents on the reaction yield is drastically increased, and higher TFA loading enormously improve the reaction yield from basically no product to a maximum of 38% at 4 °C.

In all cases, however, the final mixture contains variable amounts of side products detectable by simple TLC, making purification unfeasible.

2.3 Benchmark reaction 3

Two step novel tandem: Diels-Alder, 1,2-addition

The same combination of catalysts **3** and **1** can be used for the realization of diverse stereoselective sequences. The first generation MacMillan catalyst **3** has been extensively studied in relation to Diels-Alder reactions of α,β-unsaturated aldehydes and ketones.[42,43] Previous works have also proved the compatibility and efficiency of polymer-supported organocatalyst **3** to Diels-Alder reactions.[32,44] However, to the best of our knowledge no attempt has been made to execute any type of sequential process exploiting Diels-Alder reactivity. Since the product for this class of organocatalyzed cycloadditions is a disubstituted aldehyde or ketone such as **9**, it was reckoned that this class of molecules should easily undergo α-functionalization mediated by suitable organocatalysts (Figure 2.10).

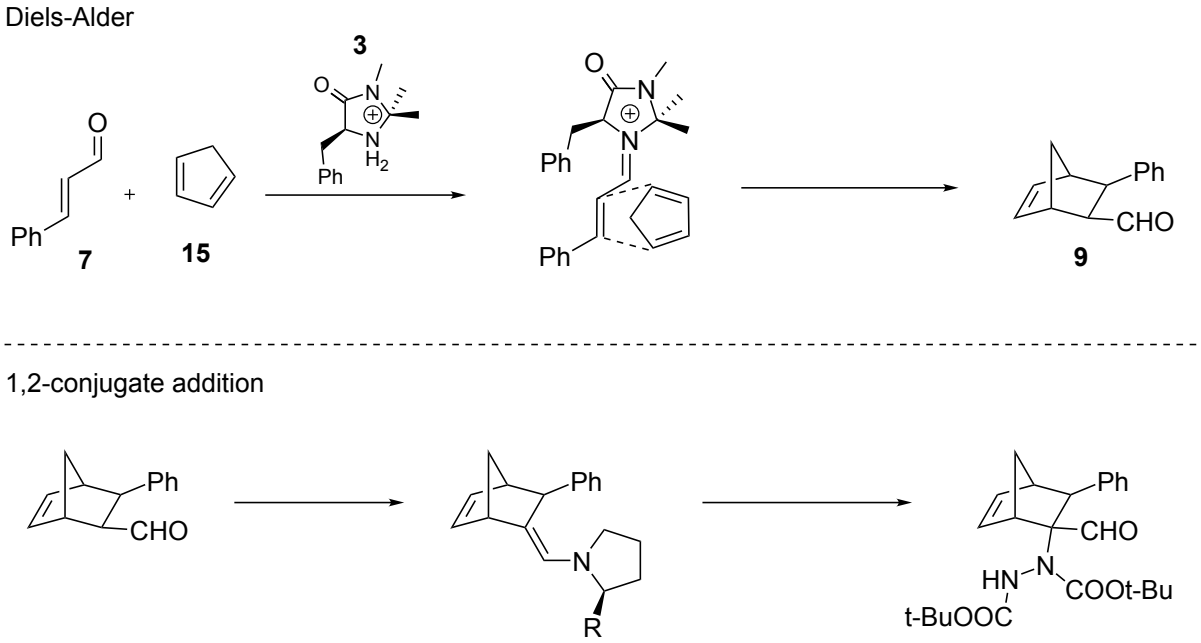

Figure 2.10: Key steps in the custom-designed tandem reaction.

The initial attempt to combine a Diels-Alder reaction between cyclopentadiene **15** and cinnamaldehyde **7** with the 1,2-addition of DBAD **8** afforded the cycloaddition product **9** in poor yield (Entry 1, table 2.4). 1,2-Conjugate addition product could not be detected. Separation of the two reactions in a step-wise procedure did not seem to improve efficiency at all for the 1,2-addition reaction (Entry 3, table 2.4), while the Diels-Alder reaction restores its normal efficiency (>65%) (Entry 2, table 2.4).

Entry	7 [mmol]	15 [mmol]	8 [mmol]	3 [mol%]	1 [mol%]	Additive	Yield
1	1	3	1.5	10	10	TFA	15%[a]
2	1	3	-	10[e]	-	TFA	66%
3	-[b]	-	0.7	-	10[c]	Ac. acid	-[d]

Table 2.4: Yields and mol % are calculated with respect to **7**. **a**) Only Diels-Alder product is isolated, but no 1,2-addition product is observed. **b**) the product from entry 1 was used as starting reagent; **c**) catalyst **16** was used as catalyst instead of **1**; **d**) no conversion. The starting reagent was recovered quantitatively; **e**) **14** was used as a catalyst instead of **3**.

Contextually to our investigations an elucidation of the mechanism was reported by Blackmond et al. concerning amine-catalyzed 1,2-conjugate addition reactions. The study points out the low reactivity observed for secondary aldehydes, in strong contrast with the high activity of primary aldehydes.[45] The rationalization of this behavior is based on the inclusion of observed cyclobutane species which were originally considered parasitic into the main cycle (Figure 2.11). The formation of this type of intermediates implies that the catalytic cycle cannot be carried out unless a pair of α-protons is available in the starting substrate, excluding the reaction designed from as valid benchmark reaction.

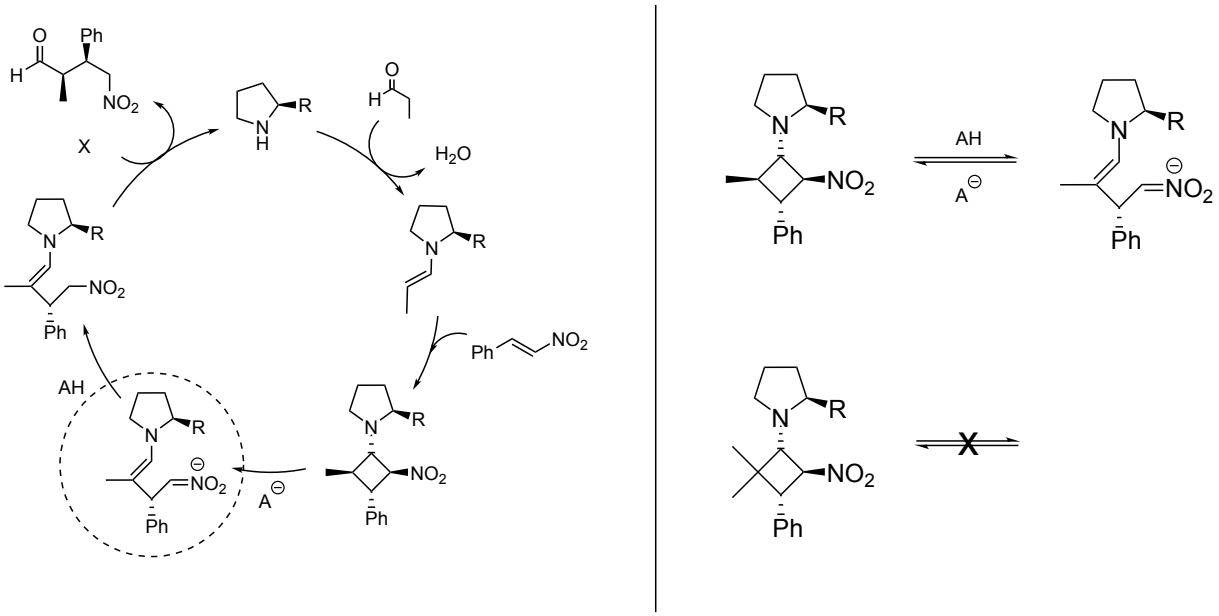

Figure 2.11: Mechanistic elucidation on the amine-catalyzed 1,2-conjugate addition on α,β-unsaturated aldehydes.

2.4 Benchmark reaction 4

Two step novel tandem: Diels-Alder, aldol reaction

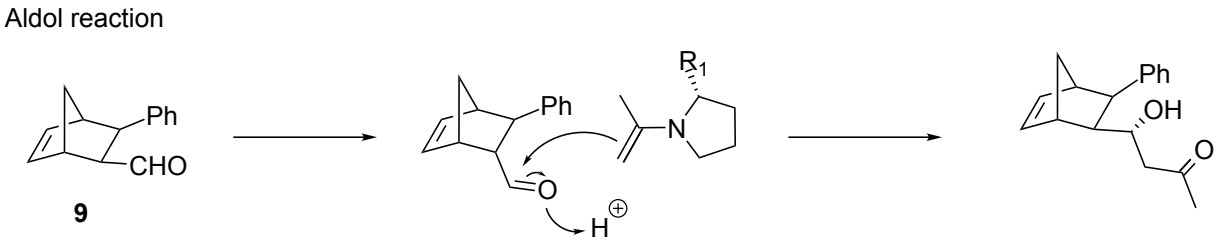

Figure 2.12: Key steps in the tandem aldol reaction.

An alternative to the 1,2-conjugate addition on the above-mentioned Diels-Alder product is the enamine-catalyzed aldol reaction between **9** and acetone (Figure 2.12). The imidazolidinone-catalyzed Diels-Alder and the proline catalyzed aldol reaction however have been reported to be most efficient in different solvents, namely water/methanol for the Diels-Alder reaction and DMSO for the aldol reaction.[42,46,47] Since the aldol reaction is known to be the most solvent-dependent reaction among the two, preliminary investigations were carried out to test the compatibility of MacMillan's catalyst in the absence of methanol, and in the presence of acetone. Absence of methanol from the reaction mixture reduced the yield to 40% (Entry 2, table 2.5); large excess of acetone however increases the yield up to 59% (Entry 1, table 2.5).

Entry	7 [mmol]	15 [mmol]	3 [mol%]	Solvent	Additive	Yield
1	1	3	10	Acetone/H_2O 1:1	**TFA**	59%
2	1	3	10	H_2O	**TFA**	40%

Table 2.5: Reaction conditions for the synthesis of 3-phenylbicyclo[2.2.1]hept-5-ene-2-carbaldehyde. Yields and mol% are calculated with respect to **7**.

All attempts to achieve the aldol reaction however failed regardless from the solvent mixture (All entries, table 2.6). In all cases the starting aldehyde could be recovered quantitatively, along with trace amounts of side-products.

Entry	9 [mmol]	Acetone [mL]	4 [mol %]	Solvent	Yield
1	0.4	0.1	20	H_2O[a]	-[b]
2	0.35	1	20	DMSO/H_2O 4:1[c]	-[b]
3	0.4	0.2	20	DMSO[d]	-[b]

Table 2.6: Yields and mol % are calculated with respect to **9**. **a**) 0.5 mL of solvent used; **b**) **9** was recovered quantitatively; **c**) 5 mL of solvent used; **d**) **4** was dissolved in the minimum volume of water prior to addition.

2.5 Benchmark reaction 5

Two step organic and organometallic tandem reaction: 1,2-conjugate addition, cyclization

The fifth benchmark reaction studied is the combination of an organocatalyzed Michael addition followed by a gold(I)-catalyzed tandem cyclization/acetalization reported by Alexakis et al.in 2009. The proposed mechanism is depicted in figure 2.13.[37] It was previously pointed out that any multi-catalytic reaction is feasible on polymer-supported catalysts only if the two catalysts operate in separate catalytic cycles, or more specifically, they do not require synergistic activation of any kind (see section 1.5.2). Unlike most other reported multi-catalytic reactions featuring a combination of organocatalysts and organometallic catalysts, this particular combination does not rely on the synergistic activation of substrates to achieve an high degree of stereoselectivity, and is therefore a suitable candidate for the present study.[19,48]

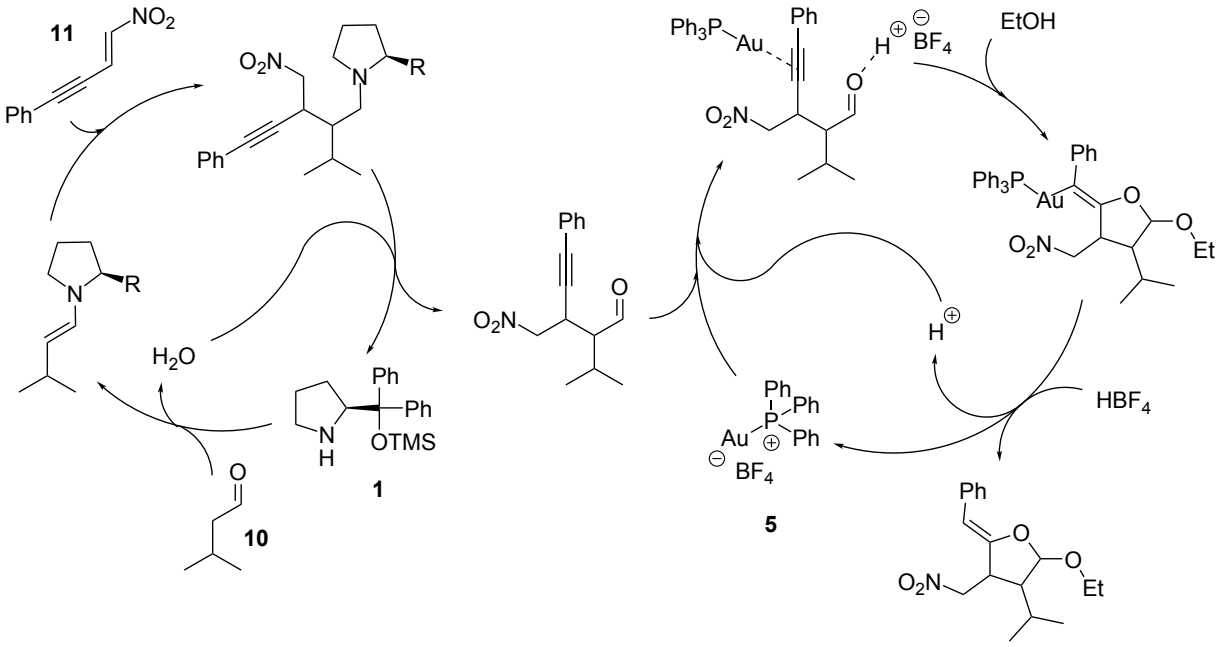

Figure 2.13: Proposed mechanism for the tandem Michael addition/cyclization.

Starting material **11** was prepared following the reported procedures in a three-step procedure. Starting from phenylacetylene **17**, propargylic aldehyde **18** was prepared in high yield by S_N2 reaction, and used as is in the following conjugate addition to afford **19** in high yield. **19** was ultimately dehydrated with TFAA to give the final product **11** in 44% overall yield (Figure 2.14).

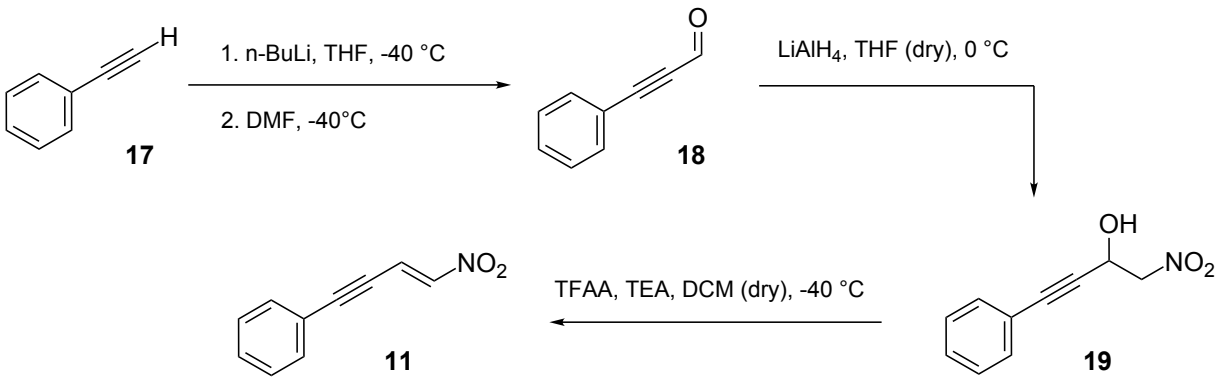

Figure 2.14: Substrate synthesis procedure.

Step-wise Michael addition was attempted using already available polymer-supported organocatalyst **16** (Figure 2.15) (all entries, table 2.7). Conjugate addition proceeds smoothly in the reported conditions, with very good yields (60-70%) in less than 24 h and virtually quantitative reaction for longer times.

Entry	11 [mmol]	10 [mmol]	Catalyst [mol%]	Solvent [mL]	T [°C]	Time	d.r.	Yield
1	0.94	10	**16** 10%	$CHCl_3$ 9	-35 → rt	14 h		71%
2	1.69	16	**16** 10%	$CHCl_3$ 15	-35 → rt	18 h		60%
3	0.15	1.5	**16** 10%	$CHCl_3$ 2	rt	7 days		Quant.

Table 2.7: Organocatalyzed Michael addition results. Yields and mol% are calculated with respect to **11**.

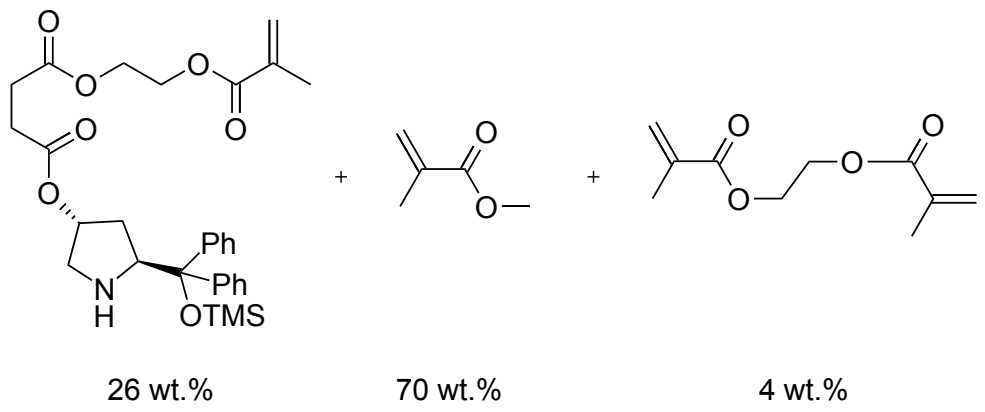

Figure 2.15: Monomer composition of PEG-methacrylic co-polymer supporting Jørgensen-Hayashi catalyst (**16**). Kristensen, T. E.; Vestli, K.; Jakobsen, M. G.; Hansen, F. K.; Hansen, T. *J. Org. Chem.* **2010**, 75, 1620–1629.

2.5.1 Polymerization design

Before attempting the gold-catalyzed cyclization reaction a procedure for the immobilization of gold(I) species on methacrylic polymer beads was designed, based on the actual knowledge of the catalyst's requirements. In the original work by Alexakis et al. the most catalytically active gold(I) specie was reported to be the one bearing triphenylphosphine as ligand and a tetrafluoroborate counterion.[37] It was considered that the most suitable site for the linking unit is the *para* position on the a phenyl ring. The most accessible monomer with this configuration is the cheap and easily available 4-(diphenylphosphino) styrene **20** (Figure 2.16).

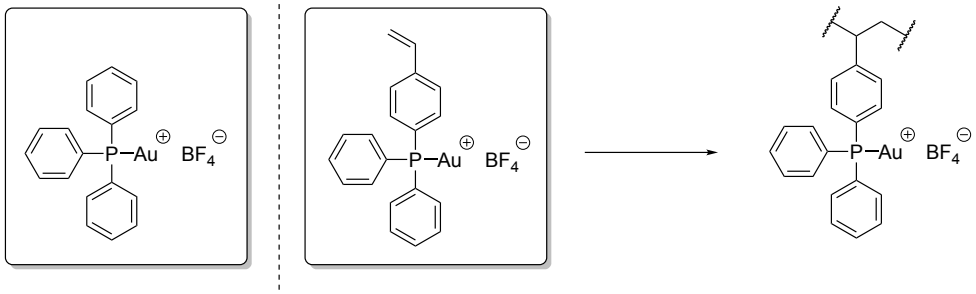

Figure 2.16: Catalyst's monomeric analogue.

The source of gold(I) ions should be cheap, highly accessible and possibly give rise to straightforward ligand substitution when exposed to phosphine ligand **20**. The specie which better fits such requirements is chloro(dimethylsulfide)gold(I) **21**. When mixed in solution with the phosphine ligand, either triphenylphosphine or **20**, the dimethylsulfide ligand is quickly exchanged for the phosphine at room temperature (Figure 2.17).[49]

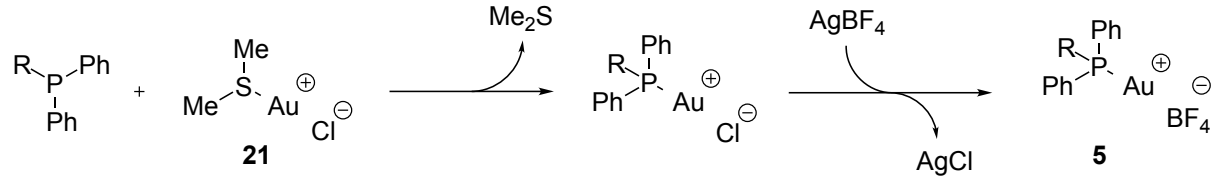

Figure 2.17: Preparation procedure of the catalytically active gold(I).

The reaction proceeds quantitatively in short times due to the high volatility of dimethylsulfide. Exchange of chloride counterions in favor of tetrafluoroborate can be easily achieved by addition of stoichiometric amounts of $AgBF_4$. The silver salt precipitates chloride ions as insoluble silver chloride, and quantitatively yields the active catalyst.

The above-mentioned procedure can be carried out using co-polymerized 4-(diphenylphosphino) styrene, in which case formation of polymer beads would be preliminary to the addition of **21** and $AgBF_4$ (post-modification strategy). Alternatively it is possible to anticipate the ligand exchange reaction prior to the actual polymerization (bottom-up strategy). Since in this case there is no obvious advantage to any strategy each was attempted to evaluate which procedure affords the most catalytically active polymer beads.

Additionally two different polymeric matrices of different solvent affinity were used in the preliminary polymerization procedures. The first polymeric materials is mostly styrenic in nature, comprising styrene, a small weight percentage of divinylbenzene as cross-linker and a variable quantity of phosphine monomer dependent on the polymerization strategy (Entries 1 and 3, table 2.8). The second polymeric material is mostly methacrylic in nature, being composed of methyl methacrylate, a small amount of ethylene glycol dimethacrylate as cross-linker and variable loadings of phosphine monomer analogous to the styrenic beads (Entries 2 and 4, table 2.8). Both materials are well compatible with the halogenated solvent required for the cyclization reaction and afford beads with good swelling properties. Much higher loadings of phosphine monomer were used for the post-modification strategy, to ensure quantitative binding of gold(I) ions to the polymer beads. For details on the polymerization procedure refer to section 4.12.

Entry	Monomer mixture	Cat. monomers [mg]	Yield
1	**A**	**20** (288)	traces
2	**B**	**20** (288)	78%
3	**A**	**20** (17); **21** (16)	Quant.
4	**B**	**20** (16); **21** (14)	Quant.

Table 2.8: Monomer mixture **A**: Styrene (1.14 mL, DVB (28 µL). Monomer mixture **B**: MMA (1.07 mL), EGDMA (36 µL).

All four types of polymer beads were used as catalyst in the benchmark acetalization reaction on the Michael adduct previously obtained. Conversion for all four reactions were estimated by ^{1}H-NMR analysis of the crude, comparing the integrals from the aldehyde proton in the starting material at 9.90 ppm and the triplet from the phenyl proton 17 at 7.07 ppm from the resulting mixture of product isomers (Figure 2.18).

Both reactions carried out using bottom-up-produced beads yielded the product with quantitative conversion (complete disappearance of the main aldehyde signal). The polymer beads

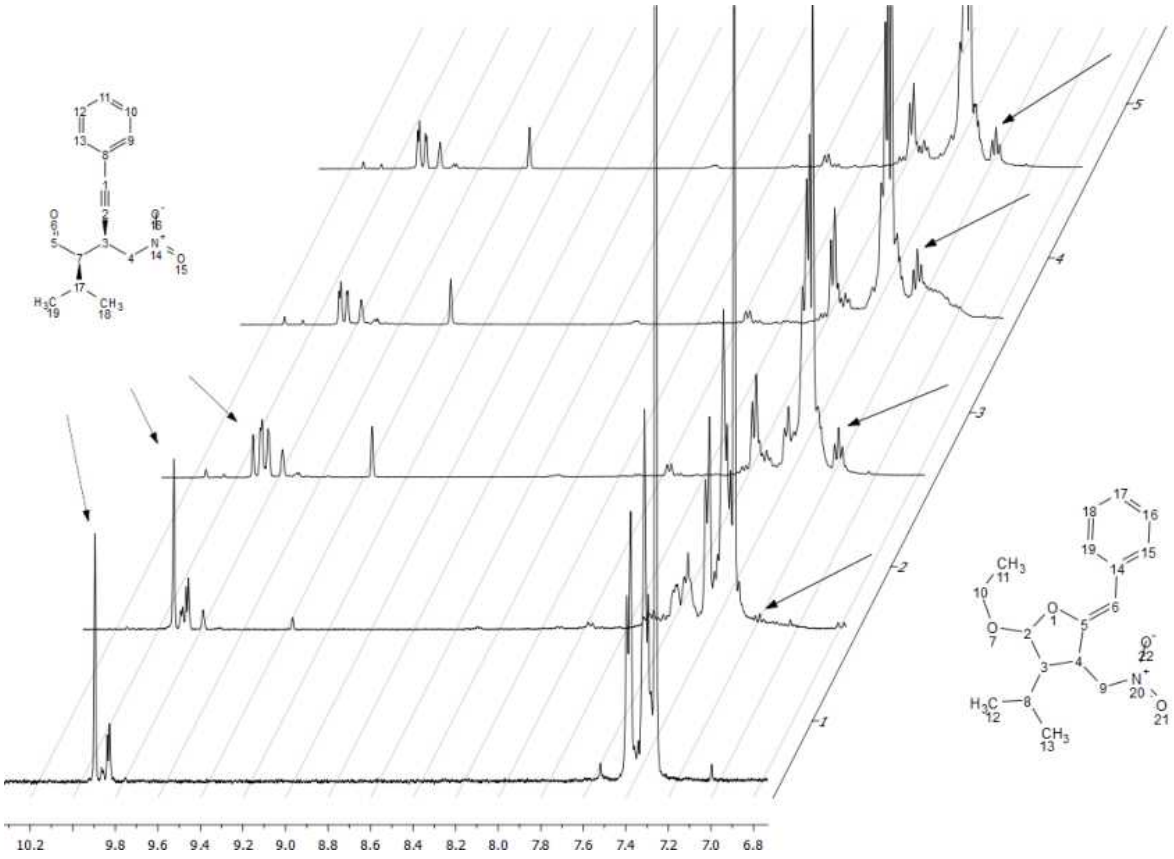

Figure 2.18: Reference peaks in the gold(I) catalyzed cyclization reaction.

produced accordingly to the post-modification procedure however managed very poorly in the case of styrenic support (traces) and less efficiently in the case of methacrylic support (78% conversion). Reduction of gold(I) to metallic gold clusters, mostly due to exposition to light,[50] was observed in all test reactions, with one major difference between entries 1-2 and 3-4: while polymer beads prepared accordingly to the post-modification procedure gave rise to metallic clusters mostly in homogenous solution, later deposited on the bottom of the reaction flask, the clusters formed on polymer beads prepared following the bottom-up strategy remained trapped well within the polymer beads and did not reach macroscopic size (Figure 2.19). The bottom-up strategy was therefore applied to all following polymerizations due to its improved immobilization properties.

2.5.2 Multi-catalytic polymer beads

To synthesize the required multi-catalytic polymer beads for the final one-pot tandem reaction tests the bottom-up procedure previously employed was extended to include organocat-

Figure 2.19: Purple metallic gold clusters trapped in polymer beads.

alytic monomer **22**. The monomer was synthesized accordingly to reported procedures, starting from pre-made unprotected monomer **23** by selective protection of its hydroxy-group (Figure 2.20).[32,51] The monomer thus obtained was used as is for all polymerizations in a 1:1 ratio with respect to the organometallic monomer (Figure 2.21).

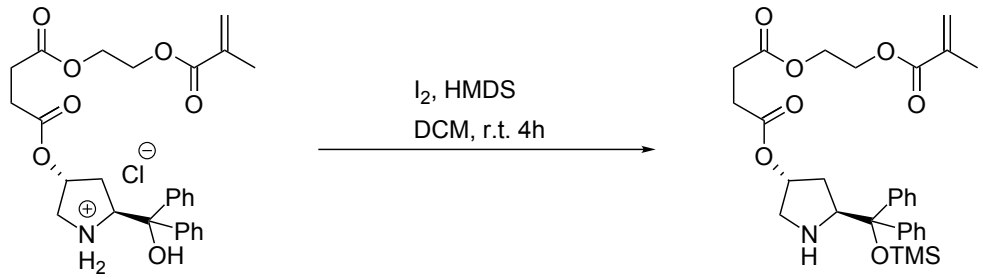

23 **22**

Figure 2.20: Catalytic monomer synthesis.

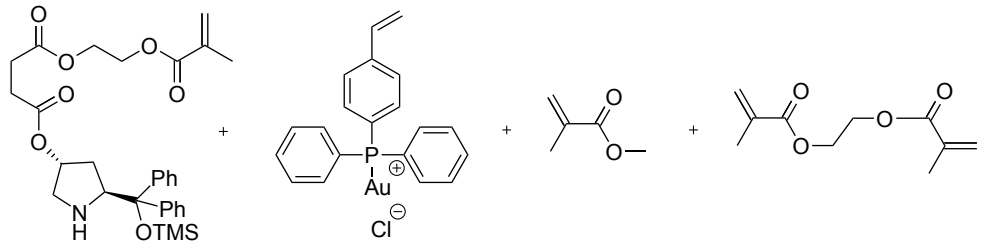

2.5 wt.% 2.8 wt.% 91.2 wt.% 3.5 wt.%

Figure 2.21: Monomer composition of methacrylic co-polymer supporting Jørgensen-Hayashi catalyst and gold(I) catalyst (**24**).

When employed in the Michael addition reaction the multi-catalytic beads **24** (1:1 catalyst ratio) did not show any loss of activity compared to the polymer beads **16** bearing only enamine catalyst, indicating the compatibility of the two catalyst within the context of the first step conjugate addition (Table 2.9).

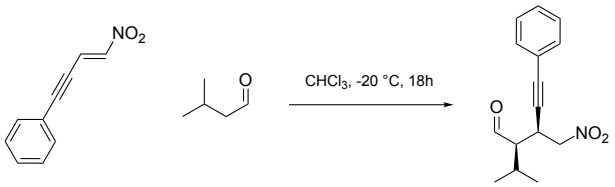

11 10

Entry	11 [mmol]	10 [mmol]	Catalyst [mol %]	Solvent [mL]	T [°C]	Time	Yield
3	0.15	1.5	**16** 10%	$CHCl_3$ 2	rt	7 days	Quant.
4	0.15	1.5	**24** 10%/10%	$CHCl_3$ 5	rt	7 days	Quant.

Table 2.9: Performance test for the multi-catalytic polymer beads bearing both organic and organometallic catalytic moieties (**16** and **24**).

2.5.3 Performance tests

The final performance tests on the multi-catalytic polymer beads were carried out accordingly to both assisted and non-assisted tandem reaction procedures. Any attempt to achieve the tandem sequence in a non-assisted fashion, adding all reagents required for the entire tandem sequence from the beginning, did not yield any Michael addition product, nor any cyclization product. In the assisted tandem reaction the multi-catalytic polymer beads were let to react for 48h prior to the addition of the second step cyclization reagents $AgBF_4$ and ethanol (table 2.10).

Entry	Polymer [mg]	11 [mmol]	10 [mmol]	Ethanol [µL]	$CHCl_3$ [mL]	Yield[c]	Yield[d]
1	**25** 206	0.37	4	-[a]	4	-	-
2	**26** 209	0.37	4	46[b]	4	19%	11%
3	**27** 209	0.37	4	46	4	27%	19%

Table 2.10: Yields and are calculated with respect to **11**. **a**) Entry 1 was halted after 24 h due to lack of any product; **b**) entry 2 was carried out in absence of $AgBF_4$ or *p*-TsOH; **c**) Michael adduct yield after 48 h reaction time, prior to ethanol addition; **d**) cyclization product yield after 24 h reaction from ethanol addition.

The observed trend for the tandem assisted Michael addition/cyclization reaction indicates that yields are mostly dependent on catalyst loading of compound **22**. For a catalysts loading as low as 5 mol % of compound **22** no product could be observed for the first step Michael addition (1:1 relative catalyst loading between **22** and gold(I) catalyst). When higher organocatalyst loadings are employed however, a clear improvement on yield is observed, with an increase of its value up to 27% for the Michael addition product (4:1 relative catalyst loading between **22** and gold(I)). The cyclization/acetalization reaction

however performs equally well whenever Michael adduct is formed, achieving up to 70% yield relative to the Michael adduct (19% overall, entry 3, table 2.10).

In no case were observed overall yield values comparable to the step-wise or homogenous reactions (70-85% overall).

3 Conclusion

Three reported multi-catalytic sequential reactions and two novel organocatalytic sequences have been studied as benchmark reactions to test the performances of polymer-supported catalysts.

Ender's triple cascade did not provide a valid benchmark reaction due to the high affinity of Jørgensen-Hayashi catalyst to all substrates in the optimal reaction conditions, therefore limiting the potential for multiple catalysis.

The sequence developed by MacMillan et al. could not be employed as benchmark reaction due to purification issues arising when polymer-supported catalysts are used. A systematic study of the most relevant variables for this cascade was performed, providing the information for future research and improvement of the sequence on polymer support. The sequence however was not further investigated due to lack of relevance with the current project.

Two novel tandem reactions based on the Diels-Alder reaction catalyzed by the first generation MacMillan catalyst were attempted but did not provide valid benchmark reactions either due to mechanistic limitations or incompatibility between the catalysts and the solvents required.

A bottom-up polymerization procedure was developed for the immobilization of gold(I) species and its catalytic activity was compared to the analogous polymer beads produced accordingly to the post-modification procedure. The bottom-up procedure showed improved gold(I) stability against reduction in the reaction conditions, and proved to be a valid strategy for the immobilization of gold(I) species.

The sequence developed by Alexakis et al. provided a valid benchmark reaction in the context of assisted tandem reactions. The multi-catalytic polymer beads prepared accordingly to the bottom-up procedure showed reduced activity in relation with the organocatalytic step of the sequence. Their activity however rapidly increases for higher loadings of organocatalyst. Sensibly lower yield values were observed for polymer-supported catalysts when catalyst loadings analogous to homogenous conditions were employed. The second step gold(I)-catalyzed cyclization does not seem to be affected by polymer immobilization procedure nor by the limited mobility of the catalyst. High levels of activity were achieved in all cases by

the gold(I) catalyst.

4 Experimental section

4.1 General information on the experimental conditions

All commercially available reagents were used as received. Equivalents for all reagents were calculated using the data reported on bottle (see 4.16). Cyclopentadiene was cracked at 165 °C, stored at approximately –20 °C and used no later than two weeks after cracking. Purity was checked via ^{1}H-NMR after cracking and prior to every use. Dry DCM and THF were obtained from a MBraun MB SPS-800 solvent purification system. Prepared compounds containing gold(I) species were stored in dark at r.t. under normal atmosphere. All chemicals synthesized and used in later reactions were stored in freezer at approximately –20 °C. Flash chromatography was performed using silica gel (Sigma 60, 40-63micometers) on the instrument Combi Flash Companion ® with Peak Trak software v.1.4.10 from Isco. TLC chromatography was performed on Merck 60 F254 silica plates. All compounds were observed under UV-light.

NMR experiments were performed at r.t. on Bruker DPX 200, DPX 300 and AVII 400 spectrometers operating respectively at 200, 300 and 400 MHz for ^{1}H, and 50, 75 and 100 MHz for ^{13}C. Chemical shifts were reported in ppm relatively to the residual solvent signal: $CDCl_3$ 7.26 ppm (^{1}H), 77.00 ppm (^{13}C). The NMR data were processed using MestReNova v.6.0.2-5475.

4.2 One-pot homogeneous Ender's cascade using multiple catalysts

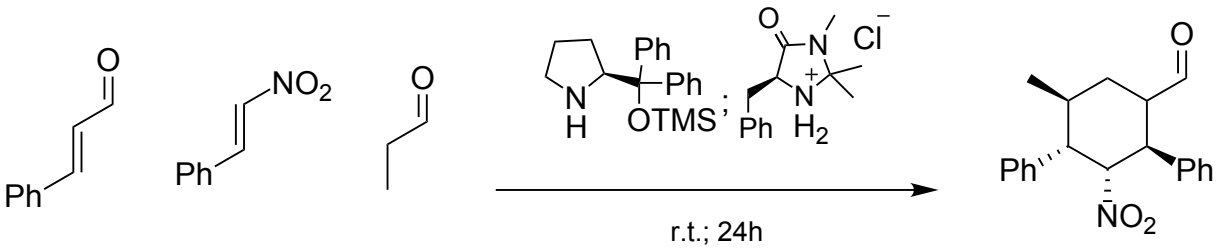

In a Schlenk tube fitted with magnetic stirrer and placed in an ice bath (0 °C) the catalysts **1** and **3** were added, followed by the solvent under constant stirring. When complete solubilization of salts occurred **7**, **12** and **13** were added in this order and the tube was closed with a glass stopper. For entry 1 glacial acetic acid was added after all other reagents (3.8 µL, 0.066 mmol).

After 24 h the reaction mixture was separated by flash chromatography (⌀= 2 cm, length = 8 cm, hexanes/ethyl acetate from 0% to 30% ethyl acetate). The product was dried with rotavap followed by high vacuum, then weighed.

Entry	7 [mmol]	12 [mmol]	13 [mmol]	1 [mol %]	3 [mol %]	Solvent	Yield
1	0.5	0.75	0.6	2	-	neat	3%
2	1	1.5	1.2	20	-	Toluene 1 mL	30%
3	1	1.5	1.2	20	20	Toluene 1 mL	28%[a]

Table 4.1: Yields and mol % are calculated with respect to **7**. **a**) Column size used ⌀= 2.5 cm, length = 9 cm.

4.3 One-pot sequential 1,4- and 1,2-addition on cinnamaldehyde

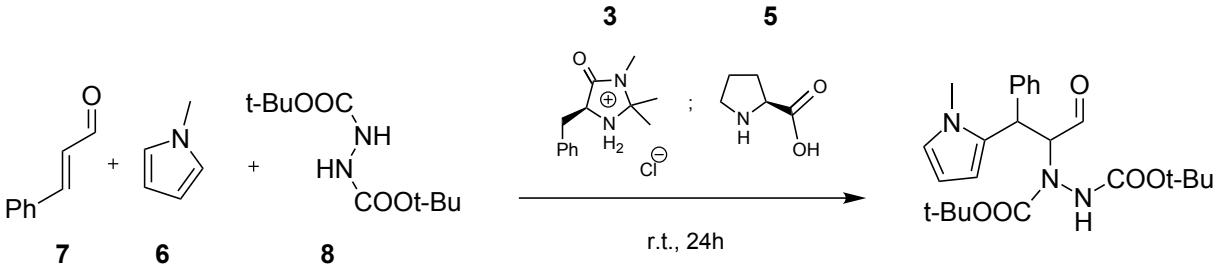

7 6 8

In a Schlenk tube fitted with magnetic stirrer were added **7** and **6**, followed by catalysts **3** and **4** and by 1 mL of solvent. After 5 min **8** was added, followed by 1 mL of solvent. The additive was added last and the tube was closed with a glass stopper.

After 24 h the reaction mixture was extracted using three portions of $NaHCO_{3(aq.)}$ (7 mL each); the aqueous layer was extracted using three portions of DCM (7 mL each). After extraction the organic layer was dried on $MgSO_4$, filtered and dried with rotavap.

The crude mixture was separated by flash chromatography (⌀= 2.5 cm, length = 9 cm, petroleum ethers/ethyl acetate from 0% to 30% ethyl acetate). The product was dried with rotavap followed by high vacuum, then weighed.

Entry	7 [mmol]	6 [mmol]	8 [mmol]	3 [mol%]	4 [mol%]	Solvent	Additive	Yield
1	1	1.2	1.2	10	30	DCM	-	-
2	1	1.2	-	10	-	THF/H_2O 7:1	-	24%
3	-[a]	-	1.5	-	30	THF/H_2O 7:1	-	40%
4	1	1.5	1.4	10	30	THF/H_2O 6:1	-	-[e,g]
5	1	5	-	10[b]	-	THF/H_2O 12:1	TFA	-[g]
6	1	5	-	10[b]	-	THF/H_2O 10:1[c]	TFA	-[g]
7	1	5	-	10[b]	-	THF/H_2O 10:1	-	-[g]
8	1	5	-	10[b,d,f]	-	THF/H_2O 10:1	TFA	-[g]
9	1	5	-	10[b]	-	THF/H_2O 10:1	Ac. acid	-[g]

Table 4.2: Yields and mol % are calculated with respect to **7**. **a**) the product from entry 2 was used as starting material; **b**) **14** was used as a catalyst instead of **3** (see Figure 4.1); **c**) 0.5 mL of solvent overall; **d**) after 24 h of reaction $NaBH_4$ was added in large excess to the crude mixture and left to react for 1 h before proceeding with extraction; **e**) 48 h reaction time; **f**) 3 h reaction time; **g**) no chromatography was possible due to by-products.

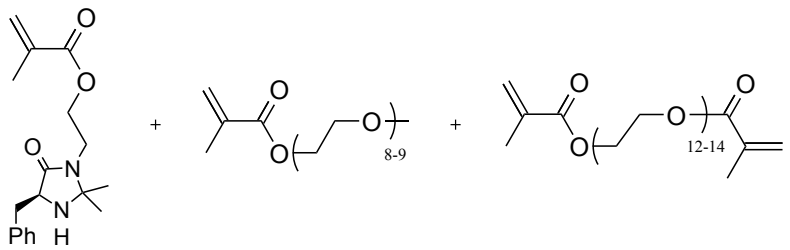

Figure 4.1: Monomer composition of PEG-methacrylic co-polymer supporting MacMillan's catalyst (**14**). For more information see Kristensen, T. E.; Vestli, K.; Jakobsen, M. G.; Hansen, F. K.; Hansen, T. *J. Org. Chem.* **2010**, 75, 1620–1629.

4.4 Experimental design for the 1,4-addition of N-methylpyrrole on cinnamaldehyde catalyzed by polymer-supported MacMillan catalyst

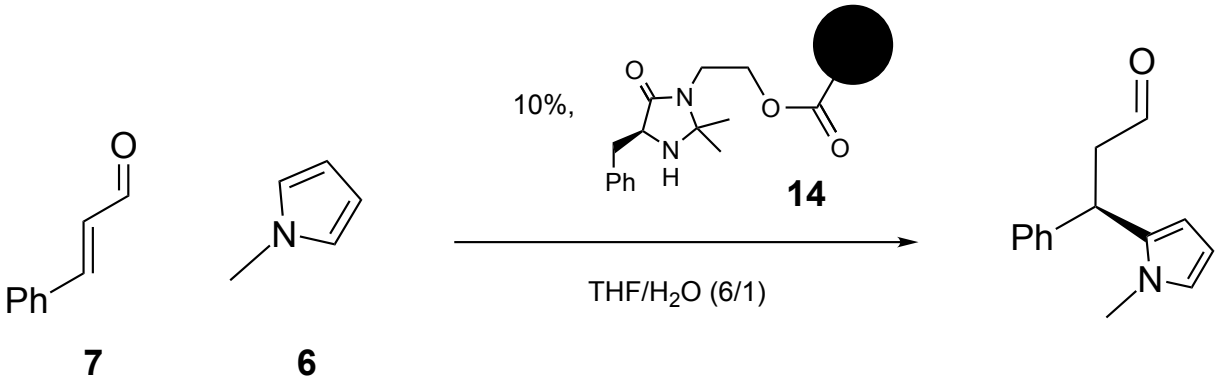

In a Schlenk tube were added in the following order catalyst **14** (156 mg, 10 %), solvent (THF/H_2O 6:1, 2.5 mL), **7** (126 µL, 1 eq.), **6** and **TFA**. The tube was closed with a glass stopper and left to react either at r.t., in an ice bath (10 °C) or in the fridge (4 °C), without stirring.

At intervals of 2, 4 and 24 h a small portion of crude solution without polymer beads was analyzed by ^{1}H-NMR and yields were calculated on the resulting crude NMR.

Entry	Temperature [°C]	TFA [eq.]	6 [eq.]	Yield
1	r.t.	0	1	0
2	r.t.	0	5	0
3	r.t.	0.1	1	0
4	r.t.	0.1	5	traces
5-6-7	10 °C	0.05	3	19% - 22% - 15%
8	4 °C	0	1	0
9	4 °C	0	5	0
10	4 °C	0.1	1	38%
11	4 °C	0.1	5	33%

Table 4.3: Experimental design for the synthesis of (R)-3-(1-methyl-1H-pyrrol-2-yl)-3-phenylpropanal catalyzed by *co*-polymer **14**. Equivalents are calculated with respect to **7**.

4.5 One-pot sequential Diels-Alder reaction and 1,4-addition on cinnamaldehyde

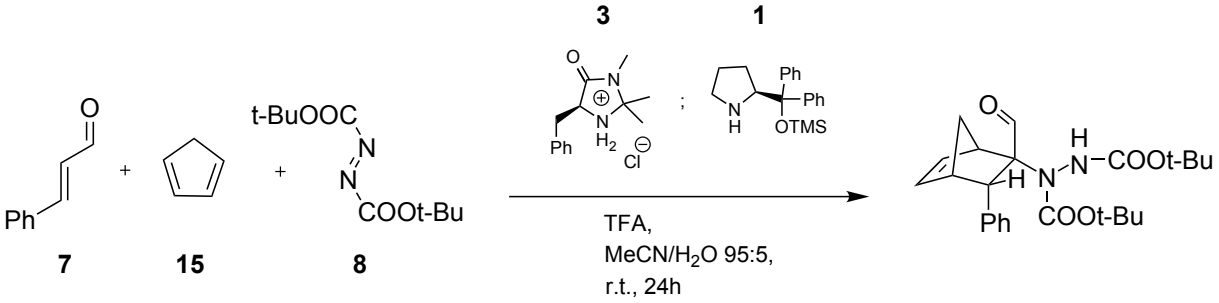

In a Schlenk tube fitted with magnetic stirrer were added catalyst **3**, **8** and the solvent ($MeCN/H_2O$ 95:5, 1 mL). When complete dissolution of powders occurred **7**, **15** and catalyst **1** were added in this order followed by the additive (0.1 mmol). The tube was then closed with a glass stopper.

After 24 h the reaction mixture was extracted using three portions of $NaHCO_{3(aq.)}$ (7 mL each); the aqueous layer was extracted using three portions of DCM (7 mL each). After extraction the organic layer was dried on $MgSO_4$, filtered and dried with rotavap.

The crude mixture was separated by flash chromatography (⌀= 2.5 cm, length = 9 cm, petroleum ethers/ethyl acetate from 0% to 30% ethyl acetate). The product was dried with rotavap followed by high vacuum, then weighed.

Entry	7 [mmol]	15 [mmol]	8 [mmol]	3 [mol%]	1 [mol%]	Additive	Yield
1	1	3	1.5	10	10	TFA	15%[a]
2	1	3	-	10[e]	-	TFA	66%
3	-[b]	-	0.7	-	10[c]	Ac. acid	-[d]

Table 4.4: Yields and mol % are calculated with respect to **7**. **a**) Only Diels-Alder product is isolated, but no 1,2-addition product is observed. **b**) the product from entry 1 was used as starting reagent; **c**) catalyst **16** was used as a catalyst instead of **1** (see Figure 4.2); **d**) no conversion. The starting reagent was recovered quantitatively; **e**) **14** was used as a catalyst instead of **3** (see Figure 4.1).

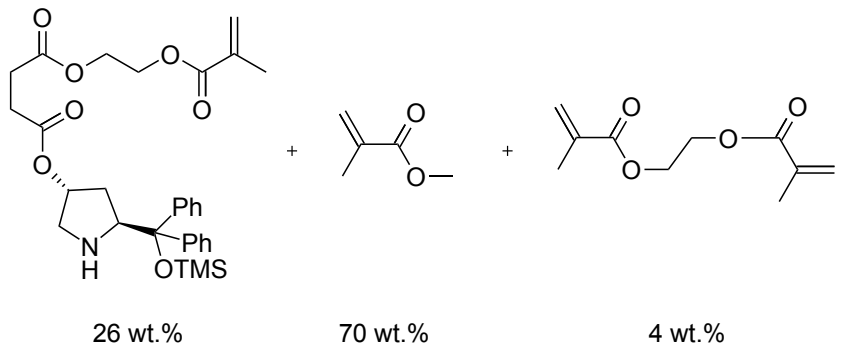

Figure 4.2: Monomer composition of PEG-methacrylic co-polymer supporting Jørgensen's catalyst (**16**). For more information see Kristensen, T. E.; Vestli, K.; Jakobsen, M. G.; Hansen, F. K.; Hansen, T. *J. Org. Chem.* **2010**, 75, 1620–1629.

4.6 Synthesis of 3-phenylbicyclo [2.2.1]hept-5-ene-2-carbaldehyde

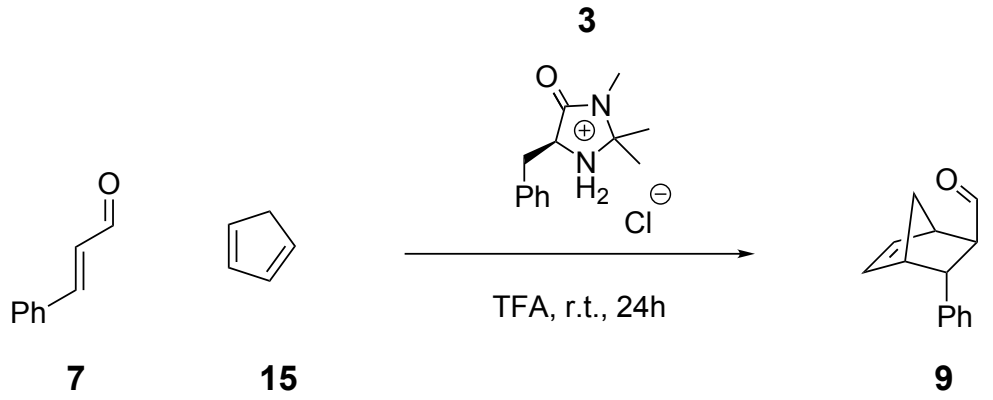

7 **15** **9**

In a Schlenk tube fitted with magnetic stirrer were added catalyst **3** and 1 mL of solvent. When complete dissolution of catalyst occurred, **15**, **7** and **TFA** were added, followed by 1 mL of solvent. The tube was then closed with a glass stopper.

After 24 h the reaction mixture was extracted using one portion of DCM (20 mL) and two portions of $NaHCO_{3(aq.)}$ (10 mL); the aqueous layers were extracted with two portions of DCM (10 mL); the organic layers were then dried with $MgSO_4$, filtered and dried with rotavap.

The crude product was separated by flash chromatography (⌀= 2.5 cm, length = 7 cm, petroleum ethers/ethyl acetate from 0% to 30% ethyl acetate). The resulting 3-phenylbicyclo [2.2.1]hept-5-ene- 2-carbaldehyde (**9**) was dried with rotavap followed by high vacuum, then weighed.

Entry	7 [mmol]	15 [mmol]	3 [mol%]	Solvent	Additive	Yield
1	1	3	10	Acetone/H_2O 1:1	**TFA**	59%
2	1	3	10	H_2O	**TFA**	40%

Table 4.5: Reaction conditions for the synthesis of 3-phenylbicyclo[2.2.1]hept-5-ene-2-carbaldehyde. Yields and mol % are calculated with respect to **7**.

4.7 Organocatalyzed aldol reaction between acetone and 3-phenylbicyclo[2.2.1]hept-5-ene-2-carbaldehyde

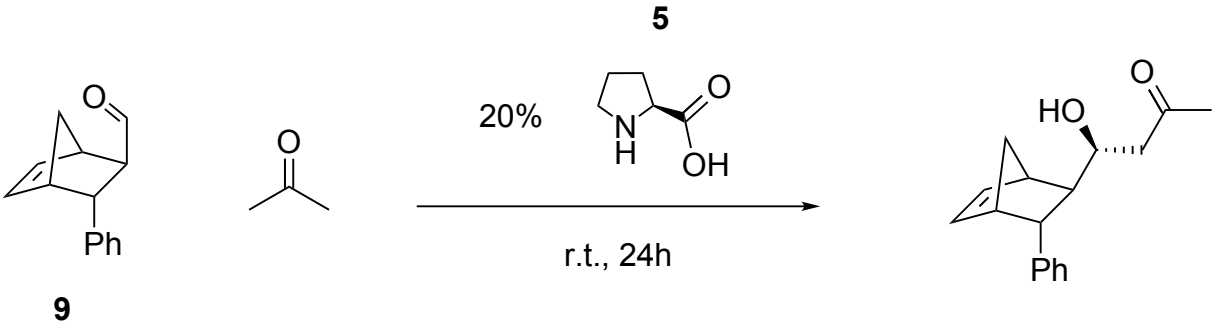

In a Schlenk tube were added in the following order under constant stirring catalyst **4**, solvent, and a solution of **9** in acetone.

After 24 h the reaction mixture was extracted using one portion of DCM (20 mL) and two portions of $NaHCO_{3(aq.)}$ (10 mL); the aqueous layers were extracted with two portions of DCM (10 mL); the organic layers were then dried with $MgSO_4$, filtered and dried with rotavap.

The crude product was analyzed by TLC and ^{1}H-NMR without further purification.

Entry	9 [mmol]	Acetone [mL]	4 [mol %]	Solvent	Yield
1	0.4	0.1	20	H_2O[a]	-[b]
2	0.35	1	20	DMSO/H_2O 4:1[c]	-[b]
3	0.4	0.2	20	DMSO[d]	-[b]

Table 4.6: Yields and mol % are calculated with respect to **9**. **a**) 0.5 mL of solvent used; **b**) **9** was recovered quantitatively; **c**) 5 mL of solvent used; **d**) **4** was dissolved in the minimum volume of water prior to addition.

4.8 Synthesis of 3-phenyl-2-propynal

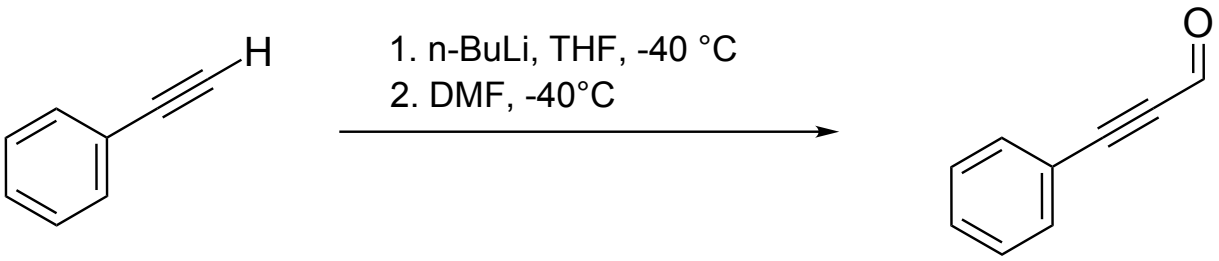

17 **18**

A three-necked round bottom flask (250 mL) with magnetic stirrer was fitted with balloon, rubber septum, and was connected to an Ar/vacuum line. The flask was exposed to three vacuum/Ar cycles, then cooled down to –45 °C in an acetone/dry ice bath. All the chemicals were added via syringe through the rubber septum.

Dry THF (50 mL) was added, followed by phenylacetylene **17** (2.26 mL, 20.6 mmol, 1 eq.); after 5 min a solution of n–BuLi in hexane was added dropwise (10 mL, 2 M, 20 mmol, 1 eq.), followed by the one portion addition of DMF (3.24 mL, 40 mmol, 2 eq.).

After 30 min the reaction was removed from the dry ice bath and let to warm up to r.t. in about 1 h. The mixture was quenched with 100 mL of $KH_2PO_{4(aq.)}$ 10 % solution, extracted with 100 mL of MTBE; the organics were extracted with two portions of water (80 mL); the aqueous layers were extracted with one portion of MTBE (60 mL).

The organics were then dried on $MgSO_4$, filtered and dried with rotavap to obtain the expected product in good purity. The resulting 3-phenyl-2-propynal (**18**) was weighed for 2.541 g (19.5 mmol, 94% yield).

4.9 Synthesis of 1-nitro-4-phenylbut-3-yn-2-ol

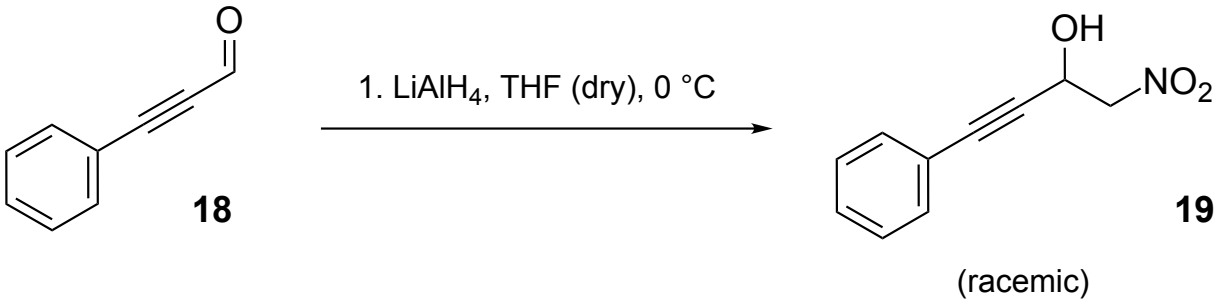

18 **19**

(racemic)

A three-necked round bottom flask (250 mL) with magnetic stirrer was fitted with a balloon and was connected to an Ar/vacuum line. $LiAlH_4$ was added to the flask and the last neck was closed with a rubber septum. The flask was exposed to three vacuum/Ar cycles and cooled down to −3 °C in an ice bath. All the chemicals were added via syringe through the rubber septum.

Dry THF was added (100 mL) under constant stirring; after 5 min nitromethane (5.5 mL, 124 mmol) was added dropwise and let react for 15 min. **18** synthesized as shown in Section 4.8 was then dissolved in a small volume of dry THF and added in one portion.

After 14 h the mixture was quenched and extracted with 100 mL of $HCl_{(aq.)}$ 1 M; the aqueous layer was extracted with two portions of DCM (100 mL each), and the organics were extracted with one portion of water (50 mL). The organics were then dried on $MgSO_4$ and with rotavap.

The product was weighed for 3.487 g (18.0 mmol, 92% yield). Purity of the resulting 1-nitro-4-phenylbut-3-yn-2-ol (**28**) was confirmed by ^{1}H-NMR and ^{13}C-NMR.

4.10 Synthesis of (E)-(4-nitrobut-3-en-1-yn-1-yl)benzene

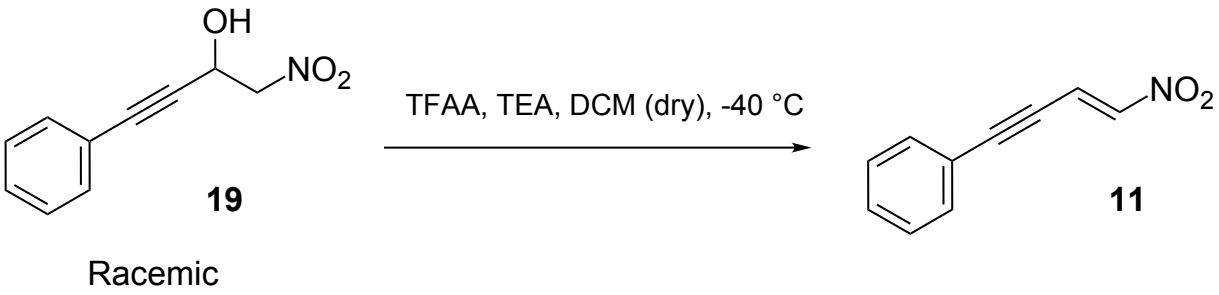

19 **11**

Racemic

The same setup discussed in Section 4.8 was used for this reaction.

The **28** synthesized as shown in Section 4.9 was added to the reaction flask, along with DCM as solvent (180 mL). Under constant stirring **TFAA** was added dropwise, followed by dropwise addition of **TEA**. 5 min after the addition of **TEA** the solution was removed from the acetone/dry ice bath and allowed to reach r.t. under constant stirring.

The reaction mixture was quenched with 100 mL of $NH_4Cl_{(aq.)}$. The organics were extracted with brine (100 mL) and water (100 mL); the aqueous layers were extracted with DCM (100 mL). The organics were then dried on $MgSO_4$ and with rotavap.

The crude mixture was purified by flash chromatography (⌀= 3 cm, length = 10 cm, petroleum ethers/ethyl acetate from 0% to 10% ethyl acetate). The product was dried with rotavap followed by high vacuum, then weighed for 1.562 g (15 mL, 9.02 mmol, 50% yield).

Purity of resulting (E)-(4-nitrobut-3-en-1-yn-1-yl)benzene (**11**) was confirmed by ^{1}H-NMR and ^{13}C-NMR. Overall yield starting from phenylacetylene (Section 4.8) is 44%.

4.11 Synthesis of O-(2-methacryloyloxyethylsuccinoyl) –*trans*–4-hydroxy-α,α-diphenyl- L-prolinol trimethylsilyl ether

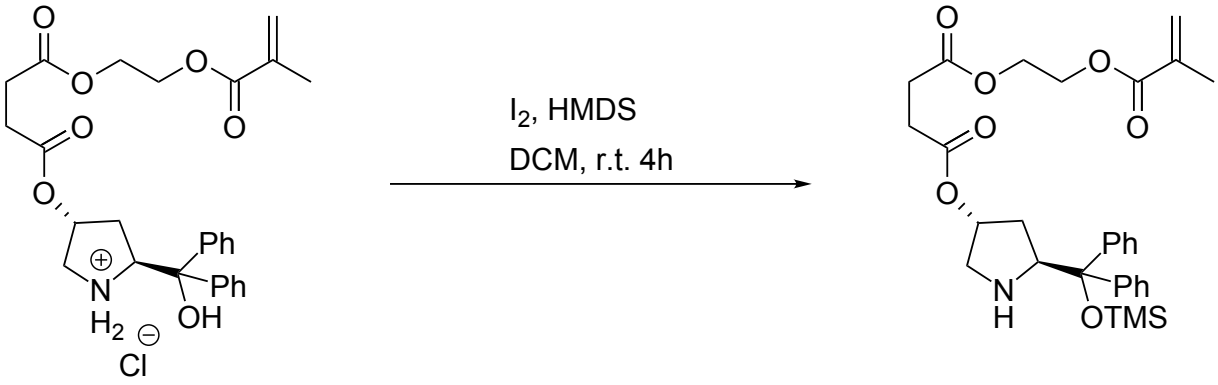

23 **22**

In a 100 mL round bottom flask with magnetic stirrer was added **23** (99.4 mg, 2 mmol) in DCM (6 mL), followed by 5 mL of 10% $K_2CO_{3(aq.)}$.

The biphasic solution was stirred vigorously for 5 min, then it was extracted with a separation funnel using 4 mL of DCM. The organics were dried over $MgSO_4$, filtered and transferred in a 100 mL round bottom flask provided with magnetic stirrer, along with 2 mL more of DCM. Under constant stirring was added I_2 (54 mg, 0.2 mmol), followed by HMDS (628 µL, 3 mmol). The flask was closed with a rubber septum.

After 4 h the solution was quenched with methanol (4 mL) and dried with rotavap. 10 mL of DCM were added to the crude product, followed by 10 mL of 10% $Na_2S_2O_{3(aq.)}$. The biphasic solution was then stirred vigorously for 30 min; reduction of iodine was followed by quick and drastic decoloration of the organic layer from dark red to light brown. After 30 min, 1 g of solid $Na_2S_2O_3$ was added to the solution, but no further decoloration occurred, indicating complete reduction of I_2.

The biphasic solution was extracted with two portions of H_2O (15 mL each), and with two portions of DCM (20 mL each). The organics were dried over $MgSO_4$, then rotavap and high vacuum.

Product purity was confirmed by NMR (quantitative yield). O-(2-methacryloyloxyethylsuccinoyl) –*trans*–4-hydroxy-α,α-diphenyl- L-prolinol trimethylsilyl ether (**22**), a brown and very vis-

cous oil, was used without further purification.

4.12 Polymerizations

General procedure: A two-necked 50 mL round bottom flask with oval stirring magnet (20 mm × 8 mm) was fitted with reflux condenser and placed into a heating mantle. An aqueous solution of PVA, KI (2 mg) and K_2CO_3 (15 mg, only **29**, **24** and **30**) was added to the flask and stirred at 500 rpm. A solution of toluene, 4-(diphenylphosphino) styrene (**20**) and $(CH_3)_2SAuCl$ (**21**) was prepared in a different flask and stirred for 5 min; to this solution were then added the major monomer, cross-linker, AMBN (14 mg) and **22**. The organic solution was slowly added to the aqueous solution and Ar was flushed into the reaction vessel for 1 min. The second neck was then closed with a glass stopper and Ar was let into the reaction vessel trough a rubber septum placed on top of the reflux condenser for 5 min. The stirring was increased up to the reported values to create a suspension, which was then polymerized for 18 to 24 h under Ar atmosphere. All polymerizations in presence of **21** were carried out in absence of light.

Figure 4.3: Polymerization apparatus.

After completion of polymerization the suspension was cooled at r.t. and poured into a beaker with 20 mL of water. The polymer beads were precipitated with 70 mL of methanol, decanted and the water/methanol solution was removed. The beads were washed/decanted with 40 mL of methanol three more times, then the beads were vacuum-filtered using 100 mL of water.

The beads were dried for 24 h under high-vacuum in a desiccator and weighed. All high vacuum drying procedures in presence of **21** were carried out in absence of light. Microscope pictures of significant polymer beads are available in Appendix III.

N°	Organocatalyst loading [mmol g^{-1}]	Phosphine catalyst loading[mmol g^{-1}]	Catalyst ratio [22:20]
31	-	0.74[a]	-
32	-	0.75[a]	-
33	-	0.75[a]	-
34	-	0.05	-
35	-	0.05	-
25	0.04	0.04	1:1
36	0.08	0.04	2:1
29	0.08	0.04[a]	2:1
24	0.04	0.04	1:1
30	0.04	0.04	1:1
26	0.08	0.05	2:1
27	0.20	0.05	4:1

Table 4.7: Theoretical loading of polymer beads. **a**) no $(CH_3)SAuCl$ was used.

N°	PVA [mL] (wt.%)	Toluene [mL]	Monomer mixture	Cat. monomers [mg]	Stirring [rpm]	T [°C]	Yield[c]
31	6 (0.3)	0.6	**A**	**20** (288)	600	85	14 % (184 mg)
32	7 (0.6)	0.6	**B**	**20** (288)	550	85	20 % (256 mg)
33	7 (0.3)	1.1	**B**	**20** (288)	600	75	41 % (552 mg)
34	6 (0.3)	1.1	**A**	**20** (17); **21** (16)	750	75	28 % (312 mg)
35	7 (0.3)	1.1	**B**	**20** (16); **21** (14)	650	75	71 % (763 mg)
25	7 (0.3)	1.1	**B**	**20** (16); **21** (15); **22** (28)	700	75	82 % (908 mg)
36	7 (0.3)	1.1	**B**	**20** (16); **21** (14); **22** (56)	650	75	40 % (456 mg)
29	7 (0.3)[d]	1.1	**B**	**20** (16); **22**(28)	700	75	76 % (861 mg)
24	7 (0.3)[d]	1.1	**B**	**20** (16); **21** (15); **22** (28)	750	75	21 % (235 mg)
30	7 (0.3)[d]	1.1	**B**	**20** (16); **21** (15); **22** (55)	750	75	71 % (809 mg)
26	7 (0.3)	1.5	**B**	**20** (16); **21** (15); **22** (28)	700 →650[a]	75	35 % (384 mg)
27	7 (0.3)	1.1	**B**	**20** (16); **21** (15); **22** (112)	700 →650[b]	75	42 % (492 mg)

Table 4.8: Monomer mixture **A**: Styrene (1.14 mL, DVB (28 µL). Monomer mixture **B**: MMA (1.07 mL), EGDMA (36 µL). **a**) Stirring was changed after 2 h; **b**) Stirring was changed as soon as the reaction temperature reached 75 °C (30 min); **c**) Yield is calculated as the ratio of weighed beads vs. the weight of the combined monomers; **d**) K_2CO_3 was dissolved in the aqueous phase prior to addition of the monomers.

4.13 Enamine-catalyzed Michael addition of isovaleraldehyde on (E)-(4-nitrobut-3-en-1-yn-1-yl)benzene

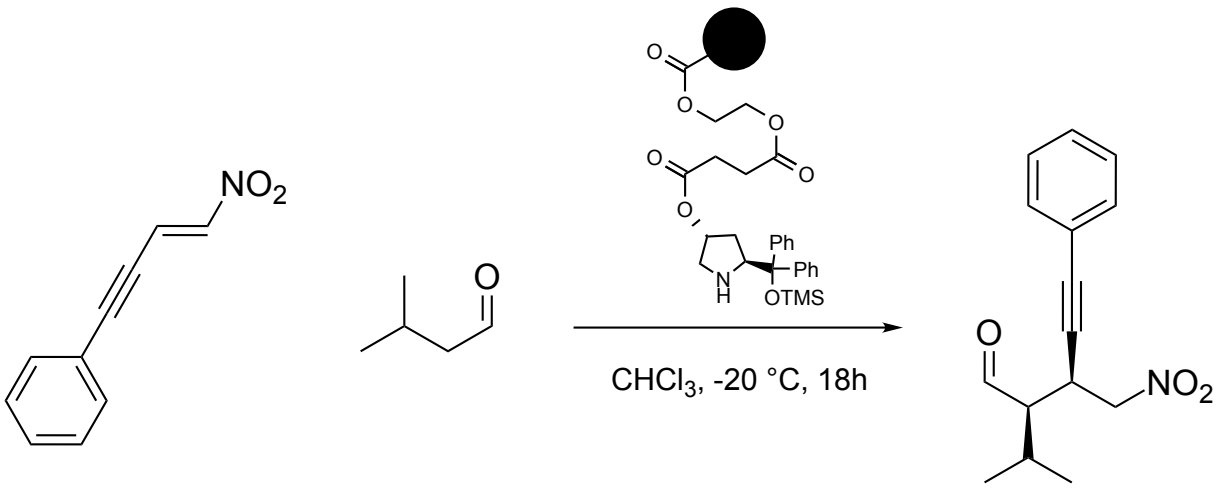

11 **10**

To a 25 mL round bottom flask with stirring magnet in acetone/dry ice bath was added the catalytic polymer, followed by **10** and solvent (1 mL); after 5 min under stirring (400 rpm) the polymer beads were fully swollen, and **11** was added, along with the remaining solvent.

After 18 h the reaction was quenched with 20 mL of $NH_4Cl_{(aq.)}$. The organics were extracted with water (15 mL); the aqueous layer was then extracted with two portions of DCM (15 mL each). The organics were dried on $MgSO_4$ and by rotary evaporation.

The resulting oil was separated by flash chromatography (⌀= 2.5 cm, length = 7 cm, petroleum ethers/ethyl acetate from 0% to 20% ethyl acetate). The resulting product (**19**) was dried with rotavap and high vacuum, then weighed.

Entry	11 [mmol]	10 [mmol]	Catalyst [mol%]	Solvent [mL]	T [°C]	Time	Yield
1	0.94	10	**16** 10%	$CHCl_3$ 9	-35 → rt	14 h	71%
2	1.69	16	**16** 10%	$CHCl_3$ 15	-35 → rt	18 h	60%[a]
3	0.15	1.5	**16** 10%	$CHCl_3$ 2	rt	7 days	Quant.
4	0.15	1.5	**24** 10%/10%	$CHCl_3$ 5	rt	7 days	Quant.

Table 4.9: Yields and mol% are calculated with respect to **11**. **a**) Column size used ⌀= 3 cm, length = 10 cm.

4.14 Gold(I)-catalyzed cyclization

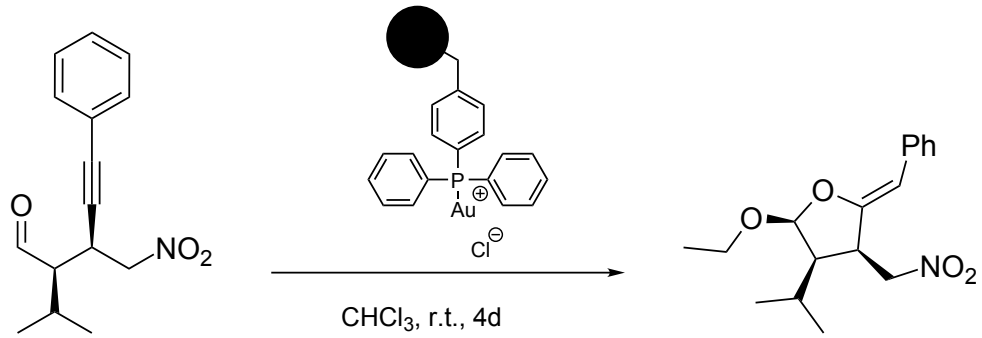

In a Schlenk tube were added the phosphine, **21** and 0.5 mL of $CHCl_3$, then the tube was cooled down at 0 °C with an ice bath. When complete swelling of the polymer beads occurred (5 min to 10 min) a reagent solution was prepared containing **19** (30 mg, 0.12 mmol, synthesized as shown in Section 4.13), *p*-TsOH (2 mg, 0.012 mmol), $AgBF_4$ (1 mg, 0.006 mmol), ethanol (21 µL, 0.36 mmol) and $CHCl_3$ (4 mL). The reagent solution was then added to the polymer beads and the tube was closed with a glass stopper.

The reaction was quenched with H_2O 5 mL, filtered and extracted with three portions of DCM (5 mL each).

The crude was analyzed by ^{1}H-NMR and TLC in all cases, showing the presence of the same products in all reactions, albeit in different ratios and yields. Eluent solution was petroleum ethers/ethyl acetate 10% ethyl acetate.

Rf = 0.67, 0.40 (product, mixture of isomers), 0.27, 0.17, 0.11.

Entry 3 was separated by prep. TLC using the same eluent system and each fraction was analyzed by ^{1}H-NMR.

Entry	21 [mmol]	Phosphine [mg]	Time [day]	Conversion
1	0.006	**31** 16	4	traces
2	0.006	**33** 16	4	78%
3	-	**34** 152	4	Quant.
4	-	**35** 152	4	Quant.
5	0.01	PPh_3 3	1	52%
6	-	**35** 200	1	Quant.

Table 4.10: Gold(I)-catalyzed cyclization test reactions.

4.15 Assisted tandem enamine-catalyzed Michael addition, gold(I)-catalyzed cyclization

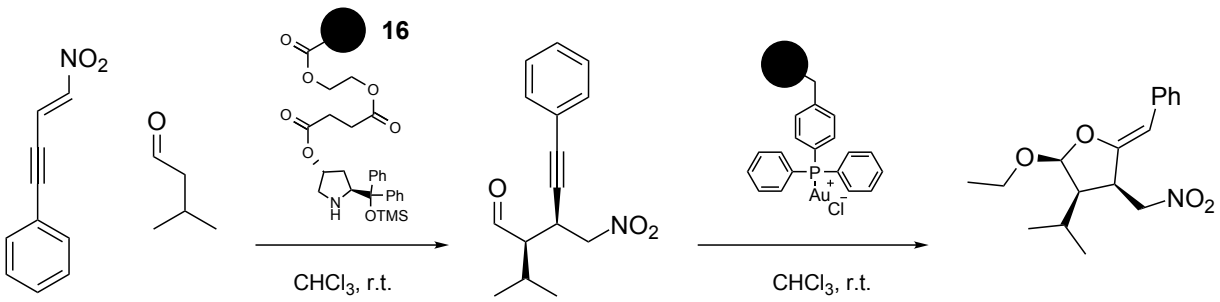

11 **10**

In a test tube were added the polymer beads, **11**, **10**, and $CHCl_3$. The tube was closed with a glass stopper and left to react for 24 h.

After 24 h ethanol, $AgBF_4$ (5 mol% of **11**), *p*-TsOH (10 mol% of **11**) and $CHCl_3$ were added, the tube was closed to light and the reaction was stopped only after 24 h.

The crude mixture was filtered with DCM (20 mL) and extracted with two portions of H_2O (20 mL each), two portions of DCM (20 mL each), then dried over $MgSO_4$, with rotavap and high vacuum.

Entry	Polymer [mg]	11 [mmol]	10 [mmol]	Ethanol [µL]	$CHCl_3$ [mL]	Yield[c]	Yield[d]
1	**32** 103; **16** 95	0.35	0.42	30	1.5	-[e]	<5%
2	**36** 103	0.41	0.47	30	1.5	-[e]	-
3	**25** 206	0.37	4	-[a]	4	-	-
4	**26** 209	0.37	4	46[b]	4	19%	11%
5	**27** 209	0.37	4	46	4	27%	19%

Table 4.11: Yields and are calculated with respect to **11**. **a**) Entry 3 was extracted after 24h, without proceeding to the second step; **b**) entry 4 was carried out in absence of $AgBF_4$ or *p*-TsOH; **c**) Michael adduct yield after 48h reaction time, prior to ethanol addition; **d**) cyclization product yield after 24h reaction from ethanol addition; **e**) yield not measured.

4.16 One-pot enamine-catalyzed Michael addition, gold(I)-catalyzed cyclization

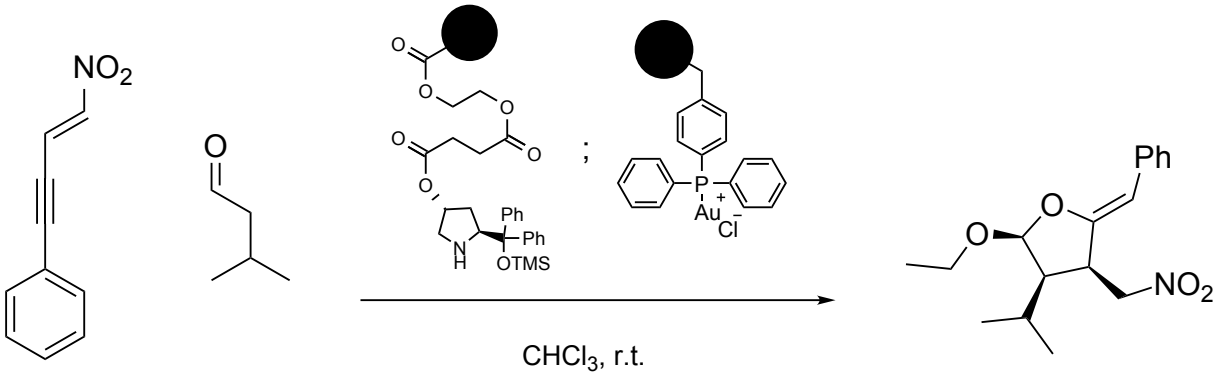

11 **10**

In a test tube were added the polymer beads, **11**, **10**, $CHCl_3$, ethanol, $AgBF_4$ (5 mol% of **11**), and *p*-TsOH (10 mol% of **11**). The tube was closed with a glass stopper and left to react in absence of light for 24 h. Entry 1 was initially placed in an ice bath (–5 °C).

The crude mixture was filtered with DCM (20 mL) and extracted with one portion of $NH_4Cl_{(aq.)}$ (20 mL), two portions of DCM (20 mL each) two portions of H_2O (20 mL each), two portions of DCM (20 mL each), then dried over $MgSO_4$, with rotavap and high vacuum.

Entry	Polymer [mg]	11 [mmol]	10 [mmol]	Ethanol [µL]	$CHCl_3$ [mL]	Yield
1	**27** 100	0.20	2	23	4[a]	-
2	**27** 100	0.20	2	23	4	-

Table 4.12: Reaction conditions for the one-pot enamine-catalyzed Michael addition, gold(I)-catalyzed cyclization. **a**) no *p*-TsOH.

Appendix I: Molecular Weight and Density of Chemicals

Name	Abbreviation	FW ($g\,mmol^{-1}$)	Density ($g\,mL^{-1}$)
(*5S*)-Benzyl-2,2,3-trimethylimidazolidin-4-one hydrochloride salt	**3**	254.8	-
(*S*)-Diphenyltrimethylsiloxymethyl-pyrrolidine	**1**	325.22	1.05
4-(Diphenylphosphino) styrene	**20**	288.32	-
Acetic acid		60.02	1.049
Azobis methylbutyronitrile	AMBN	192.26	-
Chloro(dimethylsulfide)gold(I)	**21**	294.55	-
Cyclopentadiene	**15**	66.10	0.786
Dimethylformamide	DMF	73.09	0.948
Di-tert-butyl azodicarboxylate	DBAD	230.26	-
Divinyl benzene	DVB	130.19	0.914
Ethanol	EtOH	46.07	0.789
Ethylene glycol dimethacrylate	EGDMA	198.22	1.051
Hexamethyldisilazane	HMDS	161.39	0.774
Iodine	I_2	253.81	-
Isovaleraldehyde	**10**	86.13	0.803
Lithium aluminium hydride	$LiAlH_4$	37.95	-
L-Proline	**4**	115.13	-
Methyl methacrylate	MMA	100.12	0.936
Nitromethane		61.04	1.137
N-Methylpyrrole	**6**	81.12	0.914
p-Toluenesulphonic acid monohydrate	*p*-TsOH	190.22	-
Phenylacetylene	**17**	102.13	0.93
Potassium Iodide	KI	166.00	-
Propionaldehyde	**12**	58.08	0.805
Silver tetrafluoroborate	$AgBF_4$	194.67	-
Sodium thiosulphate pentahydrate	$Na_2S_2O_3$	248.18	-
Styrene		104.15	0.909
trans-β-Nitrostyrene	**13**	149.15	-
trans-Cinnamaldehyde	**7**	132.16	1.05
Triethylamine	TEA	101.19	0.726
Trifluoroacetic acid	TFA	114.02	1.489
Trifluoroacetic anhydride	TFAA	210.03	1.487
Triphenylphosphine	PPh_3	262.29	-

Table 4.13: Molecular Weight and Density of Chemicals.

Appendix II: NMR Spectra

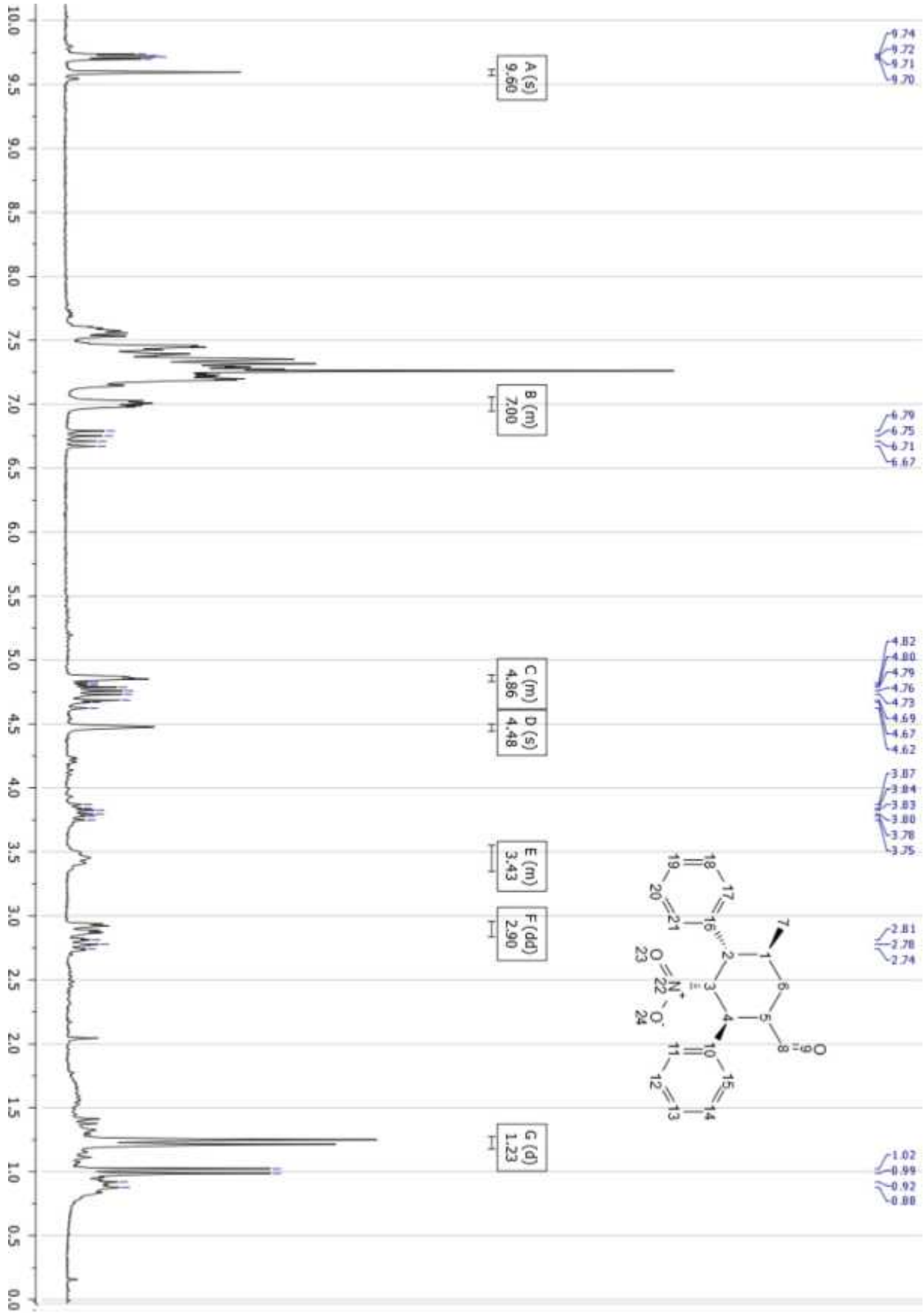

Figure 4.4: 1H NMR (200 MHz, CDCl3) 9.60 (s, 1H), 7.06 – 6.95 (m, *J* = 6.7, 2.7 Hz, 2H), 4.88 – 4.83 (m, 1H), 4.48 (s, 1H), 3.55 – 3.35 (m, *J* = 8.3 Hz, 1H), 2.90 (dd, *J* = 10.4, 3.2 Hz, 1H), 1.23 (d, *J* = 7.2 Hz, 3H).

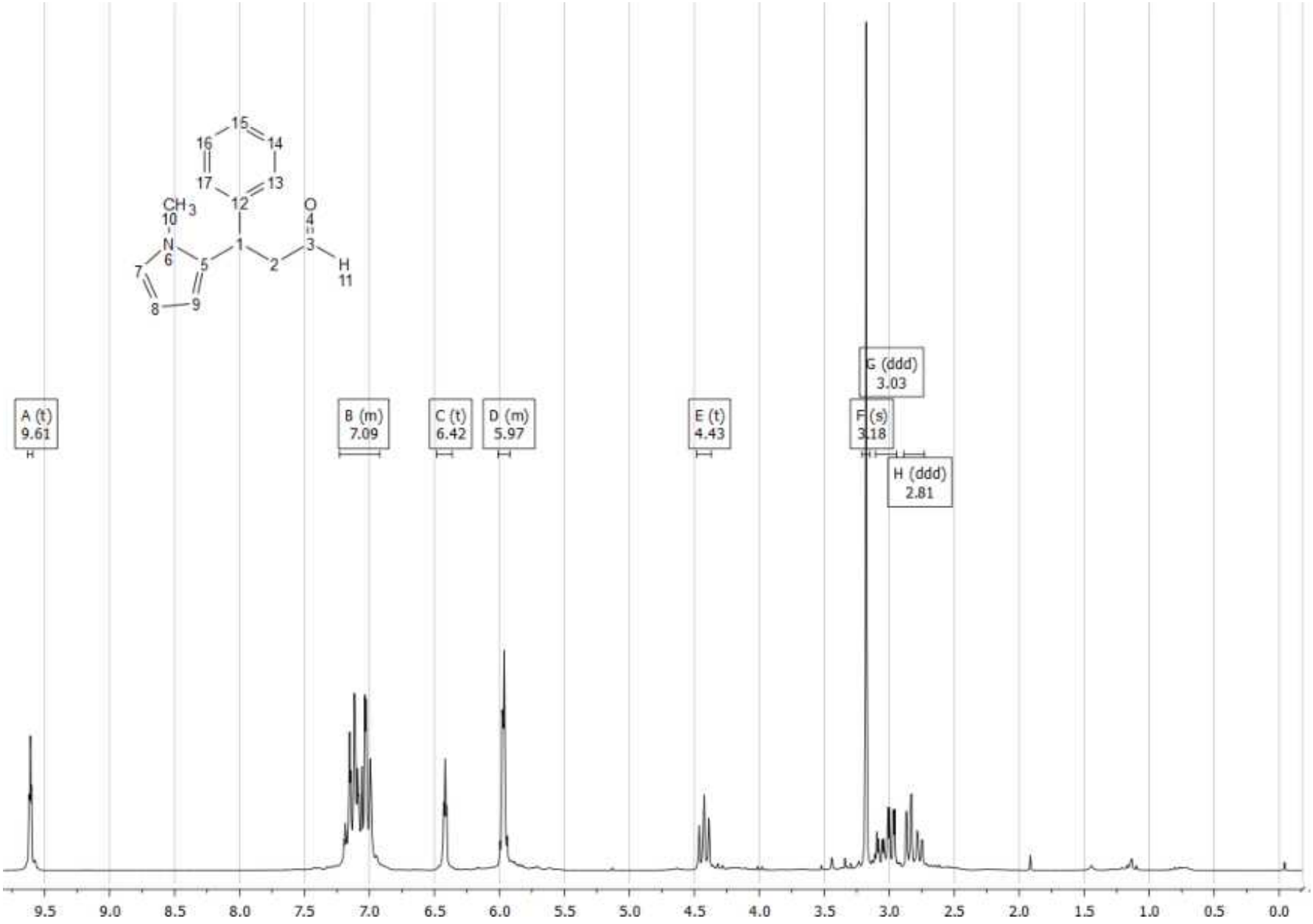

Figure 4.5: 1H NMR (200 MHz, CDCl3) 9.61 (t, J = 1.7 Hz, 1H), 7.23 – 6.92 (m, 7H), 6.42 (t, J = 2.2 Hz, 1H), 6.01 – 5.92 (m, 2H), 4.43 (t, J = 7.5 Hz, 1H), 3.18 (s, 3H), 3.03 (ddd, J = 17.1, 8.1, 2.1 Hz, 1H), 2.81 (ddd, J = 17.0, 7.0, 1.5 Hz, 1H).

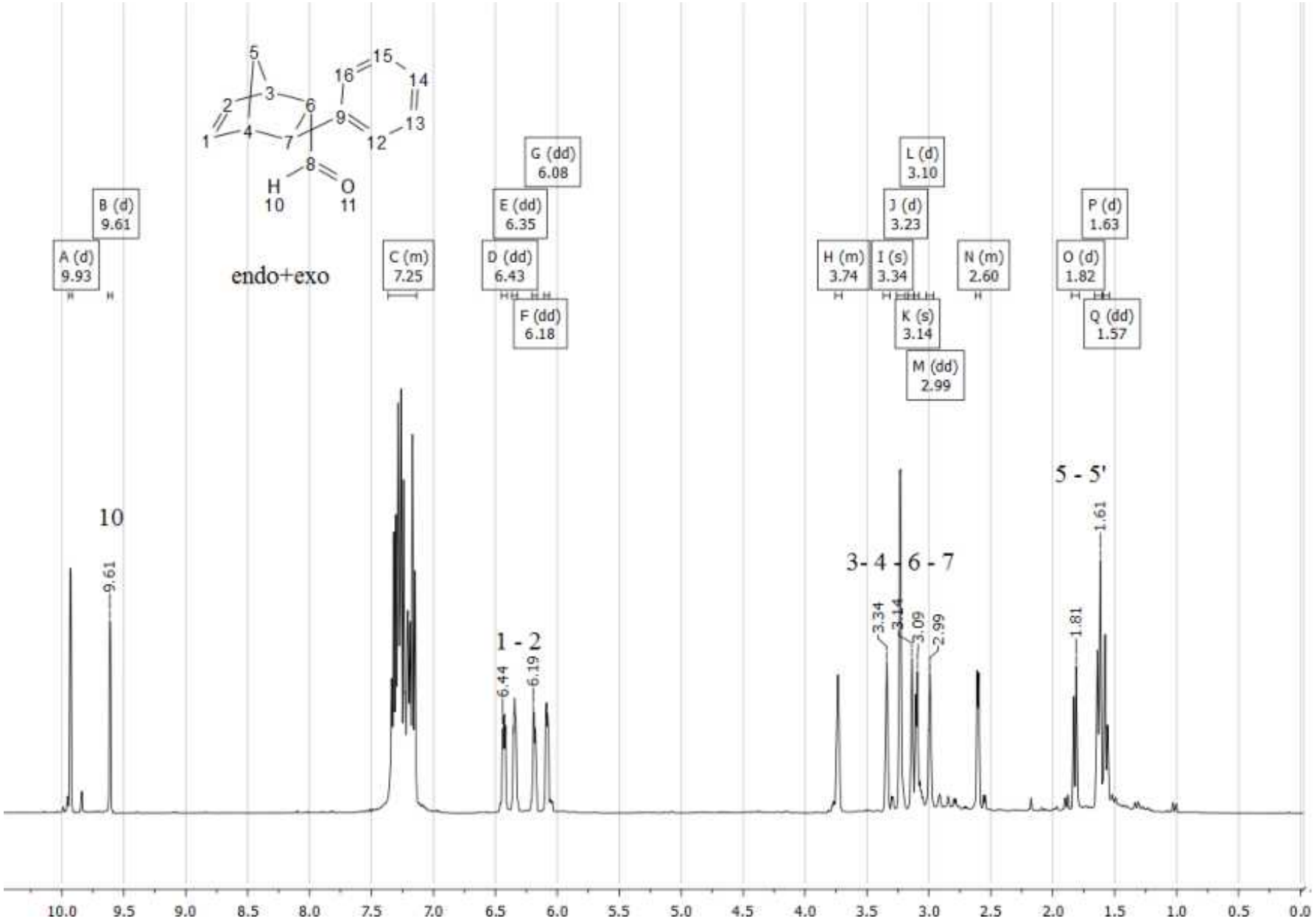

Figure 4.6: Mixture of end and exo isomers. Peak picking for the endo isomer is based on literature.[52] 1H NMR (400 MHz, CDCl3) 9.93 (d, J = 1.9 Hz, 1H), 9.61 (d, J = 2.1 Hz, 1H), 7.37 – 7.14 (m, 15H), 6.43 (dd, J = 5.4, 3.3 Hz, 1H), 6.35 (dd, J = 5.1, 3.2 Hz, 1H), 6.18 (dd, J = 5.6, 2.6 Hz, 1H), 6.08 (dd, J = 5.0, 2.4 Hz, 1H), 3.76 – 3.70 (m, 1H), 3.34 (s, 1H), 3.23 (d, J = 1.4 Hz, 3H), 3.14 (s, 1H), 3.10 (d, J = 4.9 Hz, 1H), 2.99 (dd, J = 6.2, 4.2 Hz, 1H), 2.63 – 2.58 (m, 1H), 1.82 (d, J = 8.7 Hz, 1H), 1.63 (d, J = 10.5 Hz, 3H), 1.57 (dd, J = 8.8, 1.5 Hz, 2H).

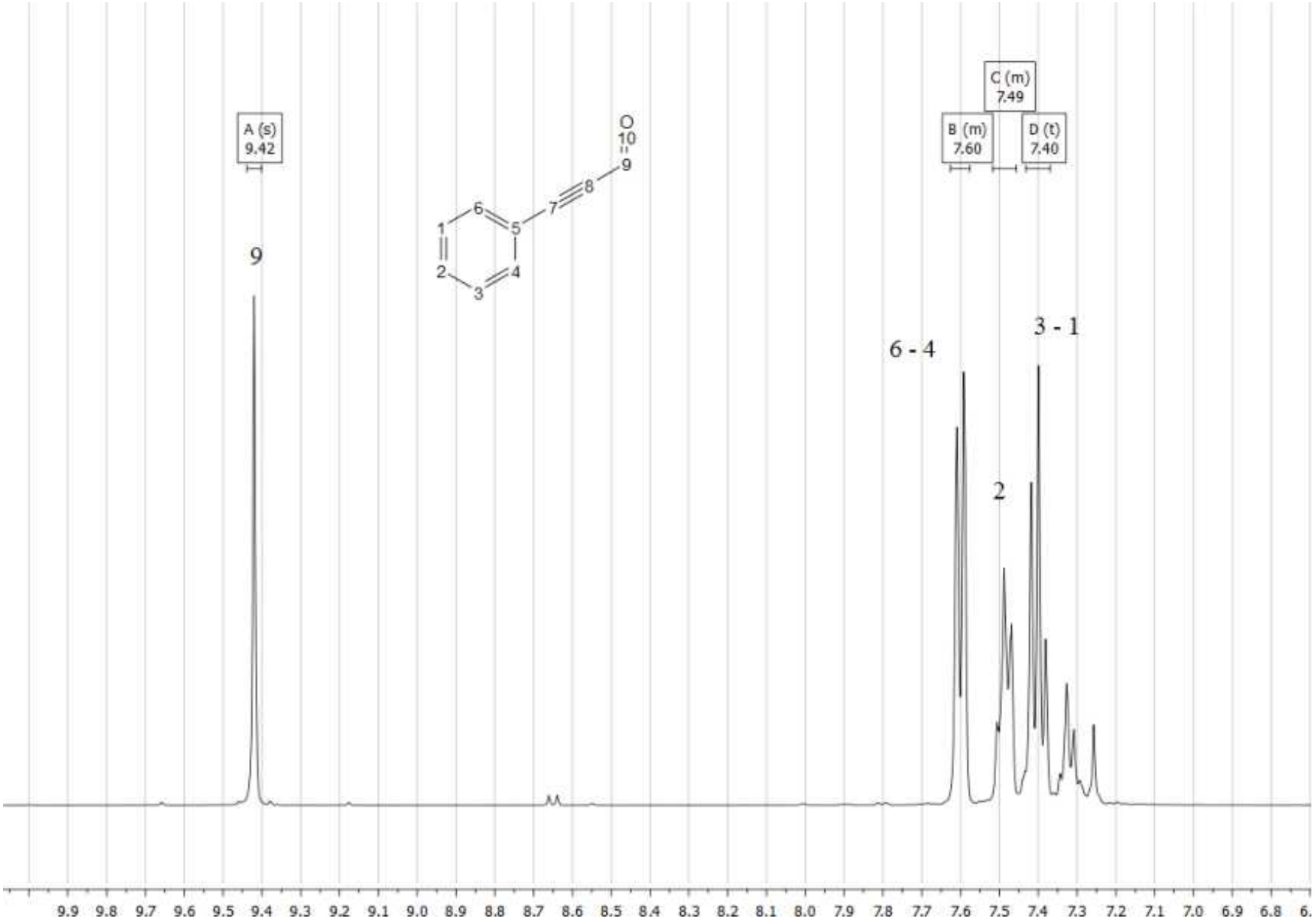

Figure 4.7: 1H NMR (400 MHz, CDCl3) 9.42 (s, 1H), 7.63 – 7.58 (m, 2H), 7.52 – 7.46 (m, 1H), 7.40 (t, J = 7.5 Hz, 2H).

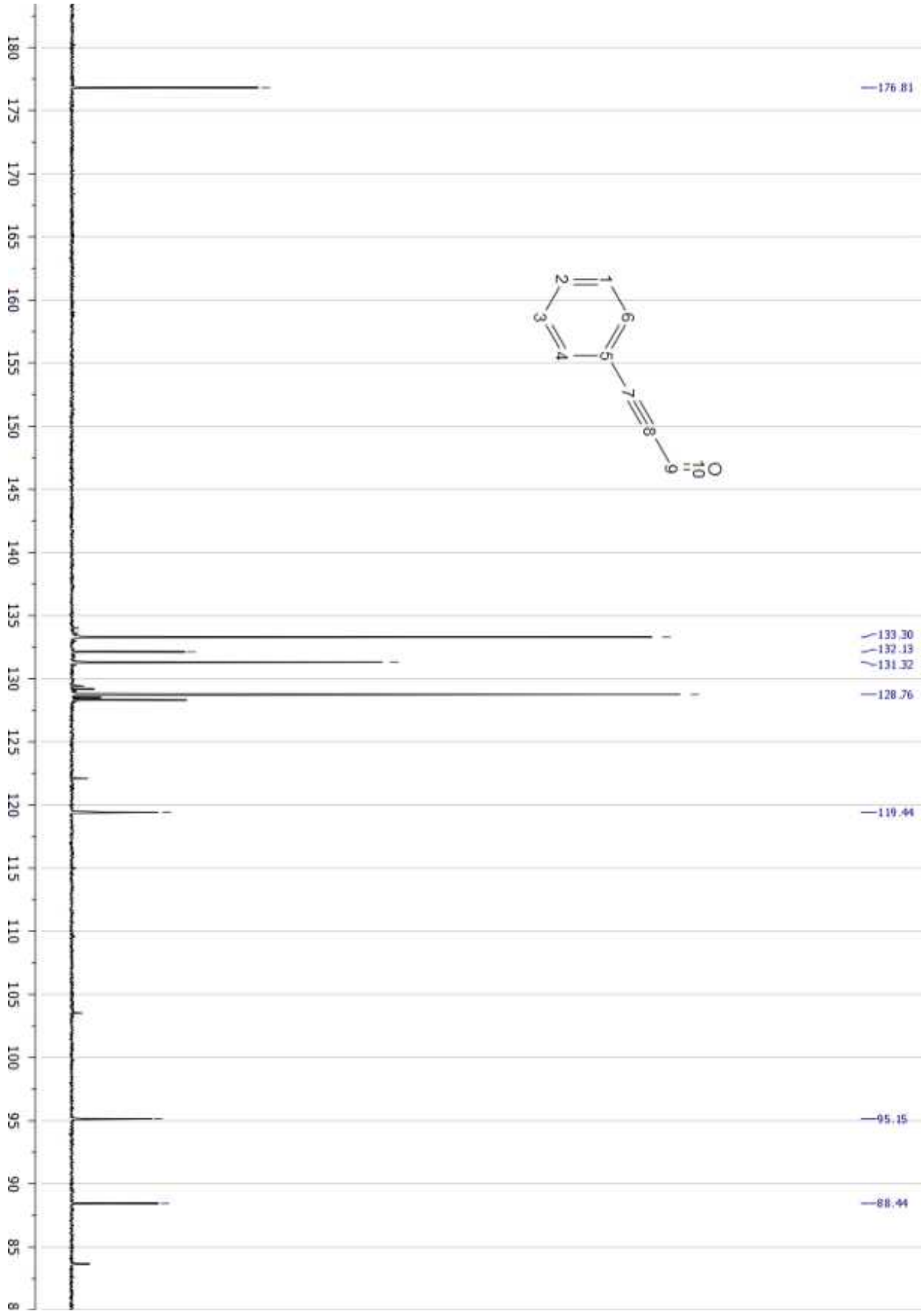

Figure 4.8: 13C NMR (101 MHz, CDCl3) 176.81, 133.30, 132.13, 131.32, 128.76, 119.44, 95.15, 88.44.

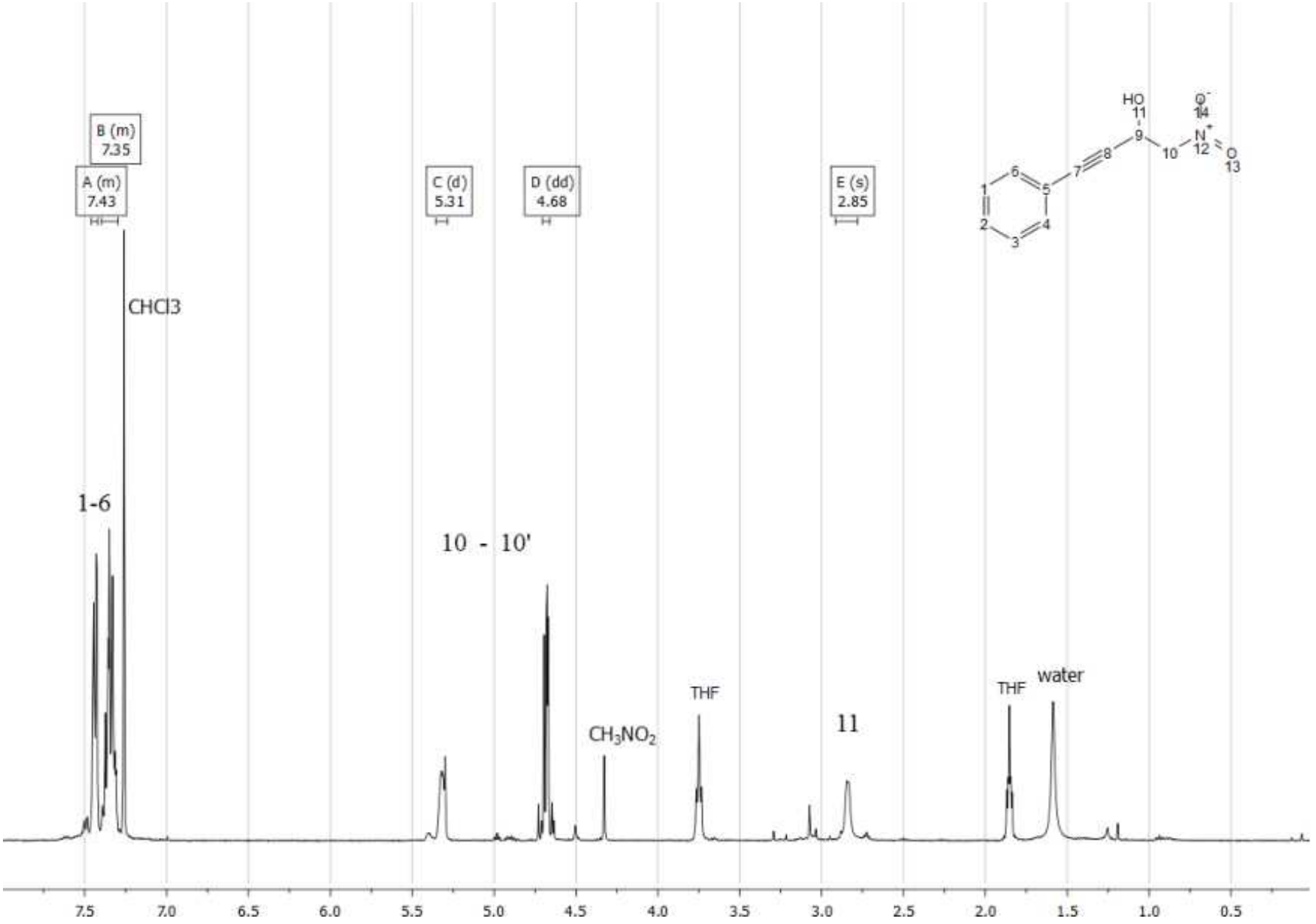

Figure 4.9: 1H NMR (400 MHz, CDCl3) 7.46 – 7.42 (m, 3H), 7.40 – 7.30 (m, 4H), 5.31 (d, J = 8.1 Hz, 1H), 4.68 (dd, J = 5.8, 4.1 Hz, 2H), 2.85 (s, 1H).

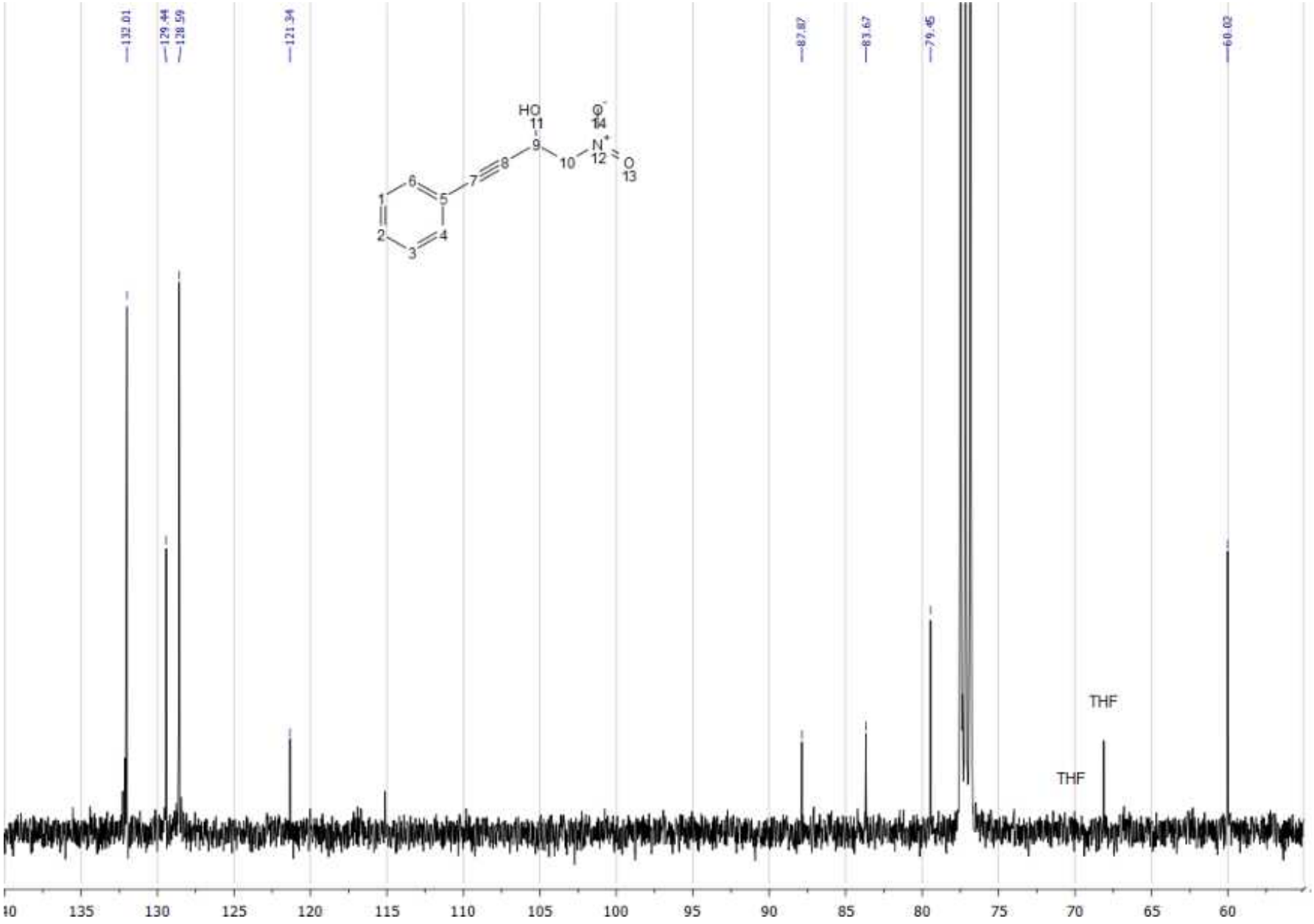

Figure 4.10: 1H NMR (400 MHz, CDCl3) 7.46 – 7.42 (m, 3H), 7.40 – 7.30 (m, 4H), 5.31 (d, J = 8.1 Hz, 1H), 4.68 (dd, J = 5.8, 4.1 Hz, 2H), 2.85 (s, 1H).

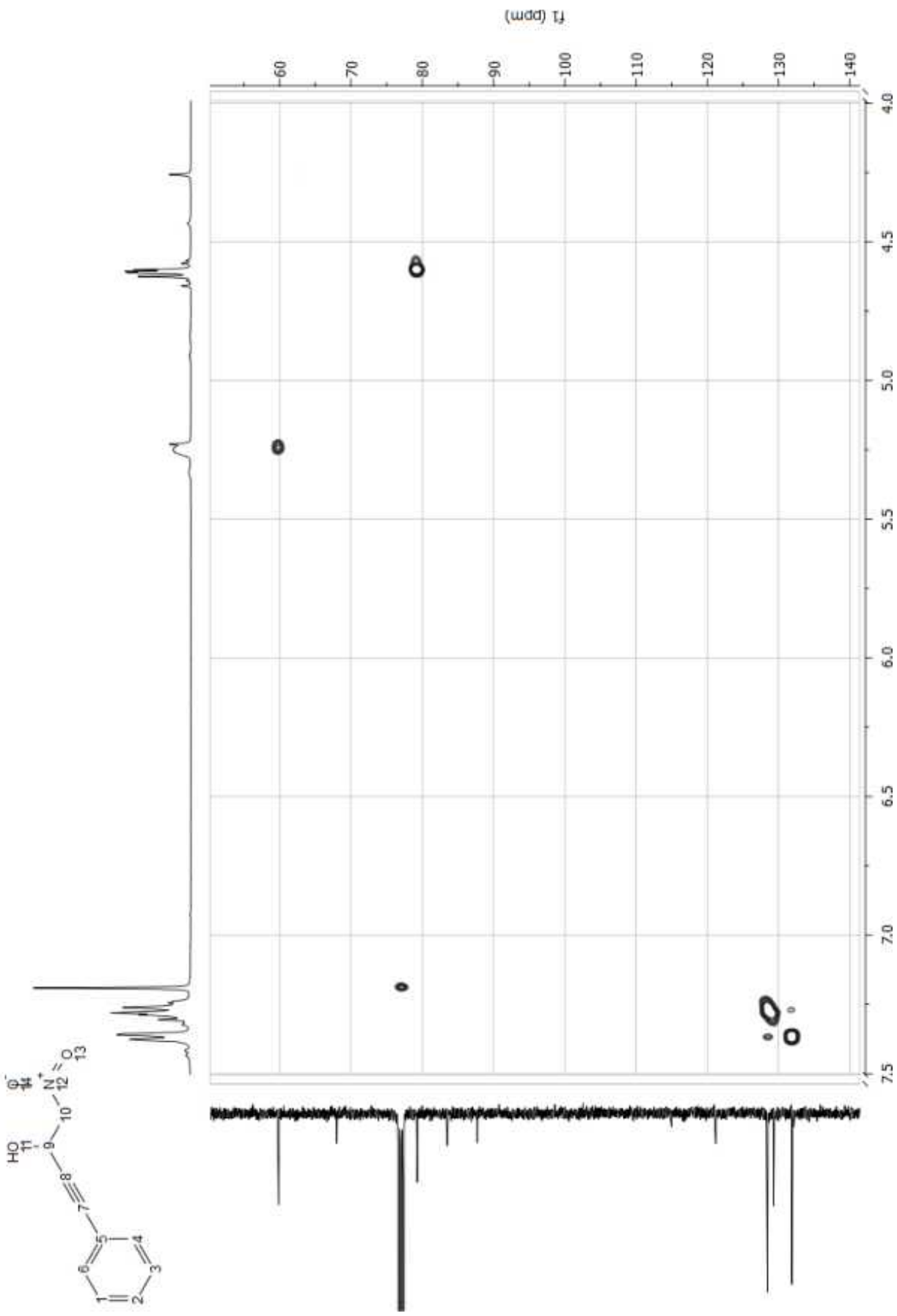

Figure 4.11: HSQC spectrum.

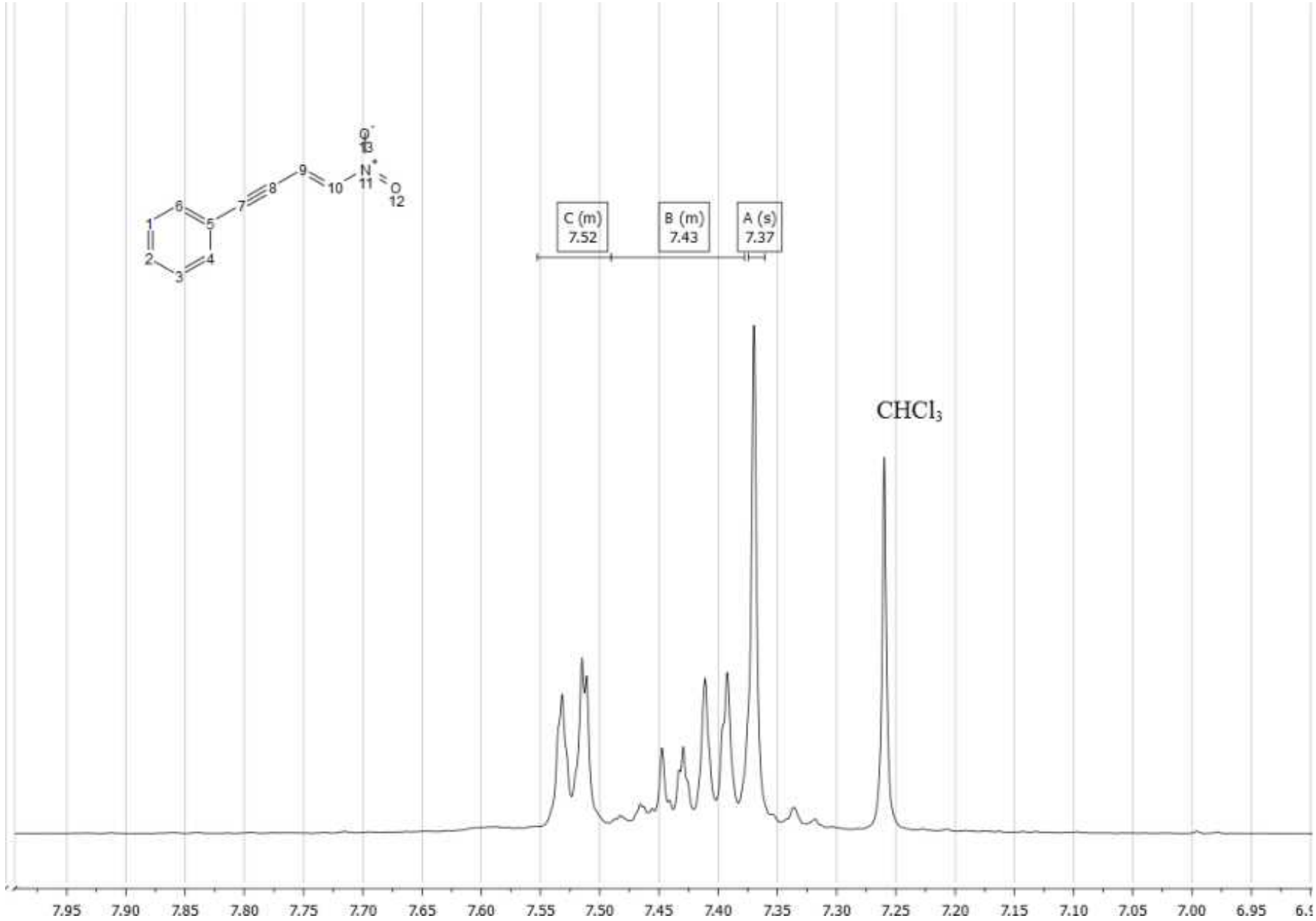

Figure 4.12: 1H NMR (400 MHz, CDCl3) 7.55 – 7.49 (m, 2H), 7.49 – 7.38 (m, 3H), 7.37 (s, 1H).

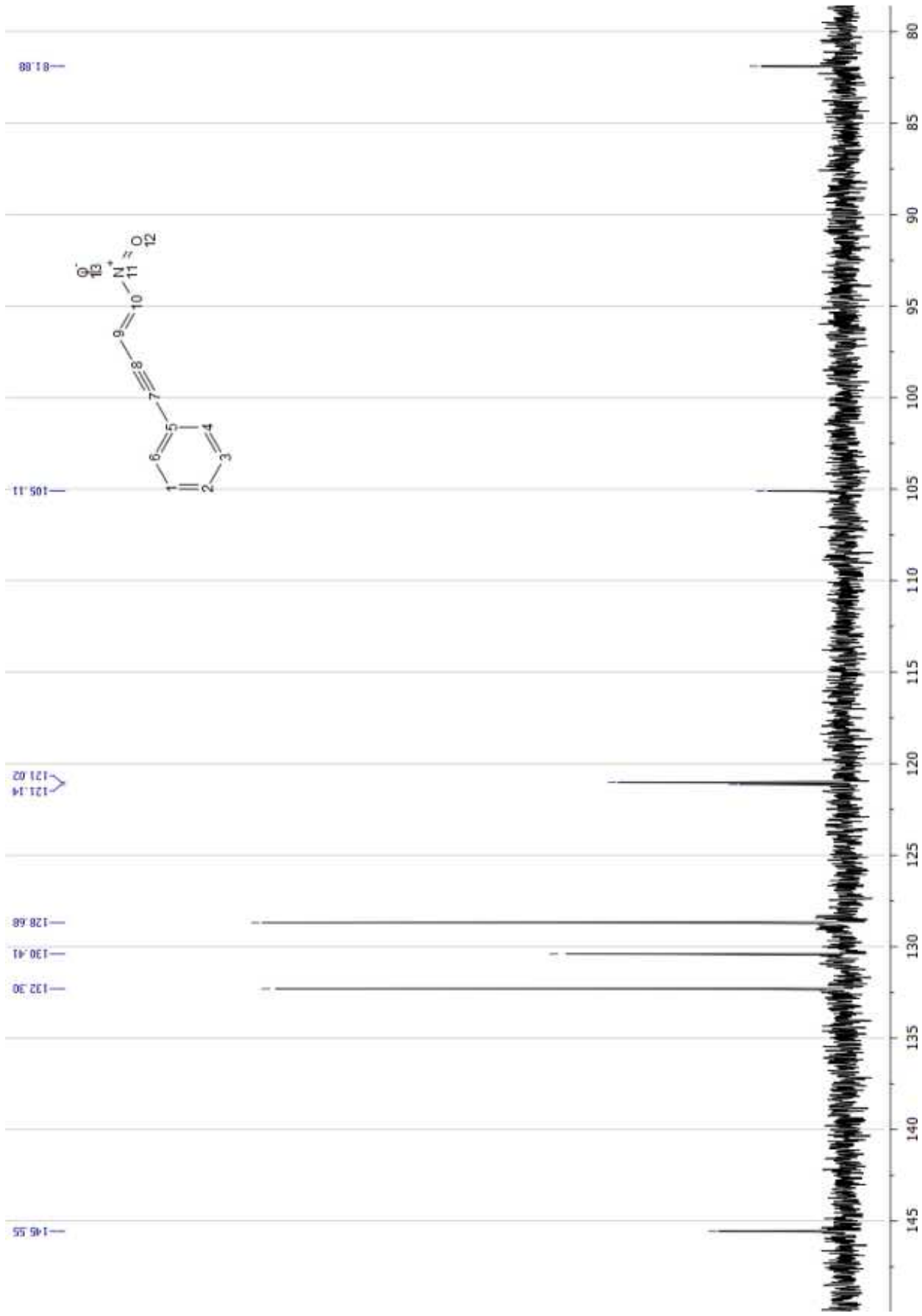

Figure 4.13: 13C NMR (101 MHz, CDCl3) 145.55, 132.30, 130.41, 128.68, 121.14, 121.02, 105.11, 81.88.

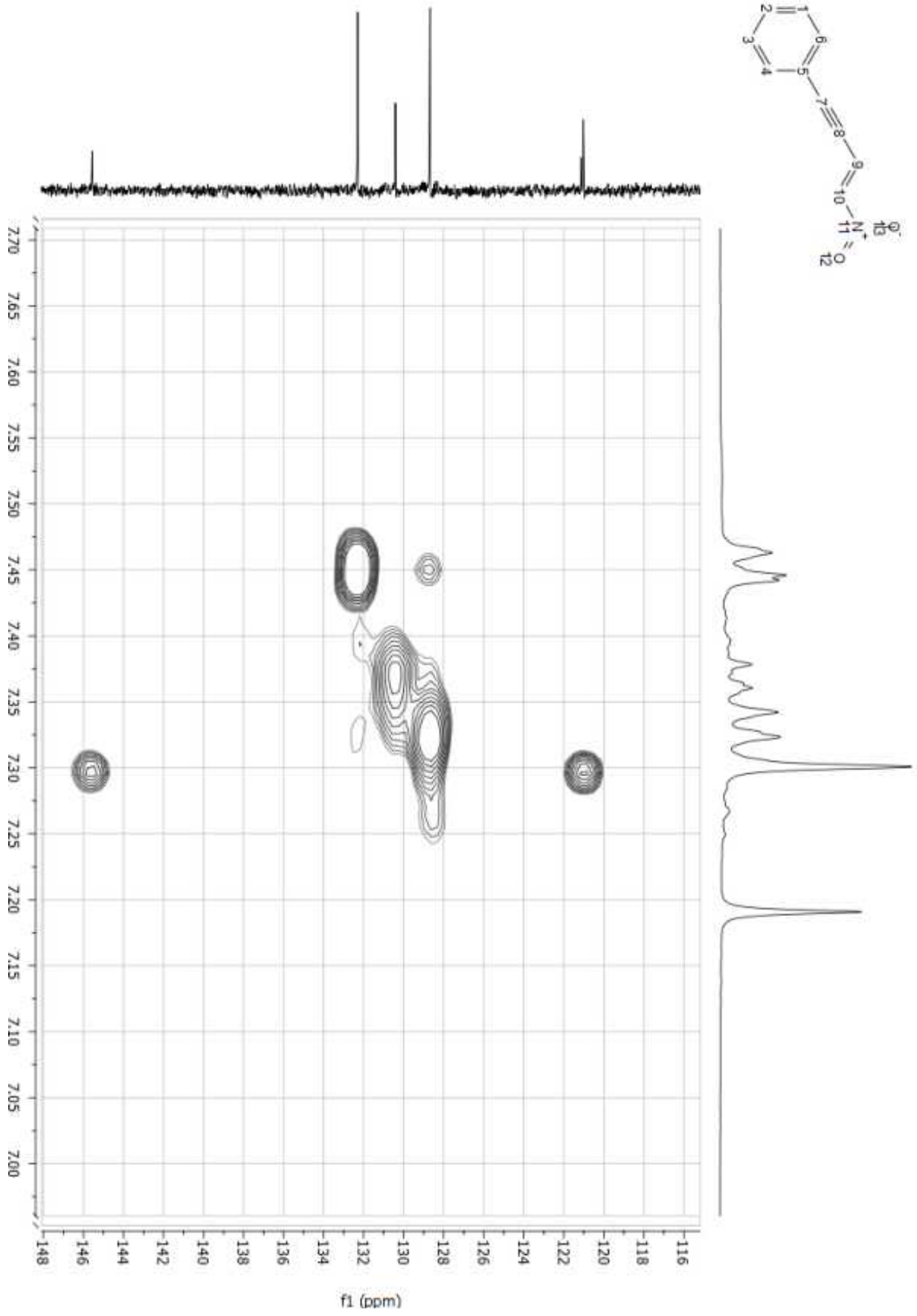

Figure 4.14: HSQC spectrum.

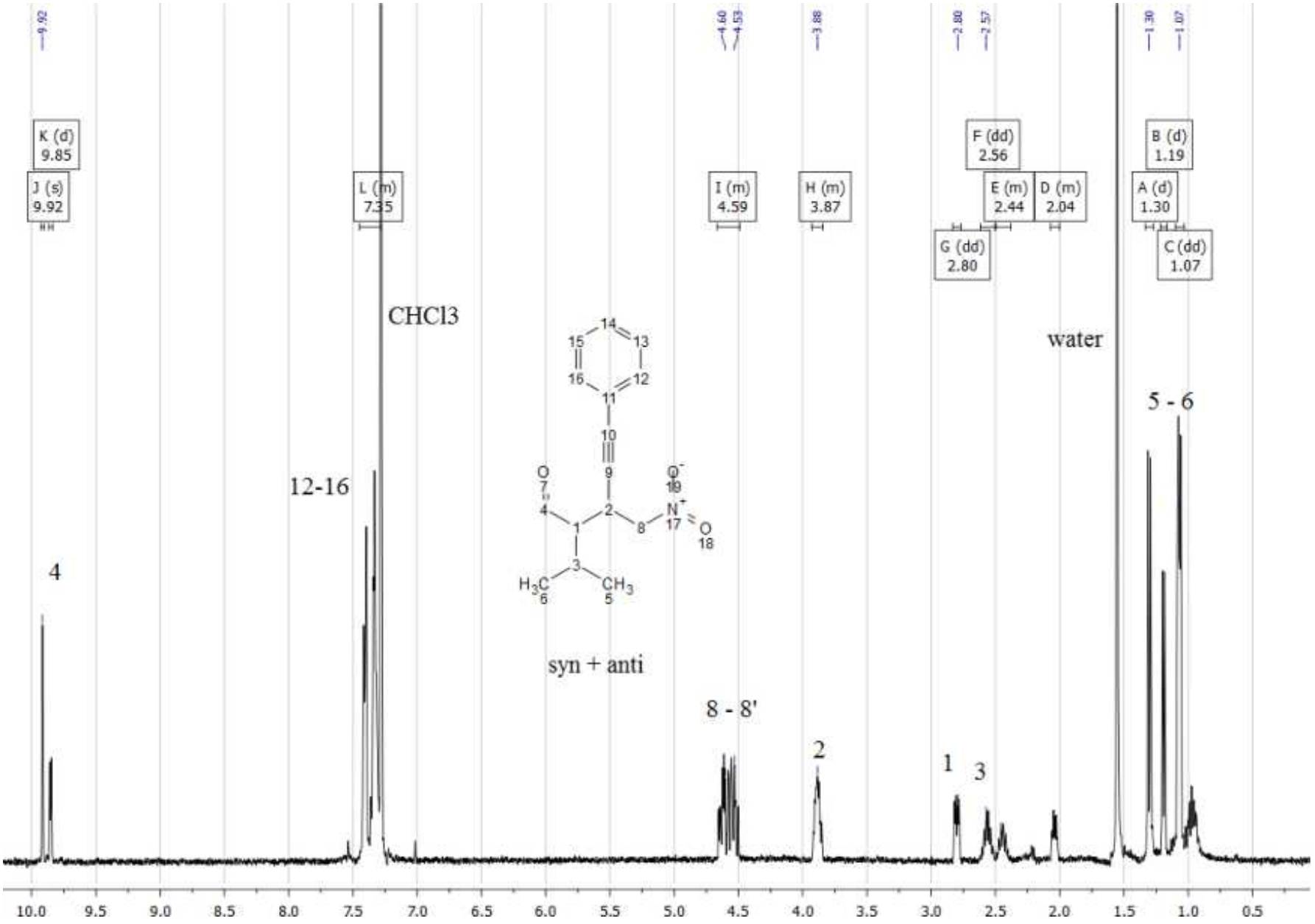

Figure 4.15: Mixture of syn and anti isomers. Peak picking for the syn isomer is based on literature and integral ratios.[37] 1H NMR (400 MHz, CDCl3) 9.92 (s, 1H), 9.85 (d, J = 4.0 Hz, 1H), 7.45 – 7.28 (m, 5H), 4.66 – 4.49 (m, 2H), 3.93 – 3.84 (m, 1H), 2.80 (dd, J = 9.4, 4.6 Hz, 1H), 2.56 (dd, J = 12.3, 7.0 Hz, 1H), 2.50 – 2.38 (m, 1H), 2.07 – 2.00 (m, 1H), 1.30 (d, J = 7.2 Hz, 2H), 1.19 (d, J = 6.7 Hz, 1H), 1.07 (dd, J = 6.7, 3.3 Hz, 3H).

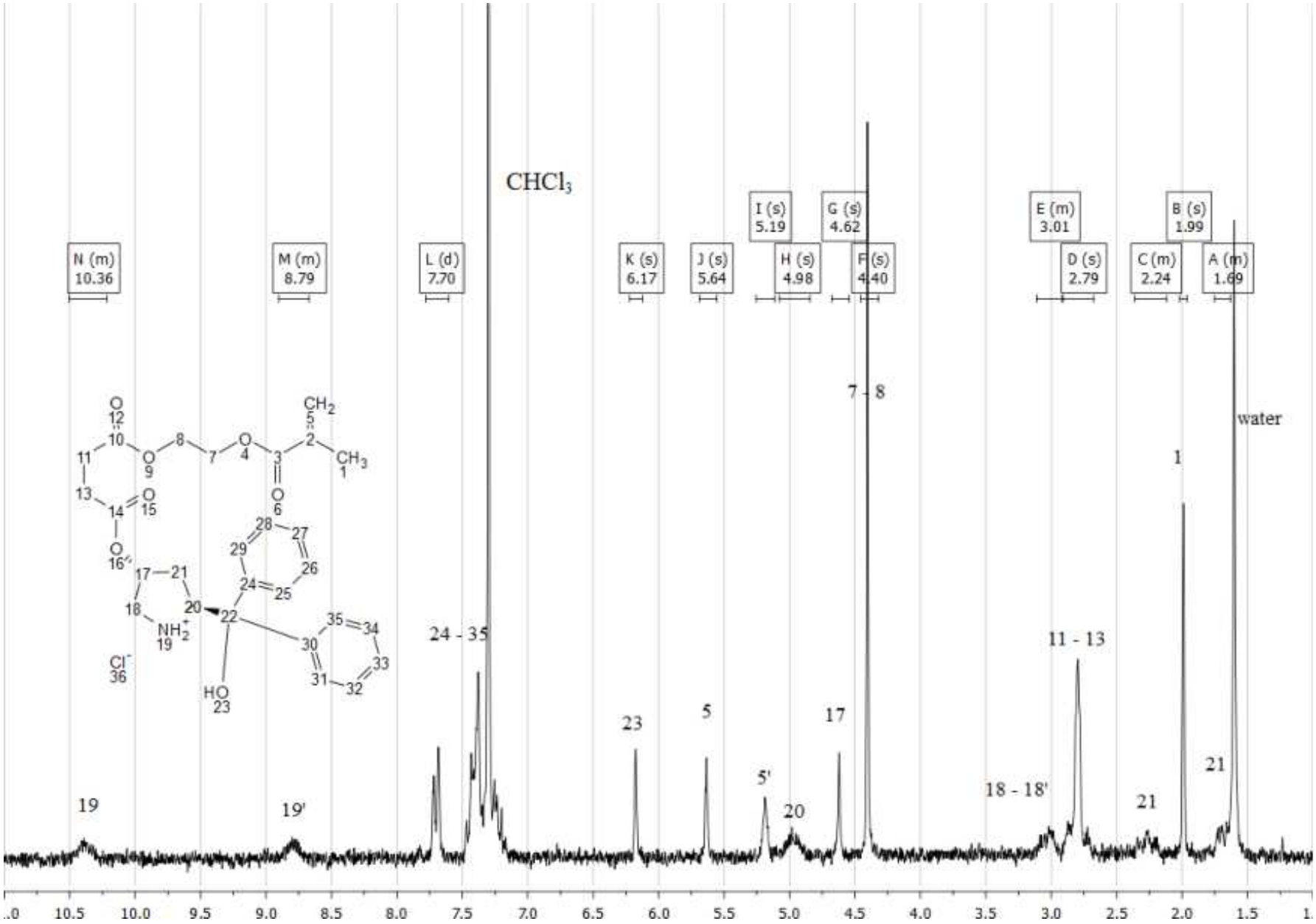

Figure 4.16: 1H NMR (200 MHz, CDCl3) 10.50 – 10.22 (m, 1H), 8.90 – 8.67 (m, 1H), 7.70 (d, J = 7.2 Hz, 2H), 6.17 (s, 1H), 5.64 (s, 1H), 5.19 (s, 1H), 4.98 (s, 1H), 4.62 (s, 1H), 4.40 (s, 4H), 3.11 – 2.92 (m, 2H), 2.79 (s, 5H), 2.36 – 2.12 (m, 2H), 1.99 (s, 3H), 1.75 – 1.63 (m, 1H).

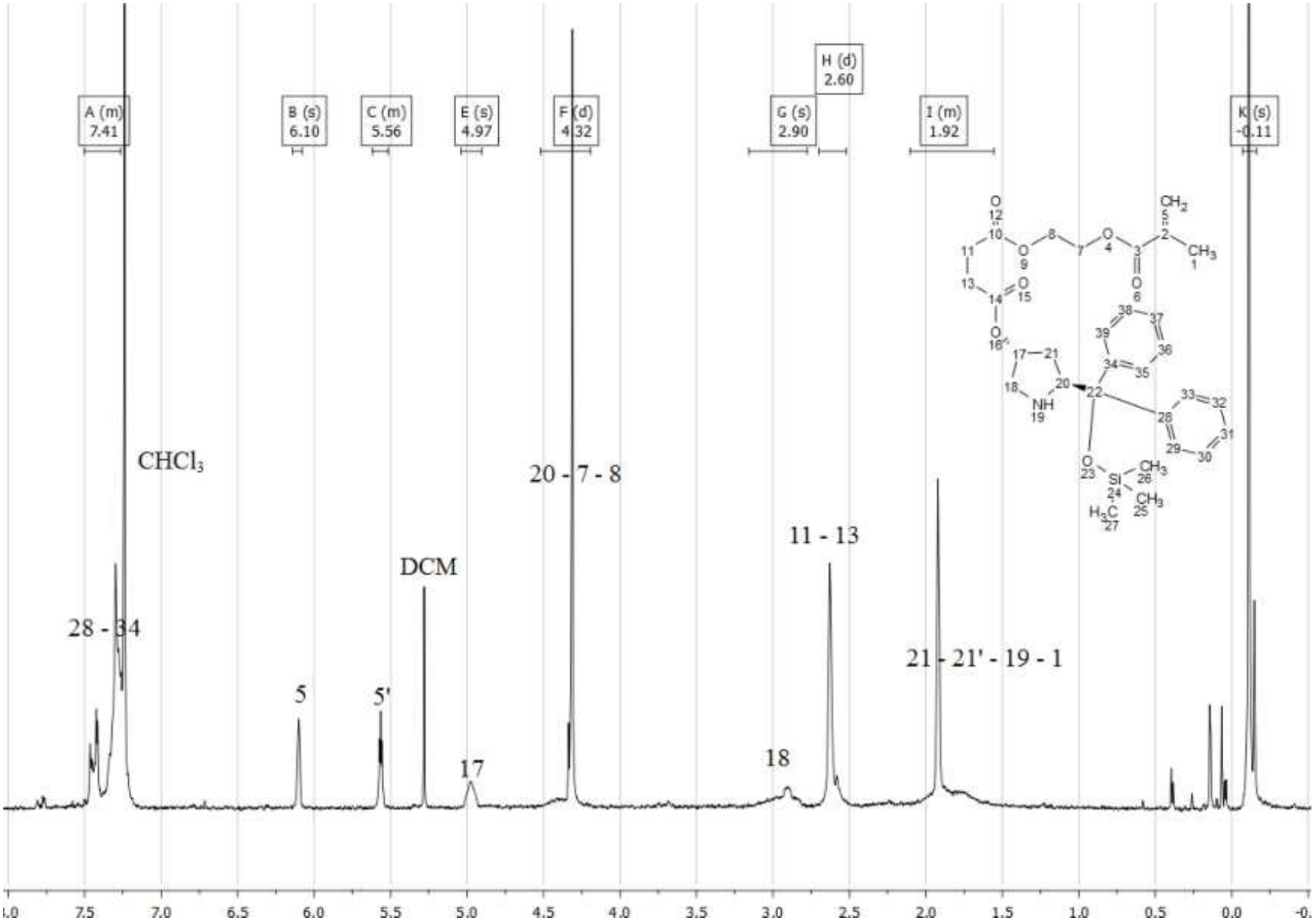

Figure 4.17: 1H NMR (200 MHz, CDCl3) 7.50 – 7.26 (m, 7H), 6.10 (s, 1H), 5.62 – 5.51 (m, 1H), 4.97 (s, 1H), 4.32 (d, J = 4.6 Hz, 5H), 2.90 (s, 2H), 2.60 (d, J = 9.3 Hz, 4H), 2.10 – 1.56 (m, 6H), -0.11 (s, 7H).

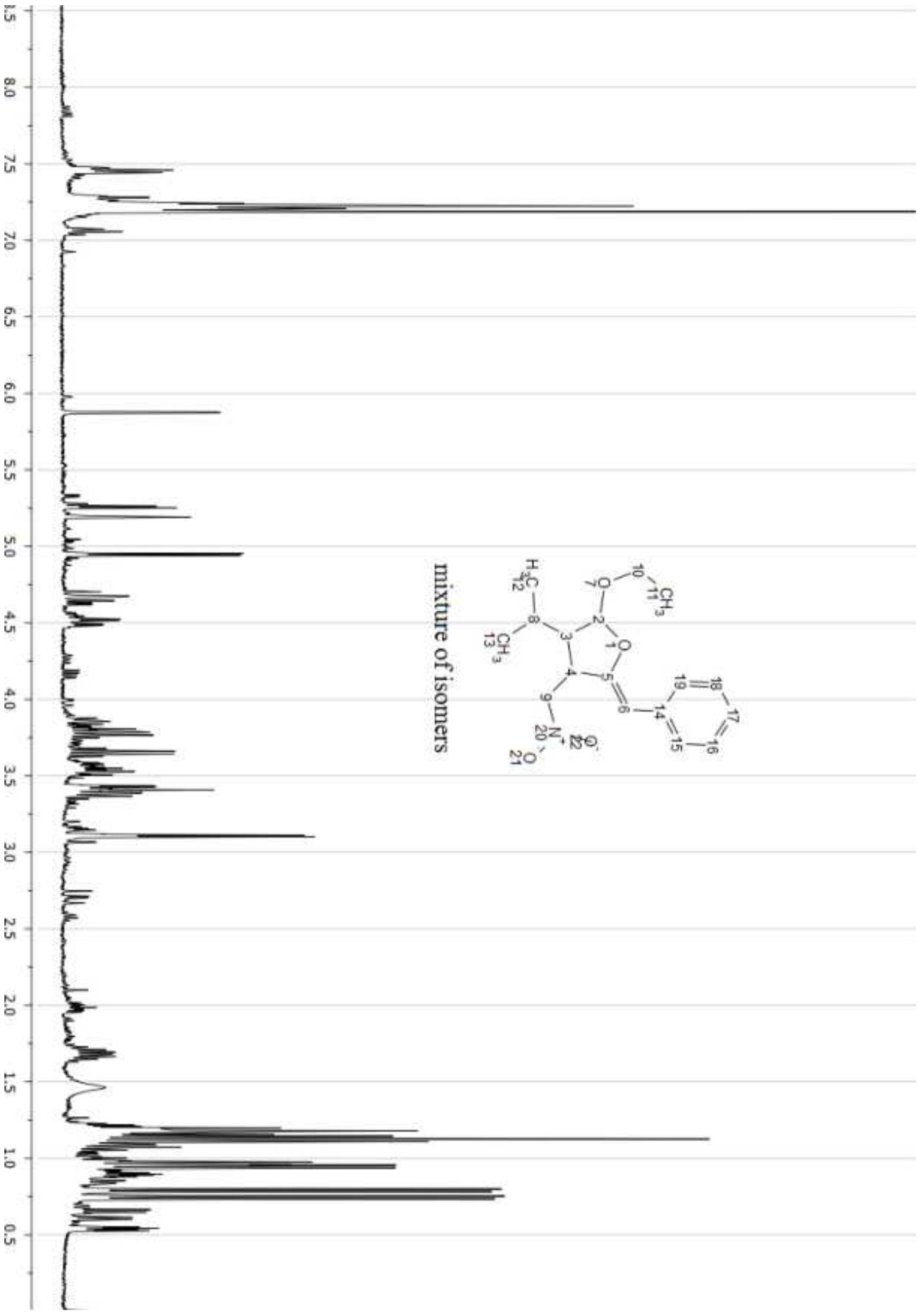

Figure 4.18

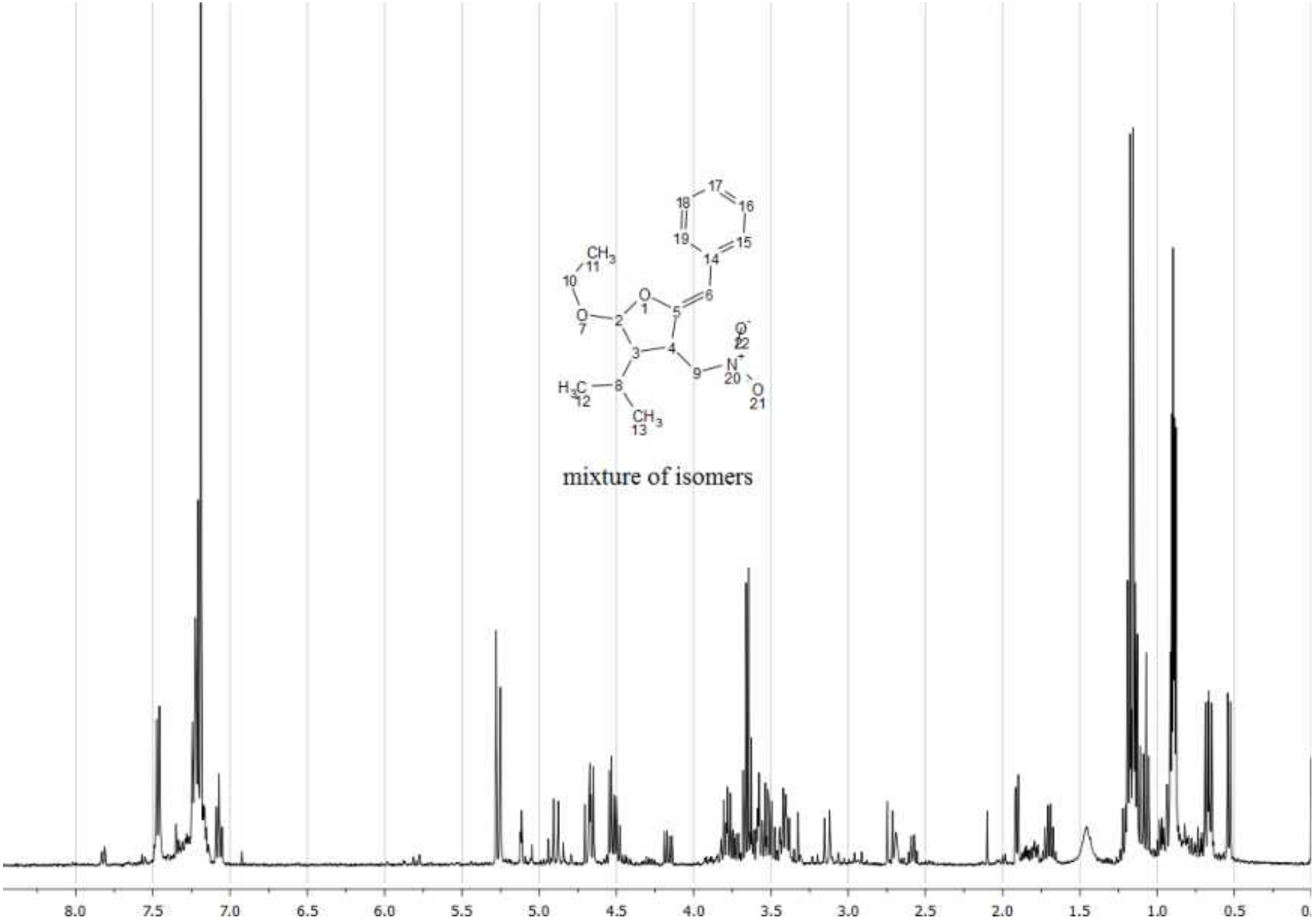

Figure 4.19

Appendix III: Microscope pictures

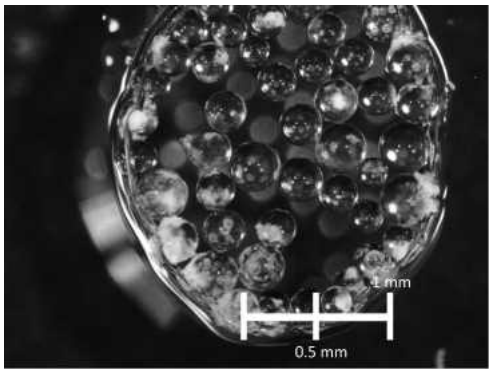

Figure 4.20: **31** in water.

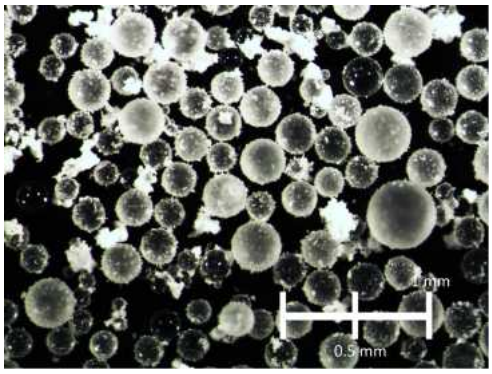

Figure 4.21: **33**

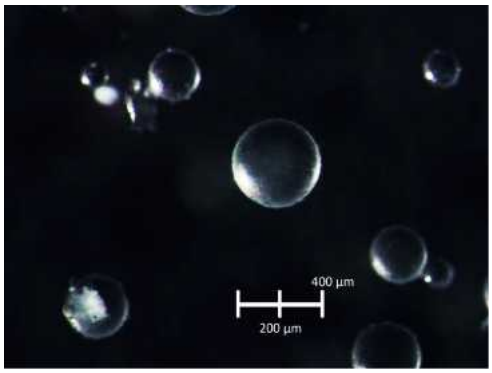

Figure 4.22: **31** in water.

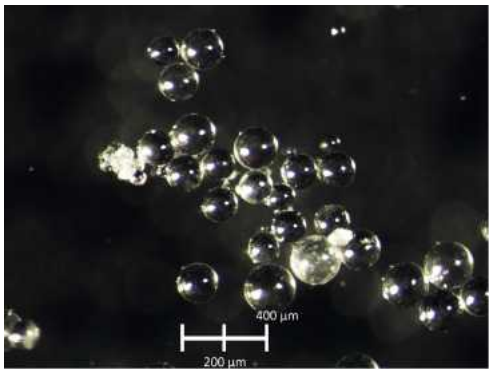

Figure 4.23: **34**

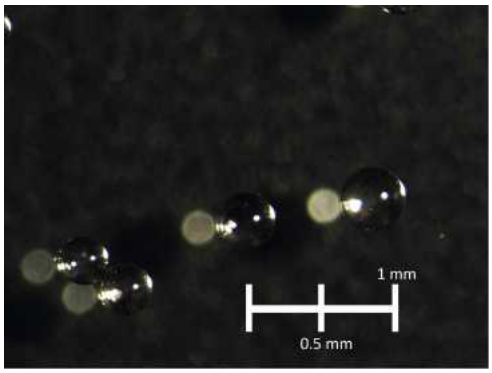

Figure 4.24: **35**

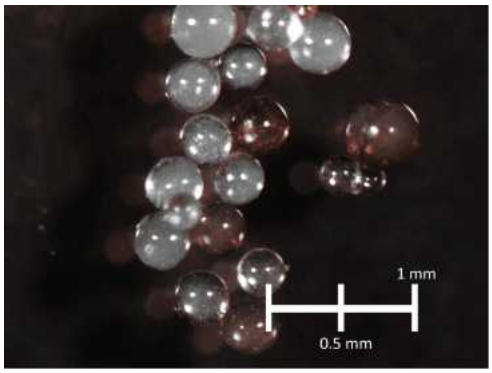

Figure 4.25: **37** after use

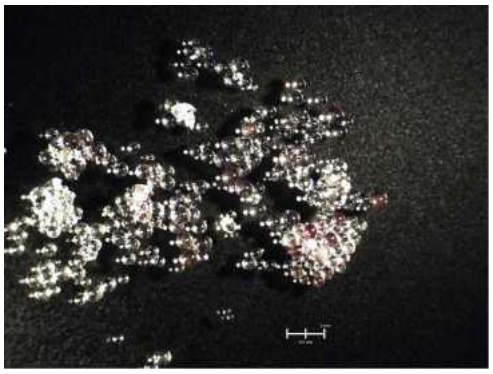

Figure 4.26: **25** after use

Figure 4.27: **25** after use

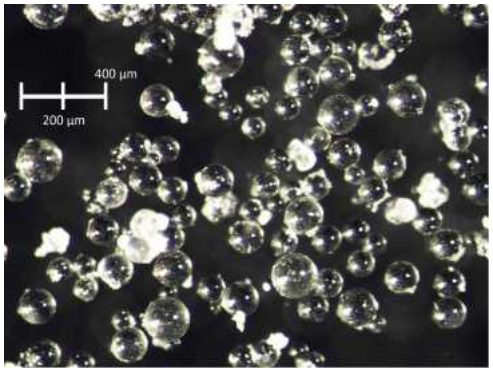

Figure 4.28: **36**

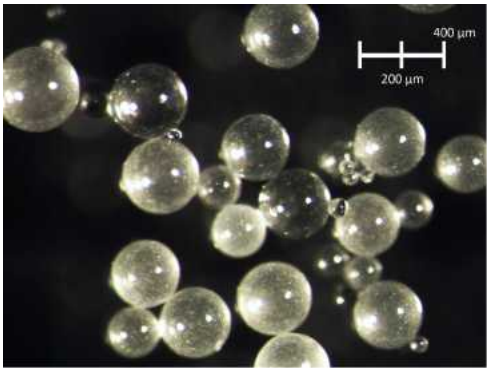

Figure 4.29: **29**

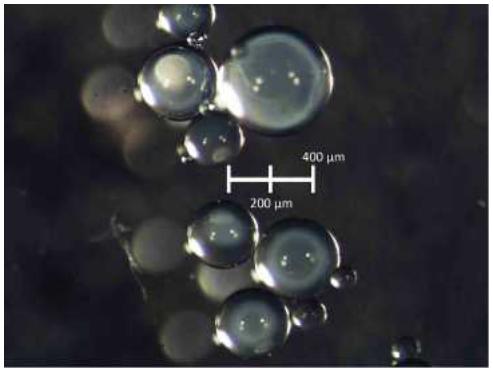

Figure 4.30: **38** after use

References

[1] Roessner, C. A.; Nayar, G. P.; Spencer, B. J.; Pichon, C.; Stolowich, N. J.; Wang, J.; Santander, J. S.; Holderman, M. T.; Scott, A. I.; Min, C. *Chemistry & Biology* **1994**, *1*, 119–124.

[2] Davie, E. A. C.; Mennen, S. M.; Xu, Y.; Miller, S. J. *Chemical Reviews* **2007**, *107*, 5759–5812.

[3] Bui, T.; Barbas III, C. F. *Tetrahedron Letters* **2000**, *41*, 6951–6954.

[4] List, B.; Lerner, R. A.; Barbas III, C. F. *Journal of the American Chemical Society* **2000**, *122*, 2395–2396.

[5] Bertelsen, S. r.; Jø rgensen, K. A. *Chemical Society Reviews* **2009**, *38*, 2178–2189.

[6] Melchiorre, P.; Marigo, M.; Carlone, A.; Bartoli, G. *Angewandte Chemie (International ed. in English)* **2008**, *47*, 6138–6171.

[7] Nielsen, M.; Worgull, D.; Zweifel, T.; Gschwend, B.; Bertelsen, S. r.; Jø rgensen, K. A. *Chemical Communications (Cambridge, England)* **2011**, *47*, 632–649.

[8] Liu, K.; Chougnet, A.; Woggon, W.-D. *Angewandte Chemie (International ed. in English)* **2008**, *47*, 5827–5829.

[9] Grondal, C.; Jeanty, M.; Enders, D. *Nature Chemistry* **2010**, *2*, 167–178.

[10] Tietze, L. F. *Chemical reviews* **1996**, *96*, 115–136.

[11] Kaneko, S.; Toshiaru, Y.; Katoh, T.; Terashima, S. *Tetrahedron* **1998**, *54*, 5471–5484.

[12] Fogg, D. E.; dos Santos, E. N. *Coordination Chemistry Reviews* **2004**, *248*, 2365–2379.

[13] Dalko, P. I.; Moisan, L. *Angewandte Chemie (International ed. in English)* **2004**, *43*, 5138–5175.

[14] Pellissier, H. *Tetrahedron* **2007**, *63*, 9267–9331.

[15] Enders, D.; Hüttl, M. R. M.; Grondal, C.; Raabe, G. *Nature* **2006**, *441*, 861–863.

[16] Allen, A. E.; MacMillan, D. W. C. *Chemical Science* **2012**, *3*, 633–658.

[17] Usui, I.; Schmidt, S.; Breit, B. *Organic letters* **2009**, *11*, 1453–1456.

[18] Du, Z.; Shao, Z. *Chemical Society Reviews* **2013**.

[19] Shao, Z.; Zhang, H. *Chemical Society Reviews* **2009**, *38*, 2745–2755.

[20] Ambrosini, L. M.; Lambert, T. H. *ChemCatChem* **2010**, *2*, 1373–1380.

[21] Chi, Y.; Scroggins, S. T.; Fréchet, J. M. J. *Journal of the American Chemical Society* **2008**, *130*, 6322–6323.

[22] Hodge, P. *Current Opinion in Chemical Biology* **2003**, *7*, 362–373.

[23] Balkenhohl, F.; Bussche-hunnefeld, C. V.; Lansky, A.; Zechel, C. *Angewandte Chemie (International ed. in English)* **1996**, *35*, 2288–2337.

[24] Bienayme, H.; Hulme, C.; Oddon, G.; Schmitt, P. *Chemistry–A European Journal* **2000**, *6*, 3321–3329.

[25] Varela, M. C.; Dixon, S. M.; Price, M. D.; Merit, J. E.; Berget, P. E.; Shiraki, S.; Kurth, M. J.; Schore, N. E. *Tetrahedron* **2007**, *63*, 3334–3339.

[26] Varela, M. C.; Dixon, S. M.; Lam, K. S.; Schore, N. E. *Tetrahedron* **2008**, *64*, 10087–10090.

[27] Selkälä, S. A.; Tois, J.; Pihko, P. M.; Koskinen, A. M. P. *Advanced Synthesis & Catalysis* **2002**, *344*, 941–945.

[28] Puglisi, A.; Benaglia, M.; Cinquini, M.; Cozzi, F.; Celentano, G. *European Journal of Organic Chemistry* **2004**, *2004*, 567–573.

[29] Kristensen, T. E.; Hansen, F. K.; Hansen, T. *European Journal of Organic Chemistry* **2009**, 387–395.

[30] Kristensen, T. E.; Vestli, K.; Fredriksen, K. A.; Hansen, F. K.; Hansen, T. *Organic*

Letters **2009**, *11*, 2968–2971.

[31] Kristensen, T. E.; Hansen, T. *European Journal of Organic Chemistry* **2010**, 3179–3204.

[32] Kristensen, T. E.; Vestli, K.; Jakobsen, M. G.; Hansen, F. K.; Hansen, T. *Journal of Organic Chemistry* **2010**, *75*, 1620–1629.

[33] Simmons, B.; Walji, A. M.; MacMillan, D. W. C. *Angewandte Chemie (International ed. in English)* **2009**, *48*, 4349–4353.

[34] Odian, G. *Principles of Polymerization*, 4th ed.; Wiley-Interscience: New York, 2004.

[35] Takemoto, K.; Ottenbrite, R. M.; Mikiharu, K. *Functional monomers and polymers*, 2nd ed.; Marcel Dekker, 1997.

[36] Lelais, G.; Macmillan, D. W. C. *Aldrichimica Acta* **2006**, *39*, 79.

[37] Belot, S.; Vogt, K. A.; Besnard, C.; Krause, N.; Alexakis, A. *Angewandte Chemie (International ed. in English)* **2009**, *48*, 8923–8926.

[38] Hechavarria Fonseca, M. T.; List, B. *Angewandte Chemie (International ed. in English)* **2004**, *43*, 3958–3960.

[39] Armstrong, A.; Blackmond, D. G. *Journal of the American Chemical Society* **2011**, 8822–8825.

[40] Paras, N. a.; MacMillan, D. W. C. *Journal of the American Chemical Society* **2001**, *123*, 4370–1.

[41] Biaggi, C.; Benaglia, M.; Raimondi, L.; Cozzi, F. *Tetrahedron* **2006**, *62*, 12375–12379.

[42] Ahrendt, K. A.; Borths, C. J.; Macmillan, D. W. C.; Organocatalyzed, T.; Reaction, D.-a. *Journal of the American Chemical Society* **2000**, *122*, 4243–44.

[43] Northrup, A. B.; MacMillan, D. W. C. *Journal of the American Chemical Society* **2002**, *124*, 2458–2460.

[44] Benaglia, M.; Celentano, G.; Cinquini, M.; Puglisi, A.; Cozzi, F. *Synthesis* **2002**, *344*, 149–152.

[45] Burés, J.; Armstrong, A.; Blackmond, D. G. *Journal of the American Chemical Society*

2012, *134*, 6741–50.

[46] Notz, W.; Tanaka, F.; Barbas III, C. F. *Accounts of Chemical Research* **2004**, *37*, 580–591.

[47] Sakthivel, K.; Notz, W.; Bui, T.; Barbas III, C. F. *Journal of the American Chemical Society* **2001**, *123*, 5260–5267.

[48] Zhong, C.; Shi, X. *European Journal of Organic Chemistry* **2010**, *2010*, 2999–3025.

[49] Mézailles, N.; Ricard, L.; Gagosz, F. *Organic Letters* **2005**.

[50] Carriedo, G. A.; Presa, A.; Valenzuela, M.; Ventalon, M. *Journal of Organometallic Chemistry* **2009**, *694*, 249–252.

[51] Karimi, B.; Golshani, B. *Journal of Organic Chemistry* **2000**, *09*, 7228–7230.

[52] Mossé, S.; Alexakis, A. *Organic letters* **2006**, *8*, 3577–80.